Short Term Exogenic Climate Change Forcing

by

Daniel Krahenbuhl

A Dissertation Presented in Partial Fulfillment
of the Requirements for the Degree
Doctor of Philosophy

Approved April 2013 by the
Graduate Supervisory Committee:

Randall Cerveny, Chair
Ronald Dorn
John Shaffer

ARIZONA STATE UNIVERSITY

May 2013

ABSTRACT

Several short term exogenic forcings affecting Earth's climate are but recently identified. Lunar nutation periodicity has implications for numerical meteorological prediction. Abrupt shifts in solar wind bulk velocity, particle density, and polarity exhibit correlation with terrestrial hemispheric vorticity changes, cyclonic strengthening and the intensification of baroclinic disturbances. Galactic Cosmic ray induced tropospheric ionization modifies cloud microphysics, and modulates the global electric circuit. This dissertation is constructed around three research questions: (1): What are the biweekly declination effects of lunar gravitation upon the troposphere? (2): How do United States severe weather reports correlate with heliospheric current sheet crossings? and (3): How does cloud cover spatially and temporally vary with galactic cosmic rays? Study 1 findings show spatial consistency concerning lunar declination extremes upon Rossby longwaves. Due to the influence of Rossby longwaves on synoptic scale circulation, our results could theoretically extend numerical meteorological forecasting. Study 2 results indicate a preference for violent tornadoes to occur prior to a HCS crossing. Violent tornadoes (EF3+) are 10% more probable to occur near, and 4% less probable immediately after a HCS crossing. The distribution of hail and damaging wind reports do not mirror this pattern. Polarity is critical for the effect. Study 3 results confirm anticorrelation between solar flux and low-level marine-layer cloud cover, but indicate substantial regional variability between cloud cover altitude and GCRs. Ultimately, this dissertation serves to extend short term meteorological forecasting, enhance climatological modeling and through analysis of severe violent weather and heliospheric events, protect property and save lives.

DEDICATION

To my mother and father.

Their selfless acts allowed me the opportunity and freedom to explore.

ACKNOWLEDGMENTS

I thank Randall Cerveny for his invaluable tutelage and mentorship throughout my graduate studies. Without his unyielding support and passion for 'unusual' projects, this dissertation would not be possible.

I also thank Ron Dorn for providing me with unique perspectives and countless meals following hikes through the Sonoran Desert.

I also thank John Shaffer for his hints, thoughtful suggestions and previous scholarship to emulate.

I also thank Matt Pace and Robert Balling, Jr. for their contributions to my investigations and publications.

TABLE OF CONTENTS

Page

LIST OF TABLES vi

LIST OF FIGURES vii

CHAPTER 1: INTRODUCTION 1

1.1 SCOPE OF THE PROBLEM 1

1.2 LITERATURE REVIEW 6

1.3 FRAMEWORK FOR INVESTIGATION 25

CHAPTER 2: LUNAR DECLINATION AND CIRCULATION 28

2.1 INTRODUCTION 28

2.2 DATA 30

2.3 ANALYSES 32

3.4 CONCLUSIONS 37

CHAPTER 3: THE SOLAR WIND AND SEVERE WEATHER 38

3.1 INTRODUCTION 38

3.2 DATA 40

3.3 METHODOLOGY 41

3.4 RESULTS 45

3.5 CONCLUSIONS 50

3.6 ACKNOWLEDGEMENTS 51

CHAPTER 4: GALACTIC COSMIC RAYS AND CLOUD COVER 52

4.1 INTRODUCTION 52

4.2 BACKGROUND 53

4.3 DATA 54

4.4 METHODS AND RESULTS 55

4.5 DISCUSSION AND CONCLUSIONS 57

4.6 ACKNOWLEDGEMENTS 61

Page

CHAPTER 5: CONCLUSIONS 62

5.1 SUMMARY OF RESULTS 62

5.2 FUTURE RESEARCH 65

5.2 SIGNIFICANCE TO FIELD 67

REFERENCES 69

APPENDIX

A GLOSSARY 78

B HCS CROSSING DATES 81

BIOGRAPHICAL SKETCH 98

LIST OF TABLES

Table Page

3.1 TORNADO AND MONTE CARLO SIMULATION DISTRIBUTION STATISTICS 49

A.B P2N HCS CROSSING DATES 78

A.B N2P HCS CROSSING DATES 81

LIST OF FIGURES

Figure Page

2.1 Longitudinal Means of Tropospheric pressure surfaces versus Lunar Declination 31

2.2 Latitudinal Means of Tropospheric pressure surfaces versus Lunar Declination 32

2.3 Longintudinal Mean 300 hpa height differences for negative to positive lunar declination transition 34

2.4 Kriged represtation of 300 hPa variations between Lunar declination maximums..... 36

3.1 Superposed Epoch Analysis of Solar Wind Parameters 42

3.2 EF3+ Tornado Distribution and Monte Carlo Simulation..... 44

3.3 Tornado Report Distributions 46

3.4 Hail and Damaging Wind Report Distribution 48

4.1 Low-Level Cloud Cover versus Solar Flux 58

4.2 Mid-Level Cloud Cover versus Solar Flux 59

4.3 High-Cloud Cover versus Solar Flux..... 60

CHAPTER 1

INTRODUCTION

1.1 SCOPE OF PROBLEM

1.1.1 Scales of Climate Forcings

Earth's climate has been changing and evolving since the planet's formation over four billion years ago. For the past 500 million years, the Earth's climate has been hospitable for complex life to evolve. In our current epoch, the Holocene, which commenced circa 10,000 years ago, the Earth, is experiencing a temperate interglacial climate regime. It is in this current epoch, the Holocene, which contains all recorded human history. Essentially, climate can be represented as the time integral of weather: the current state of the atmosphere. Earth's climate is a dynamic system, continuously redistributing and circulating energy, mass and momentum. Climate varies on numerous timescales and multitudes of processes affect the climate system.

Climate 'forcings' drive climate change, perturbing and reorganizing the climate system. These forcings are diverse and encompass a variety of temporal and spatial scales. Taxonomically, processes acting from outside the Earth system are considered exogenic forcings. Forcings acting from within the Earth system are considered endogenic forcings. Inherent modes of stability, natural system oscillations and their interconnected processes are considered autogenic forcings. Finally, changes and forcings attributed to human activity are noted as anthropogenic forcings (Versteegh, 2003).

Exogenic climate forcings include: variations in solar output, precipitation of energetic particles, impact events, electromagnetic cosmic radiation and gravitational tidal acceleration. Examples of endogenic forcings are: volcanic activity, plate tectonics (including orography, mountain building), and changes in the geomagnetic field. Autogenic forcings include land-ocean interactions, major atmospheric-ocean oscillations (PDO, ENSO), and other quasi-periodic atmospheric oscillations (NAO, AO).

Planetary climate reconstruction, current meteorological forecasting, and climatological projections prompt the maintenance of a thorough and comprehensive census of climate forcings. Not only does this provide visage into planetary evolution and habitability, but it provides invaluable reference to gauge anthropogenic effects. Through careful scrutiny, we may discern whether our current institutions should aspire to be sustainable or adaptable. Ultimately, our goals are continuous improvements of our models, concepts and ability to predict. Our numerical weather forecasting loses their predictive rigor after 2 weeks. The examination of exogenic forcings which have documented effects within the time domain established through numerical forecasting; seems the next logical step. The subsequent goal of this dissertation is the examination of exogenic climate forcings which impact upon the time scales currently limiting our meteorological and climatological forecasting and prediction.

Explicitly in this dissertation I extend the research of three exogenic topics:

a) Gravity, such that my specific research question is “what are the biweekly declination effects of lunar gravitation upon the middle and upper tropospheric geopotential heights?”

b) Solar Wind, such that my specific research question is “how do United States severe weather reports, such as tornadoes, hail and damaging wind activity, correlate with heliospheric current sheet crossings at Earth’s orbit?”

c) Galactic Cosmic Rays, such that I ask “How does cloud cover reconstructions spatially and temporally vary with respect to galactic cosmic rays?”

In order to fully address these research questions and their underlying frequencies and principles, a brief discussion of the existing literature background is necessary

1.1.1 Forcing Frequency

1.1.2 Some climate forcings are periodic or even cyclical. This results in a cumulative compounding effect. Conversely, some forcings are manifest as a singular, large magnitude impulse event.

The existence of periodic exogenic climate forcing is undeniable. From the sunrise to sunset, the ebb and flow of the tides and the march of the seasons; astronomical cycles and their effects have been known since antiquity. Lunar calendars are ubiquitous throughout history. Several ancient megalithic structures and settlements are constructed in specific alignments to chart the changing position of the Sun at solstice. Gravitational and orbital influences range from the hourly to billions of years: sub daily tidal periods (~10^{-4} years), Earth's diurnal rotation (~10^{-3} years), the lunar month (~10^{-1} years), Earth's orbital revolution (1 year), to lunar nutation (~10^{1} years), to Milankovich orbital variations (10^{4} – 10^{7} years), to Galactic spiral arm transits (10^{7}-10^{9} years).

The Sun oscillates through cycles of magnetic activity, resulting in a more powerful solar wind, and more energetic radiation. The Sun's equatorial rotation over 27 days projects a unique solar wind Earthward. Solar magnetic activity and sunspot numbers exhibit distinct periods ranging from the 11 year Schabwe cycle, the 22 year Hale, and larger periodicities. At longer time scales, the strength of the solar cycle changes as well, and the Sun exhibits lulls in activity. The magnitude of the solar wind also dictates the penetration of cosmic rays into the solar system. Cosmogenic nuclides, the results of cosmic radiation on Earth's atmosphere, comprise primary methods for paleoclimatic reconstruction.

Non-periodic impulse events are more successfully characterized by a recurrence interval. The majority of exogenic impulse forcings conform to power laws. For example, micro-meteoroids impact the planet almost constantly, a Tunguska air-blast event occurs every century, and a catastrophic impact event occurs every 60 million years or so. Similarly, solar micro-flares occur nearly constantly, large X-class flares occur with a frequency akin the 11 year solar cycle, and extremely energetic events with major geomagnetic consequences (the Carrington event) occur at centennial time scales.

Additionally, Mt. Kilauea erupts constantly, large VEI 6+ events occur roughly every couple of decades, and the last super volcano eruption occurred in Toba, Indonesia around 60,000 years ago. The events which are low impact happen continuously, and the extreme

events are considered low risk, high impact. Land-Ocean internal processes can also be low frequency, high magnitude events: such as a Heinrich event, a massive ice calving injection in the global ocean, disrupting circulation patterns.

Impulse events are intrinsically chaotic, defying forecasting. However, through identification of factors leading to the event, alerts or heightened states of awareness, can be issued. When there is unusually high seismic activity or ground upwelling, alerts may be issued for a certain volcano. When there are favorable conditions for tornadoes, watches or warning can be issued. Similarly, in new field of space weather forecasting, when a sunspot has a strong enough magnetic field classification (enough to unleash X-class flares) alerts are issued and the active region is closely monitored.

1.1.3 Ramifications

The Earth circulates mass, energy and momentum through a series of interconnected subsystems: the atmosphere, cryosphere, hydrosphere, lithosphere and biosphere. The disruption of any of these subsystems has the capability to unleash a cascade of consequences for the others.

Historically, sudden or prolonged climate changes have simultaneously allowed the spread and prosper of civilizations in one part of the world while terminating civilizations in other regions. Changing climate affects food production and fresh water resources. Throughout history, climate change has been attributed to the death of millions through widespread famine and disease. As resources are exhausted, territorialism and warfare erupt to secure remaining reserves. National economic stability, mobility and infrastructure are all subject to climate change. During the medieval warm period, wine was cultivated in the British Isles, great cathedrals were constructed throughout Europe, and the Vikings were establishing colonies in Greenland. The following little ice age however resulted in the abandonment of the Greenland settlements, the river Thames froze over, crops failed and the associated famine exacerbated the Black Death (Eddy, 1976).

Further, unpredictable solar storms pose new dangers for our technological age. Massive solar flares have the capacity to disrupt global communication, global positioning systems, and spacecraft operations. In 1943, transmissions of Allied troop deployments were hampered by solar related communications disruption (Odenwald, 2010). In 1957, the British went on full scale naval alert after the submarine Acheron was feared missing after failing to report in (Odenwald, 2010). Geomagnetic induced currents have the capacity to overload terrestrial power transmission systems. There are many accounts of telegraph workers severely shocked or killed by the overload or the fires started by geomagnetic induced currents. The Quebec blackout of 1989, which affected over 3 million people, was caused by a solar storm (Odenwald, 2010). Researchers estimate the solar storm that occurred in 1921, was more than three times as strong as the 1989 storm. The Carrington event, in 1859, produced aurorae as far south as Cuba and Hawaii. Possible damage estimates for a similar event today equates to over a trillion dollars with a recovery time of four to ten years. (American Meteorological Society, 2008) Taking into account our contemporary society's reliance on electricity, telecommunications and national information infrastructure, the grave consequences underscore the necessity of this investigation.

Understanding the magnitude and frequency of exogenic forcings are paramount to the continued prosperity of our civilization. Earth's climate is a dynamic non-linear system with complex feedback pathways, where even a small forcing can have a compounding effect including the possibility of irreversibility. The paleoclimate record exhibits abrupt changes indicating a small stimulus or perturbation has the possibility of pushing our climate over a tipping point (Gavin et al., 2011). Global climate change by definition affects the entire world population.

The following section represents a brief review of exogenic climate change forcing. This background is necessary to comprehend the scope of the issues, the unsolved issues and new questions posited.

1.2 LITERATURE REVIEW

1.2.1 Luminosity

The first exogenic climate forcing to be reviewed is the subject of solar luminosity. Firstly, a general introduction to the phenomenon is provided. Secondly, I examine the variability in the spectra of solar radiation and the constructs from which the modulations arise. I conclude with scholarship establishing links between climate phenomenon and the variance in solar radiative spectra.

Electromagnetic radiation from the Sun warms the Earth, powers the atmosphere/hydrosphere circulations and allows for photosynthetic life to thrive. The Sun is powered by nuclear fusion at its core. The Sun's core energy is radiated and convected to the visible solar surface, the photosphere. Solar luminosity is determined by the effective temperature and surface area of the photosphere (Beer, 2010).

$$L_s = 4\pi R_s^2 \sigma T_{eff}^4 = 3.8 \times 10^{28}\text{W} \tag{1.1}$$

where σ is the Stephan-Boltzmann constant:

$$\sigma = \frac{2\pi k_b^4}{15h^3c^2} = 5.67 \times 10^{-8} \frac{W}{m^2K^4} \tag{1.2}$$

with k_b the Boltzmann constant, h the Planck constant, and c the speed of light.

The luminosity peaks in visual wavelengths and is radiated out in all directions in proportion to the inverse square of the distance (Beer et al., 2006). The percentage of solar luminosity intercepted by a planet is controlled by its cross-sectional area in relation to the area of a sphere with radius d_s from the Sun:

$$P_{abs} = \frac{L_s \pi R_p^2 (1-a)}{4\pi d_s^2} \tag{1.3}$$

where a is the albedo, and R_p is the radius of the planet. Similarly, with energy emitted by a planet:

$$P_{emi} = 4\pi R_p^2 \sigma T_e^4 \tag{1.4}$$

the effective temperature of the planet can be obtained:

$$T_e = \sqrt[4]{\left(\frac{L_s(1-a)}{16\pi\sigma d_s^2}\right)} \tag{1.5}$$

The effective temperature has no relation to the size of the planet, but relies only upon the distance from the star, the star's luminosity, and the reflectivity of the planet.

The luminosity spectrum is strengthened in the extreme ultraviolet (EUV), x-ray, and radio waves due to high temperatures (10^5 to 10^6 K) in the outer solar atmosphere: the chromosphere and the corona. As such, the EUV, x-rays, and radio wavelength spectra are orders of magnitude larger than for a photospheric blackbody temperature curve.

At a distance of one Astronomical Unit or 150 Million kilometers; the total solar irradiance (TSI) is 1361 +/- 4 W m^{-2} (Gray et al., 2010). Total Solar Irradiance or TSI replaces the defunct *Solar Constant* terminology. Active regions are areas on the photosphere with very intense magnetic fields. They are more commonly known as sunspots (Foukal and Lean, 1988). Sunspot observations have measurements have continuously been refined and improved since the commencement of observation during the European renaissance (Hoyt et al., 1983; Hoyt and Eddy, 1983). Active regions cause temperature increases in the chromosphere and corona resulting in larger emittance of EUV and x-radiation. Active regions that emerge from the convective zone of the Sun are rooted into the rotating photospheric surface. The corona also has cooler areas devoid of active regions. These coronal holes have a suppressed EUV/x-ray signature; however the open magnetic field permits a faster and denser solar wind (described in detail in the following section). As the Sun rotates, the spatially unique spectral irradiance is emitted outwards illuminating the planets.

The Earth's atmosphere absorbs the higher frequency radiation from reaching the surface (Haigh et al., 2005). This radiation ionizes the upper atmosphere resulting in the Earth's ionosphere (Lockwood, 2006). Light in the visual spectrum is scattered and illuminates the

surface. Luminosity from the Sun varies with the ~11 year Schwabe cycle (Scafetta et al., 2004). During solar maximum, there are more active regions which change the spectrum of TSI. The integrated TSI does not vary largely with the solar cycle; however the amount of EUV and x-radiation varies by several orders of magnitude. Willson and Mordvinov (2003) reviewed the TSI variations over solar cycles 21 through 23 using a compellation of satellite observations. Detailed reconstruction of TSI with satellite data and sunspot observations are provided by Haigh (2003) and Solanki and Krivova (2005).

The Little Ice Age (LIA) was a period of abnormally cold climate in Europe, which corresponded with a prolonged stagnation of solar activity. The LIA has no official time span; however the effect spanned much of the latter half of the second millennium (Lockwood, 2006). Several solar activity minima occurred during this period. Although this connection is contested, it did ignite resurgence into solar-terrestrial physics (Eddy et al., 1989; Eddy, 1976).

The following research summary represents observed climatology parameters that have been found to vary with TSI. Surface temperature records for the Northern Hemisphere were found to have a 0.86 correlation with TSI reconstruction from the period 1600 – 1800AD; and extending the correlation; explains half of the surface warming from 1860 to 1970 AD (Lean et al., 1995; Lean and Rind, 1998). Scafetta et al. (2004) find that the temperature of hemispheres, land and sea surfaces, are highly correlated with TSI. Further, Scafetta and West (2006) found a pronounced solar signature within 400 years of Northern Hemisphere temperature reconstructions and Lockwood et al. (2010) using Central England Temperature found that lower TSI (during prolonged sunspot minimums) corresponds to colder winters in Europe. Similarly, Ludecke (2011) using instrument records and reconstructed proxies, argues that increasing TSI may contradict anthropogenic global warming. However, several significant volcanic eruptions were responsible for the little ice age (Lean and Rind, 1998).

Solanki and Krivova (2003a, b) found a significant correlation between TSI and global tropospheric temperature anomalies. They state that the Sun could not have contributed to more than 30% of the rise in global temperatures since 1970. Lockwood and Frohlich (2007) argue

that the decreasing trend in TSI cannot be attributed to global warming. Frohlich and Lean (1998), using five satellite radiometric observations of TSI from 1986 to 1996, find no correlation between the 0.2 degree increase in global mean surface temperature.

Global sea surface temperatures are also highly correlated with TSI over a period of 130 years (Reid, 1991). Analysis of the global averaged ocean temperatures between 1955-1994 indicate that variations in TSI are mirrored in the upper ocean (White et al., 1997). From deep sea cores, several solar periodicities (including a 1500 year cycle) were detected in sea ice proxies (Bond et al., 2001). Examining the Nile river water level time series between 622 – 1470 AD, (Ruzmaikin et al., 2006) detected multiple solar periodicities. Roy and Haigh (2010) find solar cycle signals in 155 years of global sea level pressure and sea surface temperature, and Berner et al. (2011) detect solar signals from the Voring Plateau sediment core indicating a persistent solar influence throughout the Holocene.

One of the primary forcing mechanisms proposed to explain the Sun/Earth climate connection is the effect of UV radiation influencing the stratosphere, and through vertical coupling, the troposphere. Labitzke and van Loon (1992) identified a connection between solar activity with satellite temperature data at 30 hPa geopotential height. A solar signal was also detected in the summer stratospheric vortices (van Loon and Shea, 2000). Ruzmaikin et al. (2004, 2006) and Ruzmaikin (2007) show Northern hemisphere temperature patterns controlled by the North Annular Mode (NAM) are correlated with TSI. Haigh et al. (2005) found that an increase in TSI resulted in a weakening and poleward shift of the subtropical jets. Salby and Callaghan (2006), using the NCEP/NCAR reanalysis found a modulation of the anomalous zonal wind that varies in phase with TSI. Several of these stratospheric studies include the Quasi-Biennial Oscillation (QBO). The QBO is a pseudo periodic reversal of zonal winds in the upper tropical stratosphere (Labitzke and van Loon, 1992). Roy and Haigh, (2011, pg. 11679) “suggest that solar variability, modulated by the phase of the Quasi-Biennial Oscillation, influences zonal mean temperatures at high latitudes in the lower stratosphere, in the mid-latitude troposphere and sea level pressure near the poles.”

Modeling has supported the influence of TSI on ozone production. Haigh (1996) found that ozone production in the stratosphere resulted in a poleward shift and broadening of the Hadley circulation. Polvani and Kushner (2002) established a correlation between stratospheric temperature perturbation and tropospheric response using numerical modeling. Cordero and Nathan (2005) detected a connection between TSI and the QBO with a wave-ozone feedback which altered the propagation of planetary waves. Nathan and Cordero (2007) developed an ozone-modified refractive index (OMRI) which modifies the propagation of vertical planetary waves. They propose this index as a way to quantify the connection between the stratosphere and the troposphere. van Loon et al. (2007, 1) cogently quantified the solar-climate couplings as such:

> The processes begins with an increase in solar forcing which results in a strengthening of the major convergence zones in the tropical Pacific. This then increases the precipitation in those regions and increases the southeast trade winds. Stronger trades increases the upwelling of colder water in the eastern equatorial Pacific and extend the cold tongue westward, thus reducing precipitation in the western Pacific. This redistribution on diabatic heating and associated convective heating anomalies thus produces anomalies in the tropical Hadley and Walker circulations. The former weakens as subsidence in equatorial latitudes is enhanced' the latter strengthens and extends westward. Additionally, the resulting anomalous Rossby wave response in the atmosphere and consequent positive sea level pressure anomalies in the eastern region of the Aleutian low in the North Pacific that extends to western North America, is associated with reductions of precipitation in the northwest United States. The response of the climate systems to solar forcing is manifested as a strengthening of the climatological precipitation maxima in the tropics.

TSI affects other known climate periodicities, such as the El Nino Southern Oscillation (ENSO). The ENSO is a periodic climate variance in sea surface temperature in the tropical Pacific Ocean, accompanied by an atmospheric circulation changes (Cerveny and Shaffer,

2001). Moreover, modeling indicates that the ENSO acts as a thermostat, showing a stronger positive phase at times of lower TSI (Emile-Geay et al., 2007). This mechanism coupled with a weakening of the Southeast Asian Monsoon, and an increase in North Atlantic Ice rafted debris events engenders climate variability at 10^2 to 10^3 years timescales. Simpson et al. (2009) emphasize the importance of eddy momentum fluxes modulating the tropospheric response to localized stratospheric heating. Merkel et al. (2011) confirms the results of Roy and Haigh (2010); that photochemically activated ozone from UV radiation variance influences temperature and wind patterns in the stratosphere which have tropospheric effects.

This section has introduced the electromagnetic phenomenon of solar luminosity, variations in its spectra, and its connections with Earth's climate system. However, solar influence is not limited to electromagnetic radiation.

1.2.2 The Solar Wind

This section explores the variable space environment in which the Earth is situated. First the variable solar wind, its origin, composition and parameters are introduced. Secondly, step-wise modulations of the solar wind are explored (coronal mass ejections, corotational interaction regions, etc.). Finally, I conclude with research which has linked solar wind variability with meteorological and climatological processes.

The Earth, as well as every other body in the solar system, is immersed within the outer atmosphere of the Sun. This extended solar atmosphere is known as the heliosphere. The Sun is constantly emitting a supersonic shower of plasma. This shower of electrons, protons and light nuclei is known as the solar wind (Burns et al., 2007). The Sun continuously loses mass and angular momentum due to the solar wind. Hansteen (2010) expresses balance of mass and momentum at a heliocentric distance of r, along a flow tube of area A, flow velocity v and density ρ as:

$$\frac{d}{dr}(\rho v A) = 0 \tag{1.6}$$

$$\rho v \frac{dv}{dr} = -\frac{dp}{dr} - \rho \frac{GM_s}{r^2} \tag{1.7}$$

where M_s is the mass of the Sun, and G is the universal gravitation constant. The n representing the proton or electron number density, plasma pressure can be written:

$$p = 2nkT \tag{1.8}$$

$$\rho = mn \qquad m \approx m_p/2 \tag{1.9, 1.10}$$

where k is Boltzmann's constant, m_p is the mass of a proton. As the solar wind is ejected from the corona, the charged particles are imprinted with the solar magnetic field. The magnetic field is 'frozen' into the solar wind and does not change as it travels outward through the heliosphere, known as the Interplanetary Magnetic Field (IMF) (Gray et al., 2010). The magnetic equator or the location where the radial component of the magnetic field switches polarity is known as the heliospheric current sheet (HCS) (Roldugin and Tinsley, 1998).

The solar wind in conjunction with the solar rotation produces a spiral throughout interplanetary space (Rusov et al., 2010). Using polar coordinates: the outflow of plasma, of a rotating star, assuming a monopole magnetic field: mass conservation can be written

$$\frac{1}{r^2}\frac{\partial}{\partial r}(\rho v_r r^2) = 0 \tag{1.11}$$

And the Φ component of the momentum equation is provided by either

$$\rho\left(v_r \frac{\partial v_\Phi}{\partial r} + v_\Phi \frac{v_r}{r}\right) = \frac{1}{\mu_0}\left(B_r \frac{\partial B_\Phi}{\partial r} + B_\Phi \frac{B_r}{r}\right) \tag{1.12}$$

$$\rho v_r \frac{1}{r}\frac{d}{dr}(r v_\Phi) = \frac{1}{\mu_0} B_r \frac{1}{r}\frac{d}{dr}(r B_\Phi) \tag{1.13}$$

where μ_0 is the permeability of the vacuum. The conservation of mass requires that $\rho v_r r^2$ is constant, and a divergence-free field implies that $B_r r^2$ is constant. Multiplying the latter momentum equation by r^3 yields

$$r v_\Phi - \frac{B_r r^2}{\rho v_r r^2}\frac{1}{\mu_0} r B_\Phi = const. = L \tag{1.14}$$

Under these assumptions, the ideal magnetohydrodynamic induction equation becomes

$$\frac{1}{r}\frac{d}{dr}\left(r(v_r B_\Phi - v_\Phi q B_r)\right) = 0. \tag{1.15}$$

where q is charge. Using an angular velocity and radius of the Sun: Ω, R_s, and assuming a monopole magnetic field ($B_{\Phi s} = 0$), the induction equation can be used to show:

$$r(v_r B_\Phi - v_\Phi B_r) = const. \approx -R_s(R_s\Omega)B_{rs} = -\Omega r^2 B_r. \tag{1.16}$$

Provided

$$M_A^2 = \frac{v_r^2}{v_A^2} \quad where \quad v_a^2 = \frac{B_r^2}{\mu_0 \rho} \tag{1.17}$$

we can find expressions for v_Φ and B_Φ:

$$v_\Phi = \Omega r \frac{M_A^2\left(\frac{L}{r^2\Omega}\right) - 1}{M_A^2 - 1} \tag{1.18}$$

$$B_\Phi = -\frac{B_r \Omega r}{v_r}\left[\frac{1 - L/(r^2\Omega)}{M_A^2 - 1}\right] M_A^2 \tag{1.19}$$

These expressions indicate that $1 - \frac{L}{r^2\Omega} = 0$ when $M_A^2 - 1 = 0$ and defining $r \equiv r_a$ when $M_A^2 = 1$. This allows the approximations:

$$v_\Phi \approx \frac{\Omega r_a^2}{r} \to 0 \tag{1.20}$$

$$B_\Phi \approx -\frac{B_r \Omega r}{v_r} \tag{1.21}$$

The solar winds and the magnetic field rotate as a solid body until a critical point r_a, at which the radial flow speed is equal to the Alfven speed, the field is dragged with the wind creating a Parker spiral.

The HCS is inclined to the plane of the ecliptic (the plane which the Earth orbits the Sun). The HCS crosses the orbit of the Earth at a period similar to the solar rotation rate (27 days). At these HCS crossing (previously known as magnetic sector boundary crossings) the radial component of the IMF changes polarity.

The Earth is protected from the high energy particles of the solar wind via Earth's magnetosphere. The solar wind plasma are entrained and modulated along Earth's magnetospheric field lines (Tinsley, 2000). These particles precipitate primarily at the polar

regions creating the auroras. There exists a continuous interaction and coupling between the solar wind, Earth's magnetosphere, Earth's ionosphere and Earth's lower atmosphere.

Solar activity changes the composition, velocity and density of the solar wind, influencing Earth's magnetosphere to expand or contract. As such, geomagnetic indices have often been employed as solar activity proxies. Mufti and Shah (2011) found a ~20% correlation between sea surface temperature, the Aa index and the relative sunspot number (Rz). The correlation was improved to ~65% and ~80% using an 11 year (Schwabe cycle) and 22 year (Hale cycle) moving average, respectively. Additionally, Thejll et al. (2003) found a correlation between stratospheric geopotential heights, the North Atlantic Oscillation (NAO) and geomagnetic activity indices (Ap index) for the period 1974-2000. The NAO is characterized by a circulation changes with the Icelandic low and the Azores high (Thejll et al., 2003). Their findings however show no significant correlation for the period 1949-1972. Usoskin et al. (2006) found that periods where the SSN > 70 (very active periods) exist only for 1-3% for the past 7000 years using a geomagnetic activity reconstruction. Their finding indicates that the modern maximum of solar activity is highly rare considering the past 7000 years. It should be noted that the Earth's magnetic field strength varies over timescales of millennia (Usoskin et al., 2006).

The solar wind can be accelerated, intensified or interrupted by a coronal mass ejection (CME). A CME is comprised of the same particles as the solar wind, they are however far more energetic and travel at a significant fraction of the speed of light (Bisi et al., 2010). The CME overtakes the outbound solar wind and creates a frontal shockwave. The CME (if directed at Earth) impacts on the magnetosphere, causing geomagnetic disturbances, precipitation of charged particles, inducing auroras, and alters the dimensions of the magnetosphere and the ionosphere (Tsurutani et al, 2003).

The Carrington event, an extreme magnetic storm witnessed around the world during early September 1859, produced auroras as far equator-ward as Hawaii and Cuba (Tsurutani et al, 2003). The currents induced on Earth's surface were strong enough to set several telegraph stations on fire (Tsurutani et al, 2003). The Carrington event is regarded as the most extreme

magnetic storm within recorded history, however stronger flare energies have been detected since, indicating another or stronger event are not only possible but likely (Tsurutani et al., 2003). Yeh et al. (1994) documented the ionospheric effects of the recent October 1989 X13 flare and CME event that disrupted power grids in Quebec. This study highlighted the compressive effects from the multiple shocks developed by the CME overrunning the solar wind. Additionally, a study by Pudovkin and Babushkina (1992) indicated solar flares and their accompanying CMEs affect the atmospheric circulation. They showed that the flare energy (UV/X-ray) produces an increase of the zonal circulation intensity between 45-65 degrees latitude (using the Blinova index), however after the geomagnetic event, a decrease in the circulation intensity was observed. Estimates for the energy release of the Carrington event flare are of 10^{25} Joules (Schaefer et al., 2000). A study of nine super flares, each occurring on a distant star similar to the Sun, exhibited massive flare energies to range from 10^{26} to 10^{31} Joules (Schaefer et al., 2000).

Crossings of the Heliospheric Current Sheet (HCS) have been shown to influence tropospheric and lower stratospheric vorticity (Wilcox et al., 1974). Using the Vorticity Area Index (VAI) and dates of HCS crossings, a minimum in VAI occurs immediately after, followed by a maximum in VAI 2 to 3 days after the crossing. Shapiro (1976) added that relative vorticity rather than absolute vorticity was impacted by HCS crossings. Two theories exist to explain the effect. The first is with respect to the Global Electric Circuit (GEC). For a review on the GEC and solar activity, see Rycroft et al., (2000), and Tinsley (2000).

Park et al. (1976) discovered that the vertical electric field decreased following HCS crossings at Vostok, Antarctica. The correlation between the troposphere and HCS crossings vanished during the 1970s but reappeared following volcanic injections into the stratosphere. This observation was mirrored by variations in atmospheric vertical current density (Tinsley et al., 1994; 2007). Tinsley and colleagues theorized that atmospheric vertical current density (J_z) is modulated via Relativistic Electron Flux (REF). Changes in J_z are found to influence cloud formation and microphysics (Tinsley et al., 1994, 16805):

A mechanism linking the effect of charge accumulation to changes in ice nucleation, precipitation efficiency, latent heat retention and perturbations in atmospheric dynamics is thus as an explanation for this and other solar wind – atmospheric electricity – weather and climate correlations.

Roldugin and Tinsley (2004) found that atmospheric transparency increases following a HCS crossing at high latitude observation stations. Burns et al. (2007) detected modulation of surface pressure at Vostok, Antarctica; in correlation with vertical electric field with HCS crossings. Kniveton et al., (2008) found significant high latitude cloud cover change (13-15%) with the Vostok vertical electric field using the International Satellite Cloud Climatology Project (ISCCP). It has been hypothesized that the REF is the dominate effect in which HCS crossings influence terrestrial weather (Mironova et al., 2011; Tinsley , 2012). Stratospheric volcanic aerosols compound the modulation of the GEC (Tinsley, 2012). The impact of changes in the GEC also has been proposed to alter lightning discharges (Siingh et al., 2011).

A second theory for the Wilcox effect is proposed by Prikryl et al. (2009b): that instead of Global Electric Circuit (GEC) modulations, HCS crossings produce high latitude gravity waves due to precipitating energetic particles, generating auroras and stimulating the intensification of extratropical cyclones. This theory of solar wind modulations to the climate system can be scaled up to the ~11 year and ~22 year solar cycles. The inclination of the HCS to the plane of the ecliptic increases during solar maximum. The amplitude of the magnetic reversals and subsequent REF injections would increase during a solar sunspot maximum. Particles can be accelerated to very high energies by several processes in the solar system. These energetic particles have drastic implications for planetary atmospheres and magnetic fields. There are however more energetic particles interacting with our solar system.

This section has introduced the extended solar atmosphere in which the Earth is embedded. Not only is the Earth subjected to a constant supersonic flow of energetic particles and variable magnetic fields, but is also subjected to explosions and shock waves of solar

plasma. However the solar wind has another important attribute: the modulation of galactic cosmic ray transport through the solar system.

1.2.3 Galactic Cosmic Rays

The following section introduces the high energy particles impacting the Earth known as galactic cosmic rays. First, their origins, transport, and energies are introduced. Secondly, I discuss their role in the production of cosmogenic nuclides, and the usefulness for solar activity reconstruction. I conclude with exploring the scholarship and controversy connecting galactic cosmic ray intensity with climate change.

Galactic cosmic rays (GCRs) are particles accelerated to high velocities from outside our solar system (Haigh, 2011). These particles have large energies, ranging from MeV to TeV per nucleon. GCRs are comprised primarily of protons. Other light nuclei make up the rest and a small percentage are electrons (Lockwood, 2006; Gray et al., 2011).

Galactic cosmic ray particle motion is described by the Parker transport equation (Jokipii, 2010) :

$$\frac{\partial f}{\partial t} = \frac{\partial}{\partial x_i}\left[\kappa_{ij}\frac{\partial f}{\partial x_j}\right] - v_i\frac{\partial f}{\partial x_i} - V_{di}\frac{\partial f}{\partial x_i} + \frac{1}{3}\frac{\partial v_i}{\partial x_i}\left[\frac{\partial f}{\partial lnp}\right] + Q \qquad (1.22)$$

for the quasi-isotropic distribution function (phase space density) $f(x_i,p,t)$ of cosmic rays at time t at position x_i with momentum p. Here the first term on the right side represents diffusion, the second: advection, the third: guiding-center drift, the forth: energy change, and the fifth term: the source energy (Jokipii, 2010). The diffusion term here represents a random walk of the cosmic ray scattering based on magnetic field irregularities. The advection term represents the magnetic field and cosmic rays advecting outwards with the velocity of the solar wind. The drift term represents the change in guiding center direction with the large-scale spatial variation of the average magnetic field. The energy term represents the loss of energy of cosmic rays through the divergence of the solar wind. The diffusion tensor can be expressed by the combination of its parallel and perpendicular coefficients in terms of the magnetic field B:

$$\kappa_{ij} = \kappa_{\perp}\delta_{ij} + (\kappa_{\parallel} - \kappa_{\perp})\frac{B_i B_j}{B^2} \quad (1.23)$$

Particle streaming flux can be expressed as:

$$S_i = -\kappa_{ij}\frac{\partial f}{\partial x_j} - \frac{U_i}{3}\frac{\partial f}{\partial \ln(p)} \quad (1.24)$$

with *w,* as the particle speed, the associated anisotropy is

$$\delta_i = \frac{3S_i}{wf} \quad (1.25)$$

There exists a strong ~11 year periodicity anti-correlated with solar activity (Lockwood, 2006). Solar magnetic activity during the solar maximum decreases the amount of GCRs that impact the Earth. There also exists a strong ~22 year periodicity consistent with the solar hemispheric dipole switch effecting the direction of GCR trajectories (Haigh, 2011).

Cosmic Rays are a source of ionization at the lowest levels of the atmosphere (Usoskin and Kovaltsov, 2008). As GCRs impact on the upper atmosphere, they create an intense shower of offspring particles which produces ions in the lowest parts of the troposphere (Marsh and Svensmark, 2000). GCR flux is monitored through neutron or muon detectors deep underground.

Cosmic rays also produce rare isotope species in the atmosphere, several of which have useful radioactive half-lives (Delaygue and Bard, 2010). Measuring the amounts of these cosmogenic nuclides in climate proxies (tree rings, ice cores, ocean cores, etc.) provides a means for cosmic ray activity reconstruction, and inversely, solar activity (Versteegh, 2005). Specifically, ^{14}C is produced via neutron activation, and caries a half-life of ~5000 years. ^{10}Be is produced by spallation (a nuclear reaction in which a bombarded nucleus breaks up into many particles) with atmospheric Oxygen or Nitrogen and has a half-life of over a million years (Gray et al., 2010).

Cosmic rays are also subject to Earth's geomagnetic field. Cosmogenic nuclide production are modulated by solar activity at the decade, and centennial scale; but are modulated by changes in the geomagnetic field at the millennial and longer timescales (Beer et al., 2006). As such, long timescale reconstruction of solar activity must take into account the variance in

geomagnetism, otherwise misleading changes in solar activity may be attributed (Solanki et al., 2004; Usoskin et al., 2006). The pathways and timescales in which cosmogenic nuclides are entrained into climate proxies are dynamic and complex. Often ^{14}C and ^{10}Be are compared to ensure accuracy (Delaygue and Bard, 2010).

Stuvier and Braziunas (1993) found a matching 500 year periodicity between ^{14}CO and North Atlantic deep water formation throughout the Holocene. A larger galactic cosmic ray flux during lower solar activity was proposed to increase cloudiness (Svensmark and Friis-Christensen, 1997; Svensmark, 2000; Marsh and Svensmark, 2000). Ionizing radiation creates more cloud condensation nuclei (CCN) in the troposphere. Clouds have obvious global energy balance ramifications. Using ^{14}C and ^{10}Be; Bond et al. (2001) found a matching 1500 year solar periodicity with ocean cores. Solanki and Krivova (2003) argued that GCR flux explains 30% of the atmospheric warming since 1970. Others argue that the cloud data has been misrepresented (Laut 2003). While others have found no correlation with cloudiness, or other atmosphere parameters from the United States radiosonde network with cosmic ray flux (Balling and Cerveny, 2003), Pustilnik and Din (2005) found a correlation between cloudiness and wheat production from medieval England to modern United States. Scafetta and West (2006) have determined a correlation between GCR flux and 500 years of global surface temperatures.

From 1961 to 2005, Dengel et al., (2009) found an increase in the growth of tree rings with increasing GCR flux. They argued that an increase in GCRS fosters more CCN, thereby resulting in more diffuse radiation and ultimately resulting in more photosynthesis. Ludecke (2011) found that the rise in Northern Hemisphere temperatures over the last century is not attributed to anthropogenic global warming.

An alternate hypothesis which correlates GCRs with climate, are their effects on the Global Electric Circuit (GEC) parameters (Rycroft et al., 2000; Tinsley, 2012). Tinsley (2000) argued that changes in GEC parameters: vertical current density, fair weather current, atmospheric columnar resistance, etc.; actively influences cloud microphysics, electroscavenging, and cloud opacity. Usoskin and Kovalstov (2008) further linked the GCR research with less

energetic particle events triggered by HCS crossings. They argued that all energetic particles influence the GEC causing detectable changes in atmospheric circulation, cyclogensis and vorticity.

This section has elaborated on the origin, transport and atmospheric effects of high energy particles, known as cosmic rays. It should be noted that most solar activity proxies are derived from cosmogenic nuclides produced by cosmic rays. Cosmic rays were one of the first solar activity mechanisms proposed as a quantitative link between solar variability and climate change.

1.2.4 Gravity

In this section, I review a much commonly accepted avenue of astronomical forcing, gravity. First I will examine the two most prominent sources of gravitational influence: the Moon and the Sun. Following this, I will expand on gravitational effects which have been detected in meteorological patterns and climate periodicities. Continuing, I elaborate on the long-term gravitational influences upon Earth's orbit, widely regarded as the primary agents which cause Earth's major glaciation events. I conclude with research examining solar inertial motion, and its purported link with solar activity.

According to the nebular hypothesis, the solar system contracted under mutual gravitational attraction conserving angular momentum resulting in a proto-planetary disk. The Sun, retained 99.9% of the solar systems mass, however the Jovian planets possessed the majority of the angular momentum. The solar system must be considered a coupled system due to the conservation of angular momentum and mutual gravitation.

The force exerted on the Earth (m_2) by the Sun (m_1) at a distance r is described by Newton's Universal Law of Gravitation (Beer, 2010):

$$F_{12} = -G\frac{m_1 m_2}{r^2}e_r \tag{1.26}$$

with G as the Universal Gravitation constant, and e_r is a unit vector pointing away from the Sun. Applying Newton's second and third laws:

$$F = m\ddot{r} \tag{1.27}$$

$$F_{12} = -F_{21} \tag{1.28}$$

the equations of motion of the two bodies can be written:

$$m_2\ddot{r}_2(t) = -G\frac{m_1 m_2}{r^2}e_{r2} = -G\frac{m_1 m_2}{r^3}r \tag{1.29}$$

$$m_1\ddot{r}_1(t) = -G\frac{m_1 m_2}{r^2}e_{r1} = -G\frac{m_1 m_2}{r^3}r \tag{1.30}$$

which can be combined to read:

$$\ddot{r}_2(t) - \ddot{r}_1(t) \equiv \ddot{r}(t) = -\mu\frac{r}{r^3} \tag{1.31}$$

$$where: \ \mu \equiv G(m_1 + m_2)$$

The angular momentum of the Earth (*l*) can be expressed:

$$L = m_2 r \times \dot{r} \Rightarrow \frac{L}{m_2} \equiv l = r \times \dot{r} \tag{1.32}$$

and the derivative of *l* can be used to prove the trajectory exists in a plane:

$$\dot{l} = \dot{r} \times \dot{r} + r \times \ddot{r} = r \times \ddot{r} = r \times \left(-\mu\frac{r}{r^3}\right) = 0 \Rightarrow l = const. \tag{1.33}$$

To derive the geometric description of the orbit, we employ a vector identity

$$l \times \ddot{r} = (r \times \dot{r}) \times \ddot{r} = (r \cdot \ddot{r})\dot{r} - (r \cdot \dot{r})\ddot{r} \tag{1.34}$$

$$= -\frac{\mu}{r^3}(r \cdot r)\dot{r} + \left(\frac{\mu}{r^3}r\right)r\dot{r} = \frac{d}{dt}\left(-\mu\frac{r}{r}\right) \tag{1.35}$$

$$l \times \ddot{r} = \frac{d}{dt}(l \times \dot{r}) \tag{1.36}$$

which can be combined to form:

$$l \times \dot{r} + \mu\left(\frac{r}{r}\right) = const \equiv -\mu e \tag{1.37}$$

Continuing:

$$\dot{r} \cdot \ddot{r} = -\dot{r} \cdot \left(\mu\frac{r}{r^3}\right) = \frac{d}{dt}\left(\mu\frac{1}{r}\right) \tag{1.38}$$

$$\frac{1}{2}\frac{d}{dt}(\dot{r}\cdot\dot{r}) = \frac{1}{2}\frac{d}{dt}(\dot{r}^2) \tag{1.39}$$

$$\frac{1}{2}\dot{r}^2 - \mu\frac{1}{r} = const. \equiv h \tag{1.40}$$

where h is a constant of integration, representing the conservation of energy (kinetic and potential). To derive a relation between *e* and *h*:

$$(\mu e)\cdot(\mu e) = \left(l \times \dot{r} + \mu\frac{r}{r}\right)\cdot\left(l \times \dot{r} + \mu\frac{r}{r}\right) \Rightarrow \tag{1.41}$$

which reduces to:

$$\mu^2(e^2 - 1) = 2l^2h \tag{1.42}$$

allowing the calculation of the orbit of the Earth:

$$r\cdot e = re\cos\theta \tag{1.43}$$

$$r\cdot e = r\cdot\left(-\frac{1}{\mu}l \times \dot{r} - \frac{r}{r}\right) = \frac{l^2}{\mu} - r \tag{1.44}$$

$$r(\theta) = \frac{l^2/\mu}{1 + ecos\theta} \tag{1.45}$$

yielding *e*, the eccentricity of the orbit, and the numerator representing the parameter of the curve.

In case of the Earth-Moon system, each body experiences the gravitational acceleration of the other, and the two bodies orbit about their mutual center of mass. The tidal acceleration of the Moon creates a bulge in the fluid oceans (Lethbridge, 1970). The gravitational acceleration can be expressed as:

$$a_g = -G\frac{M}{R^2(1 \pm r/R)^2} \tag{1.46}$$

However the tidal acceleration a_t, defined as the difference between the gravitational and effective accelerations:

$$a_t \approx \pm G\frac{2M}{R^2}\frac{r}{R} \tag{1.47}$$

The Earth rotates underneath this tidal bulge resulting in daily high and low tides. In combination with the Sun's tidal acceleration, the Moon's monthly synodic period creates spring and neap tides.

Lunar phase has been correlated with several climate parameters. Daily global temperatures (Balling and Cerveny, 1995), global tropospheric temperature maxima (Balling and Cerveny, 1995; Dyre et al., 1995), diurnal temperature range (Cerveny and Balling, 1999), and polar temperatures (Shaffer et al., 1997) have been found to vary with lunar phase. Precipitation (Bradley and Woodbury, 1962; Adderley and Bowen, 1962; Brier and Bradley, 1964; Hanson et al., 1987), stream flow (Cerveny et al., 2010) and thunderstorm frequency for the U.S. (Lethbridge, 1970) exhibit significant correlation with lunar phase.

The Moon is inclined to the plane of the ecliptic (the plane which the Earth orbits the Sun) by about 5 degrees (Keeling and Whorf, 1997). This results in lunar maximum declination above or below the Earth's equator can vary from of 18 to 28 degrees. Ultimately, this alters the distribution of tidal acceleration in Earth's higher latitudes (Krahenbuhl et al., 2011). The points where the orbit of the Moon intersects the plane of the ecliptic, the nodes, precess and complete their nutation over a period of 18.6 years. The lunar nutation periodicity has been detected in atmospheric pressure records (Currie, 1996), the El Nino Southern Oscillation (Cerveny and Shaffer, 2001), and global temperatures (Keeling and Whorf, 1997; Treloar, 2002).

The Moon's elliptic orbit has perigees and apogees, close and far approached in its orbit. Over long time series these perigees occur in proximity to Earth's perihelion, or close approach to the Sun. At these times, the gravitational tidal acceleration would be maximized on the Earth. Keeling and Whorf (2000) argued that such tides occur with an 1800 year periodicity and are responsible for significant climate shifts. Longer period hypertides may exist when lunar tides are compounded with Earth's orbital parameter changes (Shaffer and Cerveny, 1998).

The gravitational attraction of the other planets causes gradual changes in Earth's orbital parameters. Three orbital parameter influential on Earth's climate are the eccentricity, the obliquity and precession (Haigh, 2011; Berger, 1992; Berger and Loutre, 1989). The eccentricity

is a measure of how elliptical Earth's orbit is, determining the change in distance between perihelion and aphelion. This is the only parameter which affects the Earth's distance from the Sun, and therefore the amount of TSI incident on the Earth. Eccentricity has periodicities on the order of 100,000 and 400,000 years, and is argued to be the primary cause of the major glaciations for the past million years (Imbrie et al., 1993; Elkibbi and Rial, 2001; Muller and MacDonald, 1997).

The obliquity of the Earth measures the magnitude in the Earth's axial tilt. Currently, Earth's axial tilt is 23.5 degrees. Changes in obliquity occur at a period of 41,000 years. The obliquity impacts the seasonality, the amount of annual radiation received in the high latitudes. A smaller obliquity results in less annual radiation change at the poles promoting an expansion of ice sheets (Elkibbi and Rial, 2001).

Precession is the wobbling in the direction of Earth's axis and has periodicities of the order 19,000 to 24,000 years. It results in a slow rotation of the axial tilt with respect to the ecliptic. In 12,000 years, the North Star will be the star Vega. This ultimately rotates when the solstices and equinoxes occur in relation to the perihelion and aphelion. Currently, the Northern Hemisphere summer solstice occurs in June, near aphelion. In 12,000 years, the Northern Hemisphere summer will occur in December, at perihelion.

The Sun is not the center of the solar system. The Sun itself orbits the center of mass of the solar system, called the barycenter. Due to the varying positions of the planets, the Sun traces out a complex looping motion around the barycenter. Jupiter and Saturn have a 3:1 orbital resonance, and this results in the motion of the Sun to resemble a 3 leafed orbit, denoted as a trefoil (Charvatova, 1997). Solar inertial motion has been theorized to explain the multi-decadal modulation of the Sun spot cycle (Jose, 1965; Landscheidt, 1999).

The four gas giants planets are responsible for the evolving solar orbit. Jupiter's year is ~12 Earth years, whereas the Neptunian year takes 165 Earth years. Due to these long term periods in the gas giant planet positions, the solar inertial motion varies from the decadal to tens of millennia time scales.

Solar convective dynamo modeling has been able to duplicate Sunspot formation and emergence, but not the longer periodicities exhibited by the solar cycle. Variations in solar inertial motion modulate the angular momentum of the Sun's orbit and would impact the Sun's differential rotation. Eddy et al. (1977) linked anomalous solar rotation in the 17th century to the Maunder Sun spot minimum, confirmed by Li et al. (2011). Javaraiah (2005) found key differences in the sunspot cycle during prograde and retrograde orbital loops. Luminosity variations have been linked to variations in gravitational energy and Sun-Jupiter spin orbit coupling (Fazel et al., 2008; Wilson et al., 2008). Air temperature, and several other climate parameters have been found to vary with solar inertial motion throughout the Holocene (Charvatova, 1997; Scafetta, 2012). Palus et al. (2007) found a significant chaotic synchronization between several atmospheric oscillations (ENSO, PDO, etc.) with solar inertial motion.

In an attempt to prove this theory, Perryman and Schulze-Hartung (2010) examined the barycentric motion of other starts with detected exoplanets. They proposed several candidate stars to observe in which the stellar inertial motion is similar to our solar system, but has yet to be completed.

This section has examined the various avenues to which gravitational influences act as exogenic climate forcings. Solar-lunar tidal effects have been documented throughout human history. However, much of the newer research, the linking of major ice ages to orbital variations, and the evolving solar orbital motion linked to solar activity, have only been presented in the last century.

This concludes the literature review. What follows are a presentation of the gaps in the literature and discusses the research questions this dissertation intends to answer.

1.3 FRAMEWORK FOR INVESTIGATION

1.3.1 Research Questions

While much of the recent attention concerning climate change has focused on anthropogenic forcings, there is fierce contention on the role of exogenic forcings (Gray et al.,

2010). Although the underlying concepts are well understood, the magnitude, scale and frequency of various exogenic forcings are under debate. Regarding the exogenic/climate topics (e.g., solar luminal, solar atmospheric, cosmic ray and gravitational forcings), additional work is needed to further quantify and explain their respective degree of influence. This dissertation intends to continue the research of these following topics by examining the following specific research questions.

A. Lunar Declination and Circulation

Our ever evolving gravitational environment poses predictable orientations but unpredictable effects. The effect of the lunar phase is well documented in climate records. As is the 18.6 year lunar nutation periodicity. Nevertheless, the influence on the lunar declination on global circulation at a bi-weekly basis remains unresearched. My specific research question is what are the biweekly declination effects of lunar gravitation upon the middle and upper tropospheric geopotential heights?

B. The Solar Wind and Severe Weather Reports

Injections of energetic particles are triggered by changes in the solar wind. Atmospheric vorticity is influenced by the solar wind's magnetic polarity. Yet whether this is caused by aurora gravity waves or modulation of atmospheric electricity remains unclear. Solar wind magnetic reversals have been linked with strengthening extratropical cyclones although most of these events are from European historical records. Whether this affect is observable in other parts of the world remains unanswered. My specific research question is how do United States severe weather reports, such as tornadoes and hail and damaging wind accounts, correlate with heliospheric current sheet crossings at Earth's orbit?

C. Galactic Cosmic Rays and Cloud Cover

Although, cosmic rays have been thought to produce cloud seeding by providing ionization in the lower troposphere, there have been proposals that argue that cosmic rays alter cloud microphysics by way of atmospheric electricity. There are still unresolved issues as to whether the 22 year magnetic reversal pattern in cosmic rays is observed in cloud cover.

Additionally, the exact altitude and latitude of cloud cover change are unknown. Whether there exists geographic specificity in cloud cover modulation is undetermined. My specific research question is how does cloud cover reconstructions spatially and temporally vary with respect to galactic cosmic rays?

1.3.2 Dissertation Organization

The following three chapters comprise my attempt to answer these research questions. Chapter two discusses the connections between lunar declination tropospheric geopotential heights. A version of this chapter has published in the Journal of Geophysical Research—Atmospheres, on December 15th 2011. Coauthors for this article include: Mathew B. Pace, Randall S. Cerveny, and Robert C. Balling, Jr.

Chapter three records the correlations between heliospheric current sheet crossings and United States severe weather reports. A version of this chapter is currently under review in the Journal of Atmospheric and Solar Terrestrial Physics. Randall S. Cerveny is a coauthor for this article.

Chapter four depicts the investigation between galactic cosmic rays and cloud cover reconstructions. A version of this chapter is currently under review in the Journal of Geophysical Research—Atmospheres. This is a solo authored article.

Each of these chapters addresses the specific hypotheses, data, methodology, results, discussions and conclusions sections with regard to the individual research questions given in this chapter.

Finally, chapter five presents a summary of the dissertation with relation to the underlying framework discussed in this chapter, prospects for future research, and the fundamental significance of this dissertation.

CHAPTER 2

LUNAR DECLINATION AND CIRCULATION

This chapter records our investigation of the connections between lunar declination tropospheric geopotential heights. A version of this chapter has been published in the Journal of Geophysical Research—Atmospheres, on December 15th 2011, titled *Monthly lunar declination extremes' influence on tropospheric circulation patterns*. Coauthors for this article include: Mathew B. Pace, Randall S. Cerveny, and Robert C. Balling, Jr.

Abstract: Short-term tidal variations occurring every 27.3 days from southern (negative) to northern (positive) maximum lunar declinations (MLDs), and back to southern declination of the Moon have been overlooked in weather studies. These short-term MLD variations' significance is that when lunar declination is greatest, tidal forces operating on the high latitudes of both hemispheres are maximized. We find that such tidal forces deform the high latitude Rossby longwaves. Using the NCEP/NCAR reanalysis data set, we identify that the 27.3 day MLD cycle's influence on circulation is greatest in the upper troposphere of both hemispheres' high latitudes. The effect is distinctly regional with high impact over central North America and the British Isles. Through this lunar variation, midlatitude weather forecasting for two-week forecast periods may be significantly improved.

2.1 INTRODUCTION

A distinct cyclic variation in a multitude of global surface pressure observations has been identified in relation to variations in maximum lunar declination (MLD) with 18.61 year duration (O'Brien and Currie, 1992). A peak in United States thunderstorm frequency has been correlated with high northerly lunar declinations (Lethbridge, 1970) and cloudiness has been linked to declinational variability (Pertsev and Dalin, 2010). Additionally, spectral analysis of both observed temperature records for the United States and tree ring periodicities demonstrate significant 18.61

year variability consistent with lunar declination (Currie, 1996). The commonality between these diverse studies may be the overlying tropospheric mid- and high-latitudinal circulation pattern as defined by Rossby longwaves. If an 18.61-year cyclicity occurs in thunderstorms, cloudiness, surface pressure, precipitation and temperature then perhaps lunar declination's short-term (27.3 day) influence on the overlying circulation pattern may be the intermediate causal influence.

The long-term 18.61 year MLD cycle has been the most widely studied aspect of long-term lunar tidal stress on climate, e.g., the fifty-two articles cited by Currie (1996). Since the lunar orbit forms a 5° angle with the ecliptic and the ecliptic forms an angle of 23.4° with the celestial equator, short-term MLD occurs twice over the course of a tidal month of 27.3 days and varies between 18°21′ and 28°40′ North or South (Meeus, 1991). While the overall variation in absolute maximum declination repeats with the fundamental revolution period of the lunar nodes (18.61 years), the atmospheric effects of the short-term cyclicity of 27.3 days in lunar declination has, until recently, been neglected in climate studies. These short-term MLD variations' significance is that when the declination is greatest for a given hemisphere, the tidal forces operating on the high latitudes of that hemisphere are maximized (Burroughs, 2003).

We hypothesize that such short-term declinational tidal forces may act to deform the high latitude Rossby longwave circulation features specifically associated with the short-term 27.3 day cycle between southern (negative) and northern (positive) declinations. Recent research by Li and colleagues (Li, 2005; Li and Zong, 2007; Li et al., 2011) preliminarily supports the validity of this hypothesis but their research focused on the effects of lunar declination on length-of-day. They examined a limited number of Rossby wave height field deformations under MLD forcing, particularly focused on near-equatorial declination positions (when as they correctly stated overall planetary, but not hemispheric, tidal forcing is maximized), and consequently did not explicitly examine absolute differences between declinational extremes. Therefore, in this study, we use the global NCEP/NCAR meteorological reanalysis data for the period 1948–2010 to assess the

impact of the occurrence of short-term (27.3 day) variability from lunar declinations on the tropospheric circulation.

2.2 DATA

The NCEP/NCAR Reanalysis 1 data set is an archive of past weather patterns using observational data together with forecasting algorithms for the period 1948 to present (Kalnay et al., 1996). From that reconstruction, we extracted and analyzed the daily tropospheric 850 hPa, 700 hPa, 500 hPa, 300 hPa, 250 hPa and 200 hPa (4Xdaily) eight fields for each day of record from 1/1948 to 12/2010. The NCEP/NCAR Geopotential height data are considered the most reliable product of the reanalysis (Kalnay et al., 1996).

Lunar orbital variations were computed using the Python module, PyEphem 3.7.4.1 (http://pypi.pthon.org/pypi/pyephem/, accessed 18 May 2011), which employs algorithms to compute high-precision astronomy computations. Computed lunar declination values were cross-checked and validated against the NASA Jet Propulsion Laboratory online Horizon ephemeris (Horizons Ephemeris, http://ssd.jpl.nasa.gov/?horizons, accessed 18 May 2011).

In order to assess the atmospheric height variations as result of the most extreme tidal forcings for each month, we restricted analysis to calculation of the global height fields associated with individual monthly declinational extremes (positive and negative). For example, we extracted constant pressure surface height fields associated with the monthly northern maximum declination of +27° 04′ on 9/1/2009 and corresponding monthly southern maximum declination of −27° 05′ on 22/1/2009 and then computed the difference in the constant pressure surface heights between those two events. We repeated this for every tidal month from 1/1948 to 12/2010. In a similar fashion, we also computed the height field differences between the monthly maximum southern declination and the subsequent monthly maximum northern declination for each of the 842 tidal months.

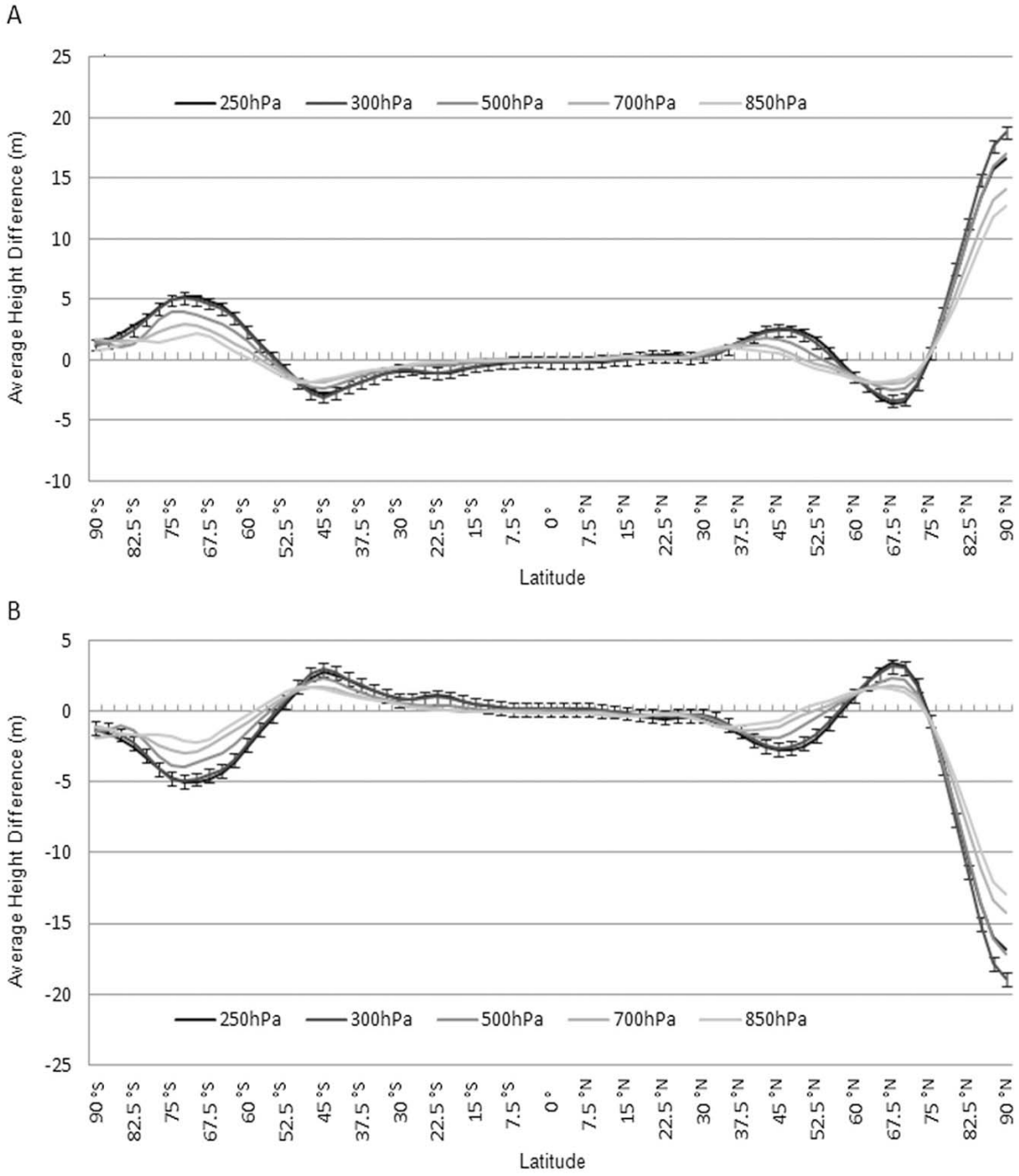

Figure 2.1. (a) Averaged height differences (m) of the 250 hPa, 300 hPa, 500 hPa, 700 hPa and 850 hPa pressure surfaces for the period 1948–2010 differences with respect to latitude (90°N to 90°S) between a given monthly negative lunar declination and the next positive lunar declination using the NCEP/NCAR reanalysis data set. (b) Same as Figure 2.1a but for averaged height differences between monthly positive lunar declination and the next negative lunar declination.

We then averaged the composites of the monthly pressure surface height anomalies (height fields associated with a monthly positive declination occurrence subtracted from the height fields associated with the same month's negative declination occurrence) across latitudinal bands. The plot of those composite anomalies indicate that the extreme lunar declination influence on circulation is most apparent in the higher latitudes of both hemispheres (Figure 2.1) with lessening effect as one approaches the equator. Inverse results occur with averaged composites of the monthly negative declination extreme height field subtracted from the height field associated with the following positive declination extreme. Standard error of the mean (over the time series) analyses for all grid points indicates low variability in the mean of the anomaly fields (average standard error of the mean over 10,512 data points ranges from 0.482 m to 10.3 m).

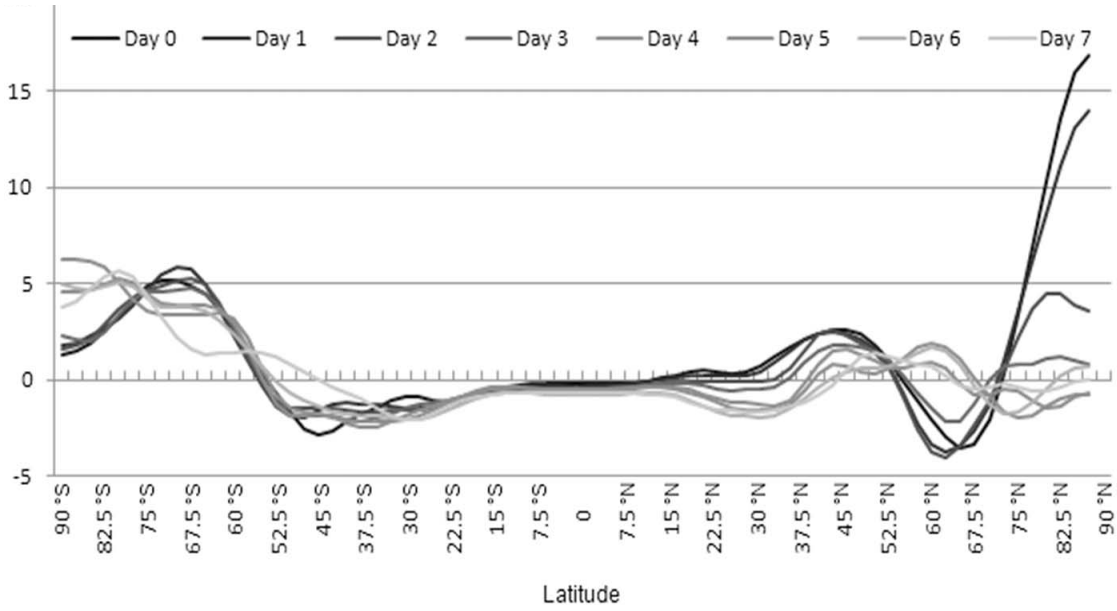

Figure 2.2. Lagged (1–7 days) averaged height differences (m) of the 300 hPa pressure surface for the period 1948–2010 differences with respect to latitude (90°N to 90°S) between a given monthly negative lunar declination and the next positive lunar declination using the NCEP/NCAR reanalysis data set.

2.3. ANALYSES

In general, the lunar cycle influence on the two hemispheres are inverse. With the notable exception of the polar latitudes, areas in the northern hemisphere displaying height

increases of a given pressure surface between monthly extremes of northern to southern lunar declination are matched with corresponding falls of heights of that given pressure surface. However, both hemispheres display an internal inverse response to declination tidal forcing between midlatitudes and the transition between the polar and Ferrel circulation cells (~60–70°). When midlatitudes show an increase in the pressure surfaces' heights between monthly extremes of declination, the 60°-70° latitude transition zone between the global circulations demonstrates reductions in heights and vice versa.

The strongest dissimilarity between the two hemispheres exists in the pressure surface height variations for the polar regions (>70°). While the polar regions of the northern hemisphere display strong increases (decreases) in heights when transitioning between negative and positive (positive–negative) declinations, the southern hemisphere's polar region shows a more muted response in comparison to the large pressure surface height changes of the northern hemisphere. The difference may be the result of the inherently more zonal circulation of the southern hemisphere and the positioning of the Antarctic continent over the South Pole.

The short-term MLD effect weakens with increasing proximity to the surface (Figure 2.1). For the troposphere, the near-tropopause pressure levels of 200, 250 and 300 hPa consistently demonstrate the stronger deviations under MLD extremes than the 850, 700 and 500 hPa. We therefore concentrate our discussion to specifically the 300 hPa surface (a pressure surface consistently in the troposphere for most times of the year in the midlatitudes). Additionally, the height anomalies are more pronounced between the days for which declinational differences for northern and southern hemispheres are maximized (Figure 2.2) with decreasing height anomalies as with lagged response from maximum short-term declinational differences.

Longitudinally averaged height differences between extremes of southern and northern declination indicate that the Atlantic and Pacific Oceans' response (Figure 2.3) are more pronounced than other regions. The 300 hPa pressure surface heights over the Atlantic and Pacific Oceans are markedly higher (lower) when transitioning from negative to positive (positive to negative) declinations over the course of a tidal month (Figure 2.3).

While the latitudinally and longitudinally averaged effects are clearly defined, the NCEP/NCAR gridded reanalysis permits identification of specific geographical locations influenced by MLD variations (Figure 2.4). While the lunar tidal influence is global in nature, it enhances the circulation patterns of specific regions depending on the long-term circulation features present and may particularly be important in individual cases. The anomaly field maps were produced by universal kriging, a stochastic interpolation method that uses weighted averages and probability models to produce an interpolated surface (Cressie, 1991; Isaaks and Srivastava,1989) and each accounts for over 98 percent of the spatial variance in the anomaly data. Geographically we identify a set of specific Rossby longwave anomalies.

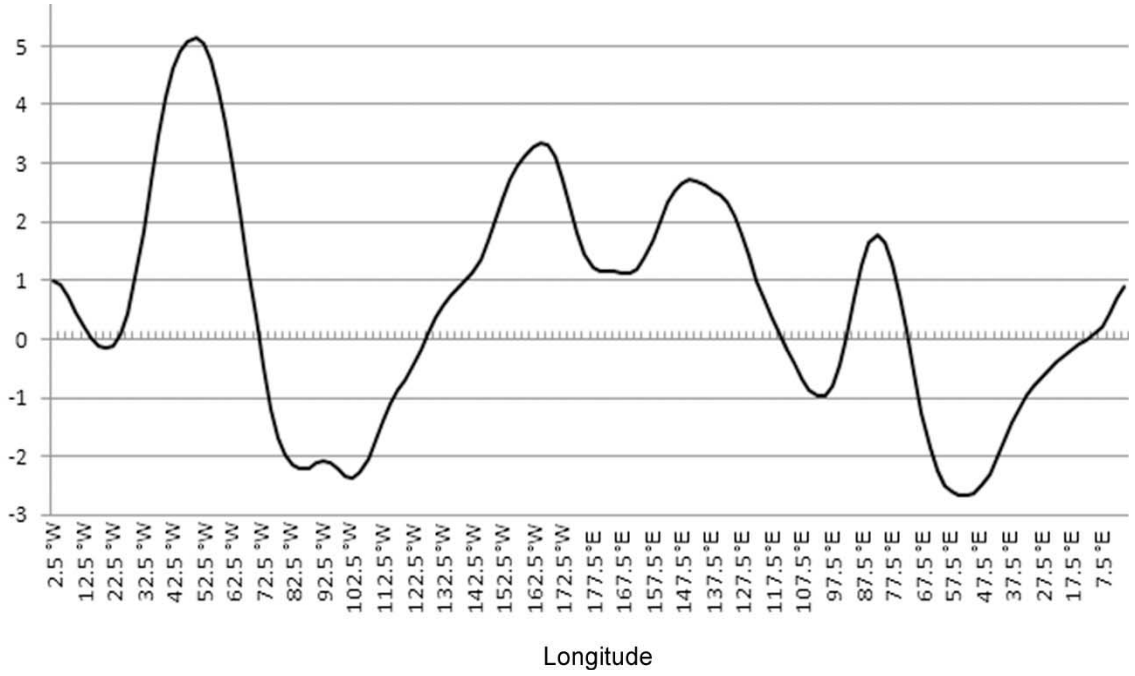

Figure 2.3. Averaged height differences (m) of the 300 hPa pressure surface for the period 1948–2010 differences with respect to longitude between a given monthly southern (negative) lunar declination and the next northern (positive) lunar declination using the NCEP/NCAR reanalysis data set.

Explicitly for negative to positive declination transition, there is a tendency for decreased pressure surface heights (troughing) to occur in the Bering Strait region, offshore of eastern North America, over the British Isles and Western Europe and the extreme northeast portion of Asia. Conversely, for positive to negative declination transition, there is a marked tendency for increased pressure

surface heights (ridging) to occur the Northwest United States to Canada's Hudson Bay, over the central Atlantic, and over Russia's Kamchatka Peninsula.

Of particular interest is the dichotomy of response in the North Atlantic Ocean transitioning between monthly positive and negative extremes of lunar declination. The region from Iceland to the British Isles (associated with the Icelandic Low) displays the opposite response to lunar forcing compared to the region of the central Atlantic high pressure. Essentially, a strengthening Icelandic Low is linked to a weakening of Atlantic high pressure and vice versa transitioning between negative and positive MLD forcing respectively. Such variability is consistent with known variations in the North Atlantic Oscillation (NAO) (e.g., Barnston and Livezey, 1987) and suggests that longterm NAO variability may be influenced by short-term MLD to a greater degree than previously thought.

In the southern hemisphere, the Rossby longwave pattern is more zonal than its northern hemispheric counterpart. Nevertheless, for negative to positive MLD forcing, there is a tendency for increased troughing to occur off the western coast of South America, in the central South Atlantic, near New Zealand and offshore of southwest Australia and in the Antarctic Ocean southwest of South Africa (Figure 2.4). Conversely, there is a tendency for increased ridging to occur from the Antarctic Peninsula to the Falkland Islands, and in eastern Wilkes Land in Antarctica.

A strong height anomaly exists between monthly lunar declination extremes off the west coast of South America. Because the upper air circulation exerts an influence on the degree of cold water upwelling along the west coast (Bjerknes, 1969), the relationship between declination and circulation for this specific region may lead to lunar influenced variations in El Niño/Southern Oscillation (ENSO). Past research (Cerveny and Shaffer, 2001) indicates a statistical relationship between long-term MLD and ENSO but did not geographically define the area most influenced by the MLD tidal effects.

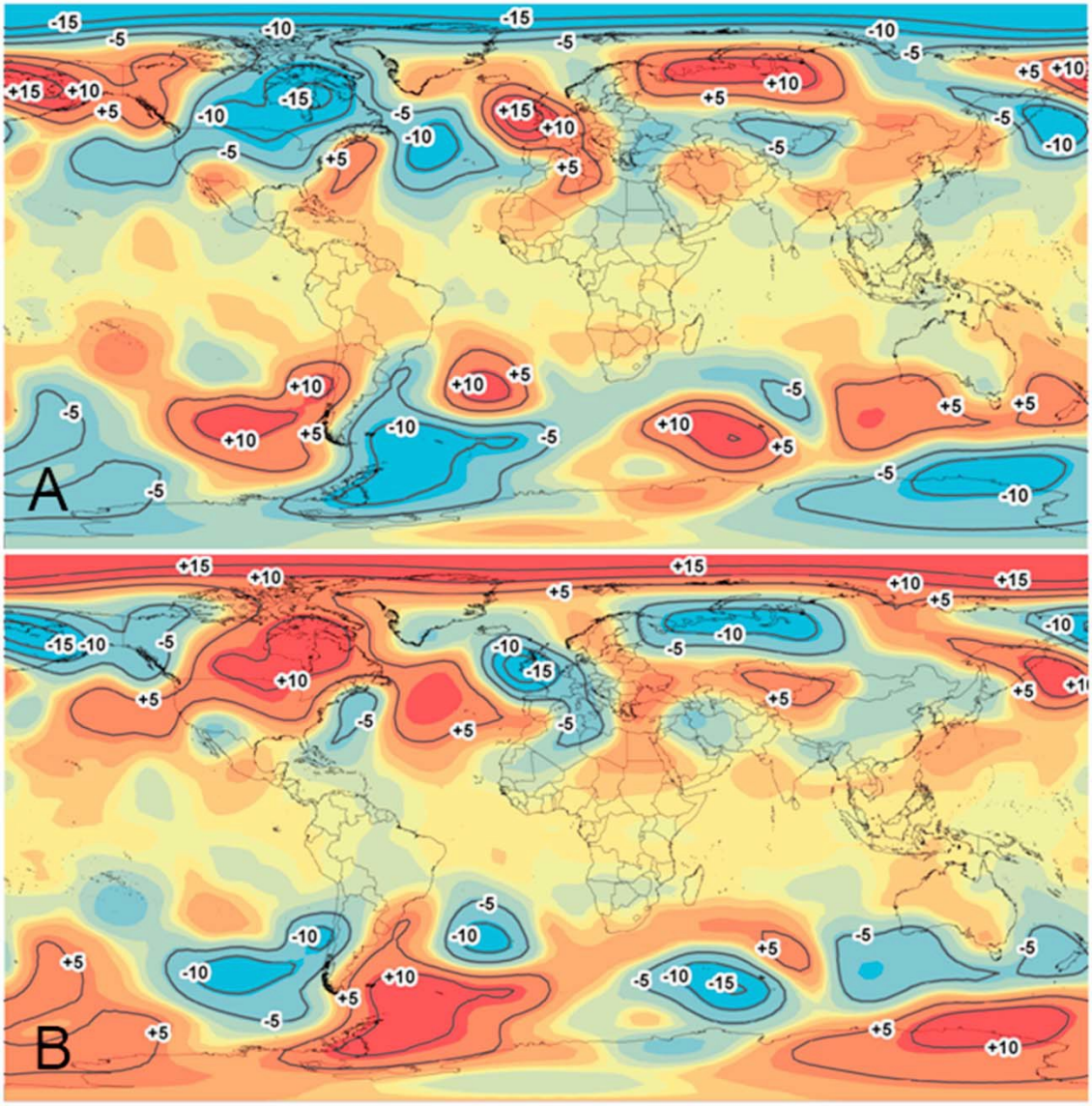

Figure 2.4. (a) Kriged representation of height variations (m) from the long-term mean for the 300 hPa pressure surface for negative–positive monthly extremes of lunar declination for the period 1948–2010 using the NCEP/NCAR reanalysis data set. (b) Same as Figure 2.4a for positive–negative monthly extremes of lunar declination.

Our research (Figure 2.4) suggests that a key controlling area for MLD effects is associated with the Humboldt Current off South American's west coast and that MLD-induced variations in wind flow over this region may be influential on ENSO.

2.4 CONCLUSIONS

The variations in pressure level heights are hypothesized to be induced by an inclined lunar orbit to the celestial equator (Li, 2005; Li and Zong, 2007; Li et al., 2011). As Li and colleagues mention, this is contrary to conclusions of previous researchers (Lindzen, 2005; Forbes et al., 2003; Hagan and Forbes, 2003; Hagan et al., 2003; Chapman and Lindzen, 1970) who have speculated that atmospheric tides are primarily excited by the solar heating of the atmosphere, whereas ocean tides are primarily induced by the Moon's gravitation pull. The complete variation in lunar declination occurs over a 27.3 day interval (Burroughs, 2003). That variation produces a switch of the hemisphere which is under the lunar declinational extreme every 13.66 days.

The upper tropospheric Rossby longwave pattern exerts a strong influence on the midlatitude synoptic storm track and on thermal/surface pressure patterns. Because of the degree of spatial consistency in the effects of MLD on the Rossby longwave pattern and given the 13.66 day variation between declination extremes, weather forecasting for a critical heretofore limited forecast period—around two weeks—may be significantly improved, especially for specific mid- and high-latitude locations.

Forecasting algorithms could conceivably utilize the concept that a slightly greater potential for storm genesis and intensification exists for specific regions during the portion of the tidal month where declinational-influenced, upper-level troughing (height falls) is occurring and decreased storm potential in those regions where declinational-influenced, upper-level ridging (height increases) is occurring. This would be particularly important in middle-range weather forecasting where these lunar declination effects could be incorporated into numerical weather forecasting models. However, distinct regional variability in response to MLD (Figure 2.4) adds the need for geographic specificity when forecasting for any given situation. The short-term nature of the forcing and the geographic variability suggest the possibility of marked improvement in a heretofore limited forecast period (~2 weeks).

CHAPTER 3

THE SOLAR WIND AND SEVERE WEATHER

This chapter records our investigation of heliospheric current sheet crossings and United States severe weather reports. A version of this chapter is currently under review in the Journal of Atmospheric and Solar-Terrestrial Physics. The article is titled *Influence of Heliospheric Current Sheet Crossings on United States Tornado Occurrence*. Randy S. Cerveny is a coauthor for this article.

Abstract: Previous studies have linked solar wind variations to terrestrial atmospheric changes. Specifically, polarity shifts resulting from the Heliospheric Current Sheet (HCS) have been shown to influence tropospheric and lower stratospheric vorticity. In this study, we establish that there is a statistical linkage between the occurrence of a HCS crossing and United States severe weather occurrence such that transition from a negative magnetic sector to a positive sector, yields more tornadoes with a significant peak occurring near the crossing event. Violent tornadoes (EF3+) are almost 10% more probable to occur near a N2P crossing, and 4% less probable to occur immediately following the HCS crossing. The deviation of hail reports, for N2P crossings, shows a higher probability before the crossing, and a lower probability following the crossing similar to the tornado anomalies. Interesting, this is not mirrored in the P2N crossing for hail reports. The distribution for damaging wind reports show minima five days prior to and following the HCS crossing date. Additionally, there are probabilistic maxima around seven/eight days prior to and following the HCS date, mirrored identically for P2N and N2P crossing dates. Although our initial study is unlikely to extend individual tornado-warning times, this type of research may be useful in improving weekly or seasonal tornado forecasting.

3.1 INTRODUCTION

Crossings of the Heliospheric Current Sheet (HCS) have been shown to influence tropospheric and lower stratospheric vorticity (Wilcox et al., 1974). Using the Vorticity Area Index

(VAI) and dates of HCS crossings, Wilcox and colleagues detected a minimum in VAI occurs immediately after, followed by a maximum in VAI two to three days after the crossing. Shapiro (1976) although unimpressed with the statistical relationship, correctly suggested that relative vorticity, rather than absolute vorticity, was predominately impacted by HCS crossings. Others argued that the correlation is limited to low pressure systems during the Northern Hemisphere winter (Bhatnagar and Jakobsson 1978).

Several theories have been posited to explain the Wilcox effect. The first incorporates the concept of the Global Electric Circuit (GEC) (Rycroft et al., 2000, Tinsley 2000). Park (1976) discovered that the vertical electric field decreased following HCS crossings at Vostok, Antarctica. This observation was mirrored by variations in atmospheric vertical current density (Tinsley et al., 1994; 2007). Tinsley and colleagues theorized that atmospheric vertical current density (J_z) is modulated via energetic particle precipitaiton. Changes in J_z are found to influence cloud formation microphysics and latent heat exchange efficiency (Tinsley et al., 1994; Tinsley 1996). Roldugin and Tinsley (2004) identified that atmospheric transparency increases following a HCS crossing at high latitude observation stations while Kniveton et al. (2008) found significant high latitude cloud cover change occurs (13-15%) with the Vostok vertical electric field using the International Satellite Cloud Climatology Project (ISCCP). It has been hypothesized that the precipitation of energetic particles is the dominant effect by which HCS crossings influence terrestrial weather (Mironova et al., 2012; Tinsley, 2012). Others find significant correlation between North Atlantic cyclone development and energetic particle precipitation (Veretenenko and Thejll 2004). Additionally, it recently has been suggested that stratospheric volcanic aerosols may compound the modulation of the GEC (Tinsley, 2012).

A second theory for the Wilcox effect has been proposed by Prikryl et al. (2009a,b). They have suggested that, instead of GEC modulations, HCS crossings produce high latitude gravity waves resulting from precipitating energetic particles. These researchers argue that high latitude gravity waves can trigger conditional symmetric instability, and via slantwise convection, promote an intensification of mid-latitude cyclones. Prikryl et al. (2009a) have provided evidence that

major North American and European mid-latitude cyclones tend to occur in close proximity to HCS crossing dates, including: the Super Tornado Outbreak (3 April 1974), the Great Blizzard of 1978, the Great Storm (14-15 October 1987), the so-called Perfect Storm of 1991, and the cyclone for the Ice Storm of the Century (7-9 January 1998). These researchers have identified tropospheric pressure deepening occurring during HCS crossings using storm track data derived from the NCEP/NCAR Reanalysis (Kalney et al. 1996).

Given that both theories imply that severe weather phenomena may be impacted by HCS crossing events, we do not undertake for this investigation, to argue one explanation over another. Instead, given the possibly of improved severe weather forecasting using the basic climate-HCS relationship (regardless of causative effect), we investigate whether significant severe weather phenomenon, the occurrence of tornadoes, is linked to HCS crossing dates. Consequently, this research specifically examines the occurrence of United States tornado activity, and other severe weather reports, over the last fifty years in relation to HCS crossing dates.

3.2 DATA

Solar wind plasma data were obtained through the National Space Science Data Center (NSSDC) through OMNIWeb interface (http://www.omniweb.gsfc.nasa.gov). The data are products of several satellite programs including the ACE, WIND, IMP, ISEE, and SOHO. The data spans from 1963 to 2011. The data are primarily composed of near Earth solar wind magnetic field and plasma variables: proton count, bulk flow velocity, magnetic mach number, etc. The data were amalgamated from fifteen geocentric spacecraft and three spacecraft upstream from the Earth. Extensive cross comparison of overlapping data provided quality control and the respective upstream records were time corrected.

Second, tornado, hail and damaging wind event data were provided by the Storm Prediction Center's Severe Weather Database (http://www.spc.noaa.gov/wcm/#data). These data were collected from observational reports of severe weather occurrence by the National

Weather Service. The database covers the period from 1950 through 2012 and provides geographic location, damage/intensity (the EF, or Enhanced Fujita scale) (Fujita, 1981; Doswell et al., 2009) fatalities of each event, as well as track vectors.

3.3 METHODOLOGY

3.3.1 HCS Crossing Dates

We calculated the Heliospheric Current Sheet (HCS) passage dates using the OMNI solar wind plasma data, specifically the heliocentric radial magnetic field component (B_Y). The solar wind magnetic sector structure is classified by reversals of the radial magnetic field component and additionally, the radial component has the greatest influence with respect to Earth's magnetosphere (Wilcox et al. 1974). A seven-day moving average Hamming window was used to smooth the time series. The result is a numerical (positive or negative) value for each day from 1963 to 2012.

We evaluated the HCS events by identifying instances where polarity reversed from a positive to negative value (P2N). This indicates a reversal of the solar wind magnetic field switching from an outward to an inward direction. Conversely, instances where a negative to positive (N2P) reversal indicated a switch from an inward to an outward radial magnetic field component. Comparing our calculated HCS crossing dates to the values used by Prikryl et al. (2009a), the mean difference between the respective crossing dates is less than 24 hours, indicating a reasonable correspondence for comparison. Additionally, several diagnostic solar wind plasma variables are subjected to a 20 day superposed epoch analysis per each HCS crossing date: the absolute magnitude of the solar wind ($|B|$), the bulk flow velocity (V), proton density (N_P), standard deviation of the vertical magnetic field (σB_Z), the magnetic mach number (M_A), and the Quasi-Invariant Index (QI). These diagnostic variables demonstrate large magnitude stepwise changes at the crossing date consistent with HCS crossing identification.

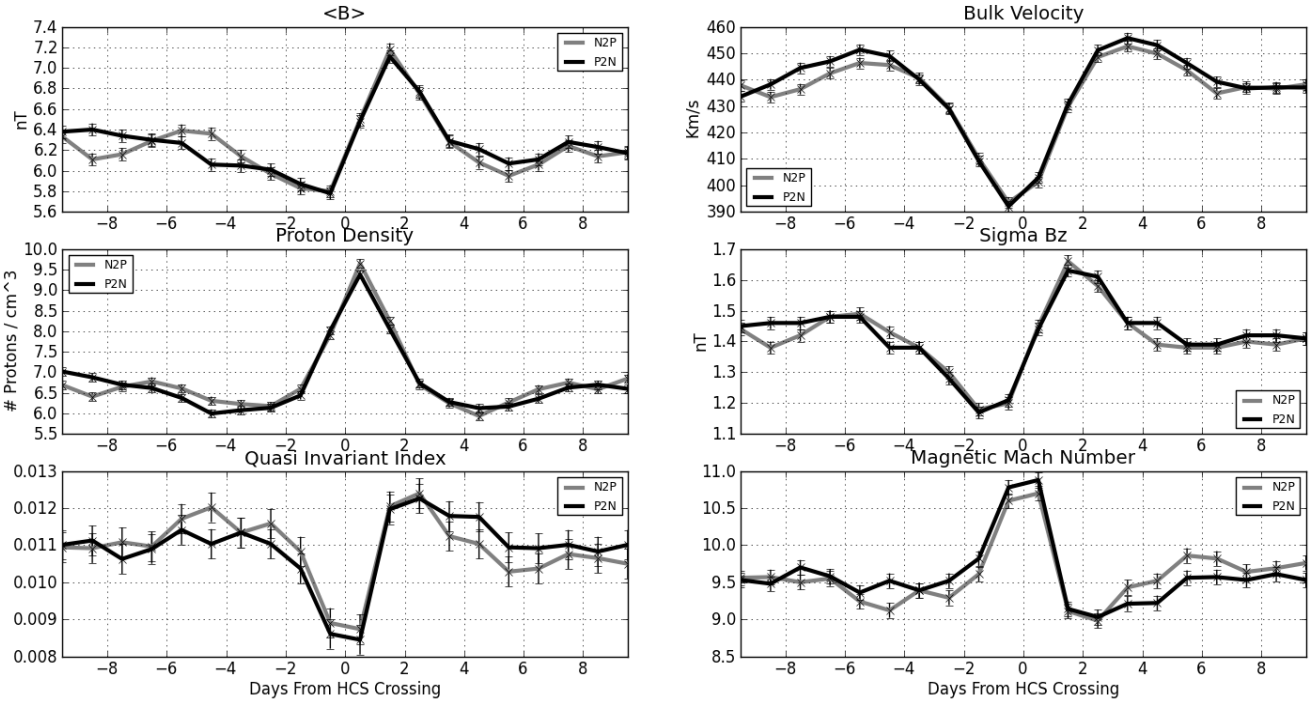

Figure 3.1: Superposed Epoch Analysis (SPE) for solar wind plasma parameters in relation to Heliospheric Current Sheet (HCS) crossing dates. The black series indicates positive to negative BY crossings, and the gray series indicates negative to positive BY passages.

This Superposed Epoch Analysis (SPE) charts the modulation of the solar wind plasma during the calculated HCS crossings (Fig. 3.1). The SPE variable signals, with the equivalence between previously utilized HCS crossing dates, provides the confidence to utilize the computed HCS dates employed in this investigation.

3.3.2 HCS Crossings and Severe Weather Events

Using the Storm Prediction Center's Severe Weather Database, we computed the time difference of each individual tornado event obtaining its temporal proximity to the nearest HCS crossing date, for either positive-to-negative (P2N) or negative-to-positive (N2P) sector crossings. The results were then amalgamated over the length of record for occurrences ranging from -30 (thirty days prior to HCS crossing) to +30 (thirty days after HCS crossing). The tornado reports were separated in to intensity categories: EF0 and greater, EF1 and greater, etc. An identical method was employed for hail reports and damaging wind reports, both of which are included in the Severe Weather Database provided by the Storm Prediction Center.

3.3.3 Monte Carlo Simulation and Hypothesis Testing

The computed distribution between severe weather reports and HCS crossings are then compared against a series of 'fake' events using Monte Carlo simulation. The simulation randomly selected dates to act as 'pseudo-events'. The number of pseudo-events generated was equivalent to the number of severe weather reports in each respective intensity category. The dates are generated randomly within the time domain established by the Severe Weather Report Database. These 'pseudo-events' were analyzed identically to the authentic tornado reports, establishing their respective proximity to the nearest N2P/P2N HCS crossing date.

To depict the results of the observed events versus what is expected through random simulation, normalized histograms of the database events are then compared to normalized histograms of the 'pseudo-events' yielding probability deviations from expected random events.

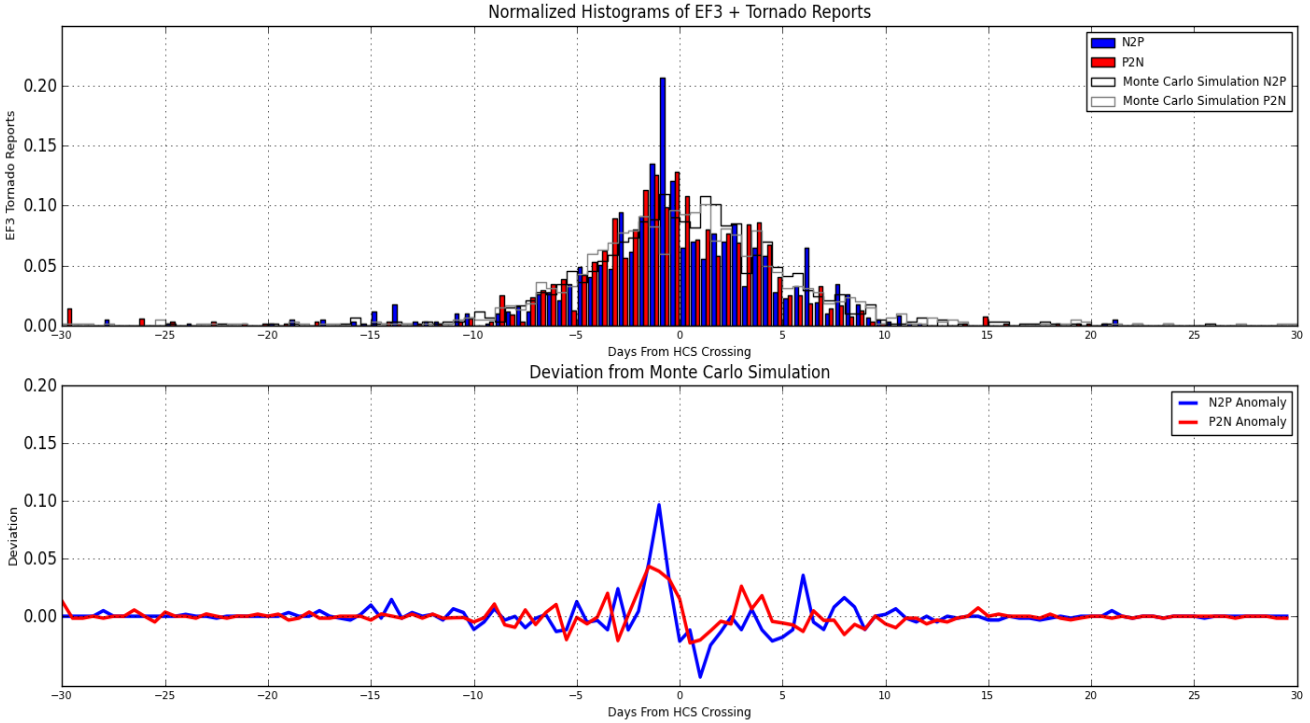

Figure 3.2: Top: Normalized histograms for EF3+ Tornado Events. Actual reports are filled histograms, Monte Carlo simulated events are stepped histograms. Bottom: Depiction of computed probability deviation between actual events versus simulated events.

Figure 3.2 (top) represents normalized histograms for EF3 and greater tornado events, with an equivalent number of Monte Carlo simulated events (represented by black and gray stepped histograms). Figure 3.2 (bottom) portrays the computed probability deviation between actual events versus expected. The deviations for tornado reports from their expected values are displayed in Figure 3.3. Six different classes are used to rank our tornado events by intensity: EF0 and greater (A), EF1 and greater (B), EF2 and greater (C), EF3 and greater (D), EF4 and greater (E), and EF5 (F).

3.3.4 Distribution Statistics

Distribution statistics for both tornado reports and Monte Carlo generated pseudo-events are provided in Table 1. Included in the statistics are measures of symmetry (skewness) and the peakedness (kurtosis) of the distribution. Table 1 is organized with respect to intensity of the tornado reports similar to Figure 3.3.

3.4 RESULTS

3.4.1 Tornado Reports

There are more than 20,000 reports for each P2N and N2P for EF0 and above, and more than 12,000 reports for EF1 and above. For EF1 tornadoes and weaker, the collective probability deviations between observed reports versus expected events is below 5 percent. However, there is a noticeable increase and subsequent decrease before and after N2P crossings. However, violent tornadoes (EF3+) are almost 10% more probable to occur near a N2P crossing, and 4% less probable to occur immediately following the HCS crossing. The signal is muted in the P2N deviation series: slightly less than 5% probability, however the negative probability following the HCS crossing is similar. There is a noticeable asymmetry in the event distribution, immediately before and after the HCS crossing. With increasing EF scale, there appears to have an increasing peakedness.

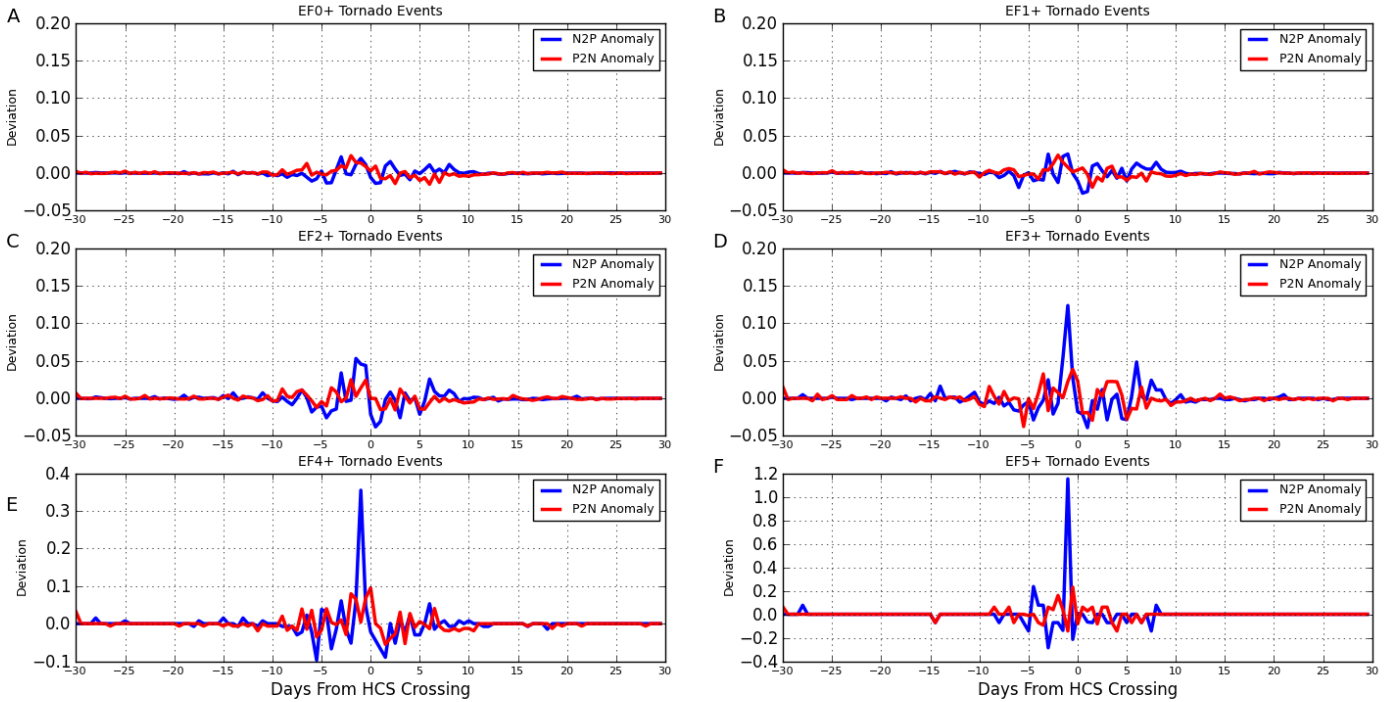

Figure 3.3: Observed Tornado events deviation from expected (N2P: Negative to Positive Crossings--gray and P2N: Positive to Negative Crossings--black): A: EF0 and above, B: EF1 and above, C: EF2 and above, D: EF3 and above, E: EF4 and above, F: EF5 and above.

The numbers of events for EF3+, for N2P and P2N crossings, are above 1000. Increasing tornado intensity results, however, with decreased reports.

For events at EF4 and greater: there exists a very sharp increase in deviation from expected probability. Our results show EF4+ are ~35% more likely to occur immediately before the N2P HCS crossing. Additionally, these events are almost 10% less likely to occur immediately following the HCS crossings. For the deviation of P2N crossings from expected: EF4 and greater tornado events are 10% more probable to occur before the HCS crossing. These extreme tornadoes are rare events (~ 250 per N2P and P2N). As the number of actual events decrease; the random simulation of dates and the corresponding probabilistic comparison, is less vigorous.

For EF5 reports: there exists much higher probability for EF5 tornadoes to occur near the HCS crossing (N2P) and almost 20% for the P2N crossing. However, the amount of tornado events for N2P and P2N are only between 20 and 40 events. In the event of a single massive outbreak event, the Monte Carlo simulation fails to generate sufficient fake dates which reduces the robustness of our probabilistic comparison.

3.4.2 Hail and Damaging Wind Reports

We additionally applied our analysis to severe weather reports of hail and damaging wind. The reports were examined with an identical analysis as the tornado events, including Monte Carlo simulation of pseudo-events; results are depicted in Figure 3.4. For both hail and damaging wind reports, there is less than 3% deviation in probability for N2P and P2N crossings. The deviation of hail reports, for N2P crossings, shows a higher probability before the crossing, and a lower probability following the crossing similar to the tornado anomalies. Interesting, this is not mirrored in the P2N crossing for hail reports. This lack of correspondence is likely the result of the occurrence of hail not being as strongly linked to vorticity as tornado formation.

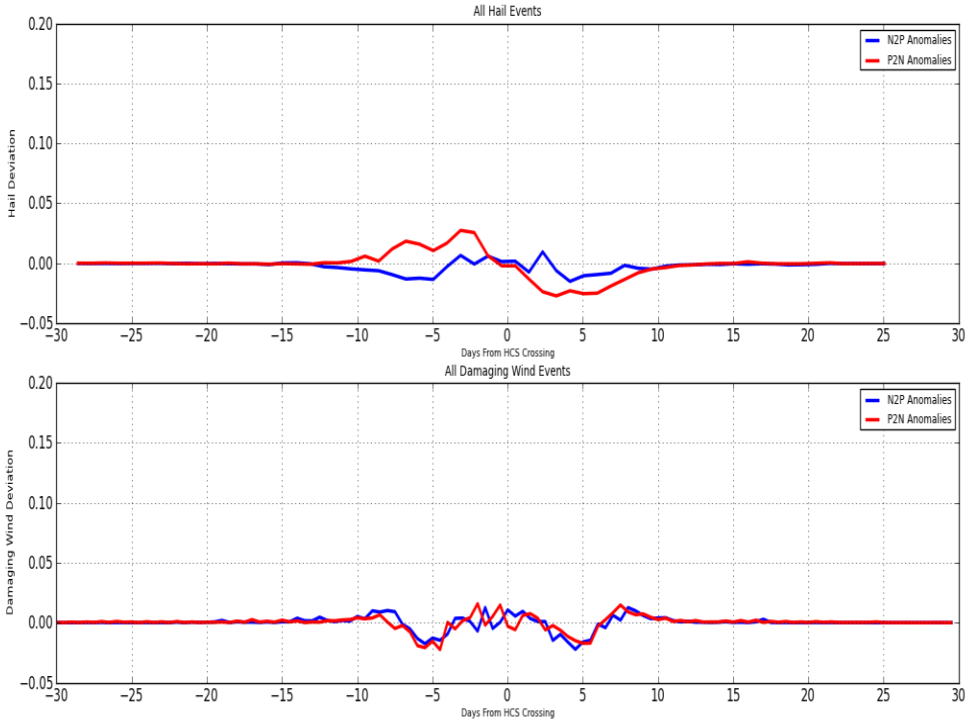

Figure 3.4: Top: Depiction of computed probability deviation between hail events versus simulated events. Bottom: Depiction of computed probability deviation between damaging wind events versus simulated events

Since hail occurrence is a function of sustained vertical uplift and not primarily dependent upon rotation (Guo and Huang, 2012), such a weaker linkage to HCS crossing is reasonable given the assumption that HCS crossings influence vorticity (Wilcox et al., 1974).

The distribution for damaging wind reports show minima five days prior to and following the HCS crossing date. There is no familiar peak near the HCS crossing date. Additionally, there are probabilistic maxima around seven/eight days prior to and following the HCS date, mirrored identically for P2N and N2P crossing dates.

3.4.3 Distribution Statistics

A normal distribution displays a skewness value of 0.00. Given an equal number of days prior to and proceeding the HCS event, the skewness values therefore indicate the asymmetry or

the degree to which the distribution of tornadoes are centered around the given HCS event. Overall, there is an increased skewness for the authentic tornado reports versus the simulated events, indicating a preference between solar wind polarity regimes. The distributions exhibit a statistically significant preference for events to occur before a HCS crossing and a disinclination following the HCS crossing.

		N	Mean	Var	Skewness	Kurtosis
EF0+	N2P	23800	0.06	22.73	-0.43	2.64
	P2N	23469	-0.51	28.01	-0.69	5.52
	M.C. N2P	20461	-0.16	26.78	-0.12	3.01
	M.C. P2N	20594	0.04	30.45	-0.22	4.40
EF1+	N2P	12107	-0.05	25.05	-0.48	2.60
	P2N	11964	-0.45	29.39	-0.72	5.59
	M.C. N2P	11283	-0.22	25.20	-0.16	2.87
	M.C. P2N	11522	0.05	30.85	-0.33	4.81
EF2+	N2P	4409	-0.28	26.13	-0.71	3.36
	P2N	4216	-0.57	31.66	-1.00	6.03
	M.C. N2P	4470	-0.07	25.71	-0.09	2.34
	M.C. P2N	4578	0.23	31.26	0.00	4.51
EF3+	N2P	1232	-0.30	26.20	-0.75	3.97
	P2N	1096	-0.54	28.72	-1.71	8.67
	M.C. N2P	1213	-0.18	22.18	0.01	2.59
	M.C. P2N	1211	-0.03	36.17	-0.24	4.26
EF4+	N2P	265	-0.60	26.83	-1.24	7.62
	P2N	256	-0.93	24.88	-2.95	15.47
	M.C. N2P	280	-0.33	27.30	-0.06	0.61
	M.C. P2N	295	0.33	32.33	0.58	4.41
EF5+	N2P	26	-2.06	33.21	-3.34	13.66
	P2N	33	-1.93	31.36	-3.92	17.09
	M.C. N2P	36	0.89	21.08	0.47	0.08
	M.C. P2N	33	1.05	34.98	0.84	2.01

Table 3.1. Distribution statistics for tornado events and Monte Carlo (M.C.) simulated events with HCS crossings proximity

Kurtosis, or distributional peakedness, indicates the magnitude of the distribution. The method was employed to gauge the peaked anomaly near the HCS crossing. Extreme violent tornado events exhibit very kurtotic distributions. However, method is very sensitive to outliers resulting in very inconsistent values for actual and simulated distributions.

3.5 CONCLUSIONS

The distributional analyses demonstrate that United States tornado reports exhibit significant linkages to Heliospheric Current Sheet crossing dates. Since severe thunderstorm and tornado formation requires vorticity (Fujita et al., 1970); the established Wilcox effect could potentially provide the atmosphere with more rotation at times of HCS crossings. The more intense tornadoes exhibit a more pronounced association with HCS crossings. This leads to a conjecture that the association may be related to a synoptic scale rotational strengthening of mid-latitude cyclones; engendering tornado outbreaks. When employing a larger population of less violent tornadoes, the signal is minimalized.

Interestingly, the HCS crossing from a negative magnetic sector to a positive sector (N2P), correlated to more (particularly severe) tornadic activity, most notably near the crossing event. If vorticity is modulated by energetic particle precipitation, the polarity switch of the HCS would be critical in determining the magnetospheric response or reorganization. A potential validating test would utilize severe storm reports from the southern hemisphere, in the identification of the possibility of a reciprocal effect. Unfortunately, at this time, the authors have not been able to obtain a comparable database of tornado reports for Australia or other southern hemispheric locations.

The Wilcox effect has a documented influence on vorticity in the atmosphere. Even though there are numerous sources to provide vorticity to storms engendering tornadoes (shortwaves, jet stream sector structure, etc.); the configuration of the solar wind, its modulation of Earth's magnetosphere, and the subsequent precipitation of energetic particles may impart an

additional amount of vorticity to severe storms. Our results show an asymmetry between sector crossings and tornado events and a unique peakedness in the distribution in distance from HCS crossings with severe violent tornadoes.

We stress that this research is not intended to support one theory over another with regard to explaining the Wilcox effect. However, our study speaks to the importance of future case studies, specifically those which analyze the diversity of heliospheric events (coronal mass ejections, corotational interaction regions, coronal holes, etc.) and their connections with Earth's magnetosphere, ionosphere and atmosphere. It is likely that continued investigations would elucidate the causes behind the Wilcox effect (relativistic particle precipitation, ionospheric joule heating, auroral gravity waves, etc.). This and future research are dependent upon the establishment and maintenance of a continued observational presence within the magnetosphere, heliosphere, and local cosmos.

Although our initial study is unlikely to extend tornado-warning times, our research could be useful in perhaps improving weekly or seasonal forecasting as well as developing additional severity indices regarding the modeled locations and arrival dates of HCS crossings. Fundamentally, this study suggests that continued attention to the frequency/magnitude of HCS crossings and their timing in a given tornado season may be significant in better assessing the number and timing of tornadoes.

3.6 ACKNOWLEDGMENTS

Solar wind plasma data were obtained through the National Space Science Data Center (NSSDC) through their OMNIWeb interface (http://www.omniweb.gsfc.nasa.gov). Severe weather event data were provided by the Storm Prediction Center's Severe Weather Database (http://www.spc.noaa.gov/wcm/#data) via the National Weather Service.

CHAPTER 4

GALACTIC COSMIC RAYS AND CLOUD COVER

This chapter records my investigation of galactic cosmic ray flux and North American regional cloud cover. A version of this chapter is currently under review in the Journal of Geophysical Research—Atmospheres, titled: Solar Influence on High, Mid-Level and Low Cloud Cover: Results using the North American Regional Reanalysis (NARR). This was a solo authored article.

Abstract: Although global linkages between solar variability and terrestrial cloud cover have been made in the past, detailed regional evaluations of such linkages have not been conducted. In this study, correlations between high-resolution (32-km) low, mid-level, and high cloud cover and solar activity are investigated using the North American Regional Reanalysis (NARR). Pearson's product-moment correlations are applied to monthly cloud cover averages and 10.7cm solar flux. Results confirm previous studies' findings of a general negative correlation between solar flux and low-level marine-layer cloud cover, specifically over the central, northeast Pacific, and the central Atlantic oceans. Additionally, negative correlation is observed in high cloud cover over the majority of Canada. However, the fine-resolution NARR dataset also indicates a positive correlation exists between solar activity and low-level cloud cover over the Arctic and tropical continental Central America. Additionally, positive correlations between solar flux and mid-level cloud cover are observed throughout the ITCZ, the subtropics, the southern, gulf coast, Atlantic seaboard states and the Arctic. These results indicate substantial regional variability between cloud cover altitude and solar flux; and have implications for accurate climatological modeling.

4.1 INTRODUCTION

As integral parts of the climate system, clouds mediate radiative and latent heat fluxes between the atmosphere and the ocean. Variations in cloud cover directly influence Earth's

radiation budget. Clouds simultaneously reflect shortwave solar radiation and capture long-wave radiation emitted by Earth's surface. The net climate forcing of cloud cover is dependent upon region and altitude. The accuracy of climate modeling projections are highly dependent upon feedback quantification. Although cloud-extraterrestrial linkages have been made in the past; few detailed regional evaluations of such linkages have been attempted. In this study, the influence on regional cloud cover of solar activity (and galactic cosmic ray GCR) flux is assessed using the high-resolution gridded reconstruction from the North American Regional Reanalysis Project. Such an analysis serves to improve our understanding of radiative-modulated cloud cover and substantially improve future climatological simulations.

4.2 BACKGROUND

Modulation of atmospheric cloud cover has been proposed as one of the processes linking solar activity to terrestrial climate variability. Galactic cosmic rays, and other energetic charged particles, penetrate the atmosphere and produce ionization in the deepest parts of the troposphere (Usoskin and Kovaltsov, 2008). As GCRs transit the solar system, they are entrained and deflected by the interplanetary magnetic field. There exists a strong eleven-year periodicity in GCR flux, which is inversely correlated with solar activity (Lockwood, 2006). There also exists a strong twenty-two-year periodicity consistent with the solar hemispheric dipole switch affecting the direction of GCR particle drift (Haigh, 2011).

Enhanced GCR flux has been proposed to increase cloudiness (Svensmark and Friis-Christensen, 1997; Svensmark, 2000; Marsh and Svensmark, 2000). Solanki and Krivova (2003) have argued that GCR flux explains 30% of the atmospheric warming since 1970. Scafetta and West (2006) have determined a correlation between GCR flux and five hundred years of global surface temperatures. Conversely, it has been argued that the cloud data have been misrepresented (Laut, 2003) and others found no significant correlation with cloudiness using the United States radiosonde network (Balling and Cerveny, 2003).

GCR-induced ion production in the lower atmosphere provides more favorable conditions for cloud droplet formation (Haigh, 2011). Documented positive correlations exist with the tropical marine low cloud cover and GCR flux (Gray et al., 2010). However, laboratory experiments have yet to support cloud microphysical modeling used to establish consecutive processes supporting the observed climatological variations.

Discrimination between high and low cloud cover variability is important. With regards to climate radiative forcing, an increase in thin high cloud cover results in a net warming, whereas increased thick low altitude cloud cover results in a net cooling. Evidence suggests that low cloud cover variability exhibits positive correlation with GCR flux, while high cloud cover variability has found to have a negative correlation with GCR flux (Yu, 2002; Kristjansson et al., 2004; Palle, 2005). Voiculescu et al. (2006) found a positive correlation between low cloud cover variability with GCR flux over ocean regions and dry continental air masses, and a negative correlation between high cloud cover variability with GCR flux, specifically over the oceans and moist continental areas. Voiculescu and Usoskin (2012) have stressed the importance of examining the correlation between GCR flux and cloud cover, at the regional level, at climate defining regions.

Because of the aforementioned research, assessing the regional impact and the spatial resolution of cloud cover modulation is useful for appraising climate/extraterrestrial linkages; as is developing a convergence of evidence of such linkages through multiple data set and reconstructions. This study utilizes the high-resolution gridded reconstruction from the North American Regional Reanalysis Project to analyze the spatial and altitude correlations of cloud cover with solar activity and inversely with GCR flux.

4.3 DATA

Cloud data used in this investigation were obtained from the North American Regional Reanalysis (NARR), a high-resolution gridded reconstruction (Mesinger et al. 2004). The NARR project is a recent extension of the NCEP Global Reanalysis, compiled over North America

(Mesinger et al. 2004). The NARR utilizes a combination of the Eta Weather Model, or the WRF-NMM or NAM model as it was renamed in 2005, used by NCEP as well the Regional Data Assimilation System (RDAS) (Mesinger et al. 2004). The NARR dataset has a 32 kilometer resolution at the lowest latitudes. Grid vertices are located at approximately 12N; 134W, 55N; 153W, 57N; 49W,14N; 65W.

Cloud cover fractions considered at individual 'monolevels' were used. Specifically, monthly mean cloud cover fraction for high, mid-level and low level cloud heights. Cloud cover below 800 hPa are designated low cloud cover, and cloud cover above 450 hPa are considered high cloud cover. Cloud cover between 450 and 800 hPa is designated as mid-level cloud cover (Mesinger et al. 2004). NARR data are provided by the NOAA/OAR/ESRL PSD, Boulder, Colorado, USA; from their Web site at http://www.esrl.noaa.gov/psd/.

The 10.7cm (2800 MHz) solar radio flux timeseries (F_s) is the solar activity proxy selected for this investigation. Solar flux measurements are commonly used to inversely estimate cosmic ray flux (Yu, 2002; Haigh, 2003; Voliculescu et al., 2006; Lockwood and Frohlich, 2007; Gray et al., 2010). Due to multiple GCR observatories, discontinuity of the respective timeseries, and varying calibration and scattering adjustments, the F_s are employed to inversely gauge monthly GCR counts. The time domain used for this investigation ranges from 1 January, 1979 to 1 December, 2010. Monthly means of solar radio flux were averaged from the daily F_s values provided by the National Research Council of Canada based on observations at Algonquin Radio Observatory, near Ottawa, later transferred to the Dominion Radio Astrophysical Observatory, near Penticton, British Columbia.

4.4 METHODS AND RESULTS

Following previous studies (Scafetta and West, 2006; Balling and Cerveny, 2003), Pearson's product-moment correlation analysis is applied to the three levels of NARR cloud data (low, mid, and high) with respect to the 10.7 cm F_s datasets. Correlations are computed for each grid-point of the NARR dataset separately resulting in high-resolution spatial matrices of

correlation coefficients and their respective two-tailed confidence values. For visualization purposes, the NARR dataset is projected upon a Northern Lambert Conformal Conic grid. Dark shaded regions of the correlation figures indicate grid-points whose correlations do not satisfy a 95 percent level of confidence.

A significant negative correlation between low cloud cover and F_s (as noted in the previous section, thereby connoting positive correlation with GCR flux) regionally over maritime ocean regions (Figure 4.1). Specifically, strong negative correlations are evident in the Mid-Atlantic, the Northeastern and equatorial Pacific, and off the coast of Baja California. Conversely, there exists a positive correlation between low cloud cover and F_s (implying negative correlation with GCR flux) near tropical Central America continent, the northern tip of South America, regions of Quebec, and the Arctic.

No statistically significant negative correlation with F_s and mid-level cloud cover (connoting no positive correlation with GCR flux) (Figure 4.2). However, there exists extensive and significant positive correlation between medium cloud cover and F_s (implying negative GCR correlation). The regions displaying the highest statistically significant correlations include the Central Pacific and US west coast, the southern and Gulf coast states of the U.S., lower Central America and the northern tip of South America, and off the coast of Baja. Other areas which show positive correlation are the Arctic, the Mid-Atlantic, and on and near the east coast of Labrador.

A negative correlation between high cloud cover and F_s (implying positive GCR flux) over the majority of continental Canada with the exception of the Yukon Territory and British Columbia (Figure 4.3). There is also a significant negative correlation evident near the southern tip of Greenland. Conversely, the results show a statistically significant positive correlation between solar flux and high cloud cover over the Atlantic seaboard, the southeast and Gulf Coast states of the U.S., the Mexican Plateau, Baja California, and north of Eastern Siberia.

4.5 DISSCUSSION AND CONCLUSIONS

These high-resolution spatial statistical analyses confirm a relationship established in previous studies between solar and galactic cosmic ray (GCR) flux upon global cloud cover. However, using the high-resolution North American Regional Reanalysis dataset, highly specific regional significant correlations between solar activity and cloud cover are evident. These correlations exhibit distinct and different spatial patterns with regard to respective cloud altitudes (low, mid-level and high).

In general, these regional patterns are in good agreement with established findings (Yu, 2002; Kristjansson et al., 2004; Palle, 2005) indicating a negative correlation between F_s and low cloud cover (and implying positive correlation between low clouds and GCR flux) exists over maritime regions. However, these results indicate that this negative Fs/low cloud finding is not globally uniform and that the significant positive correlations exist over the Mid-Atlantic Ocean, the North Pacific Ocean and parts of the Inter-Tropical Convergence Zone (ITCZ). Additionally, these results show positive correlation between dry continental land mass and low cloud cover.

These results exhibit substantial positive correlation between F_s and midlevel cloud cover (connoting negative correlation with GCRs) across the subtropics and the Arctic. No significant negative correlation exists with midlevel cloud cover with F_s (implying positive correlation with GCR flux) at all within the NARR spatial domain.

These results agree with the positive correlation between high cloud cover and F_s (connoting negative correlation with GCRs) over moist continental areas, specifically the US Atlantic seaboard and gulf coast states. However the correlation is not extended over the oceans, with the exception of the Pacific Ocean off the coast of Baja California. Additionally, a strong negative correlation exists between high cloud cover and F_s (implying positive correlation with GCR flux) over large parts of Canada. Although these initial regional results are revealing, there are several limitations that require mention. First, use of the 10.7 cm radio flux to estimate solar variability and inversely, galactic cosmic ray flux may be problematic.

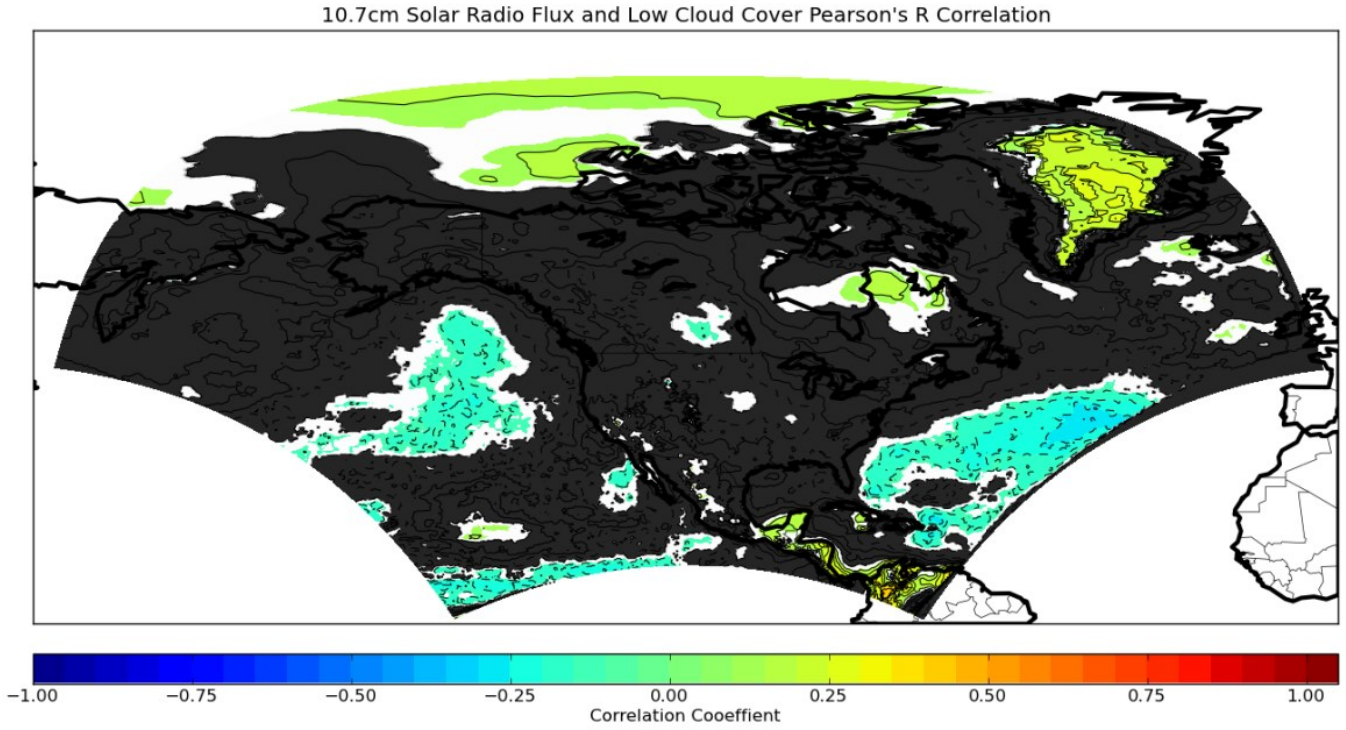

Figure 4.1: Mapped Pearson's product-moment correlation values between the NARR low cloud cover and 10.7cm solar flux (Fs) for the period from 1979 to 2010. Shaded gray regions represent values that do not satisfy a 95 percent level of confidence

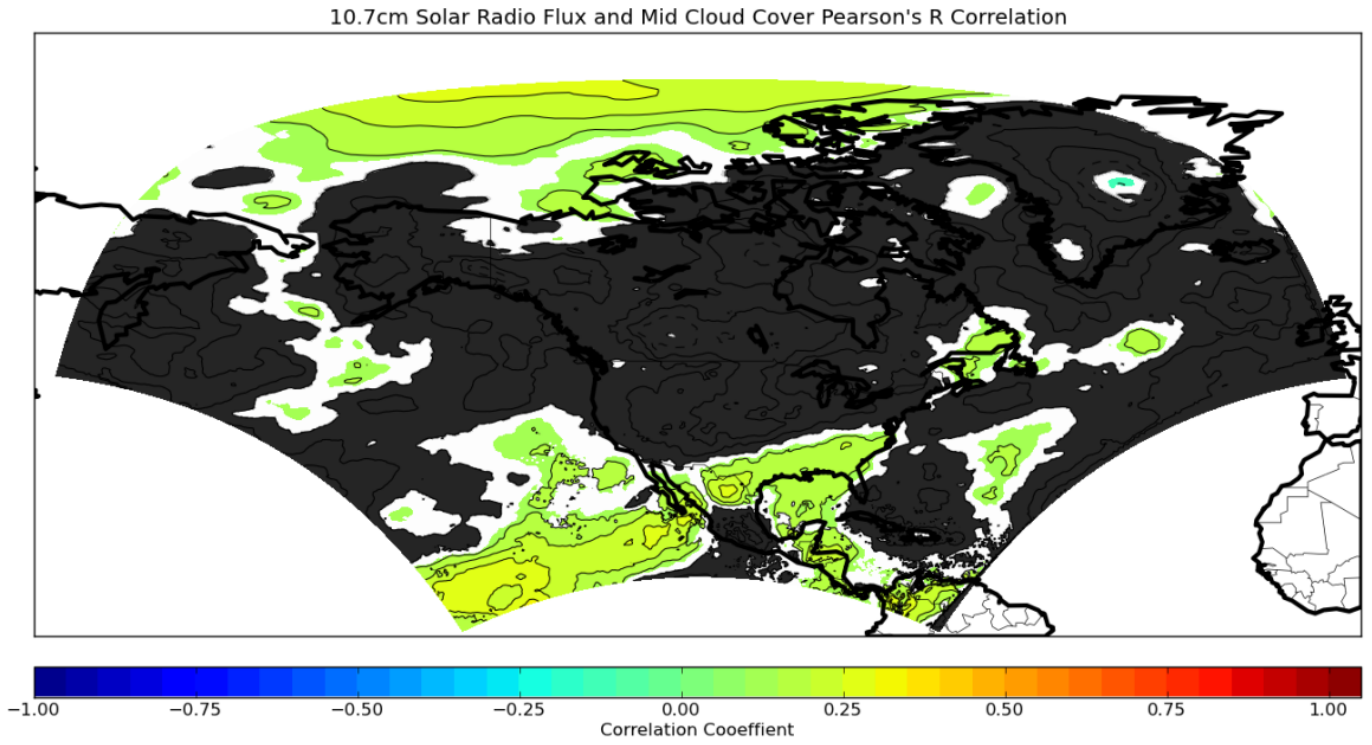

Figure 4.2: Mapped Pearson's product-moment correlation values between the NARR mid-lvel cloud cover and 10.7cm solar flux (Fs) for the period from 1979 to 2010. Shaded gray regions represent values that do not satisfy a 95 percent level of confidence.

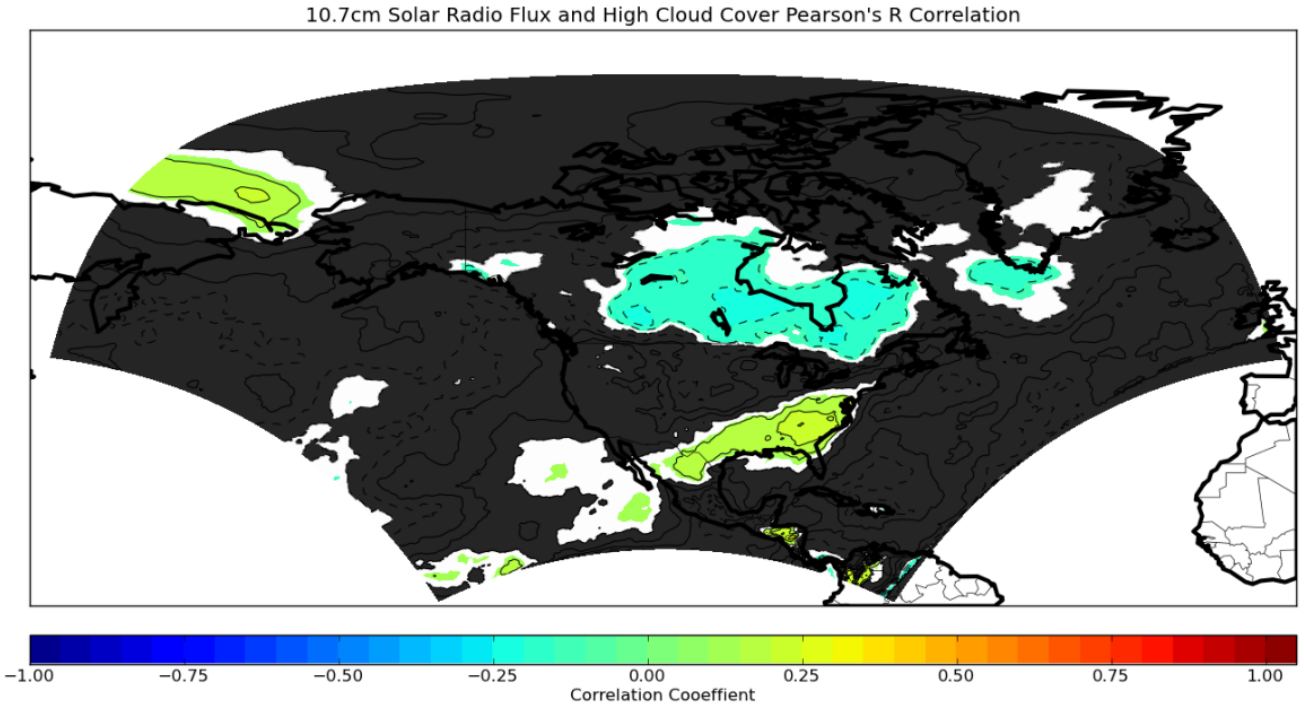

Figure 4.3: Mapped Pearson's product-moment correlation values between the NARR high cloud cover and 10.7cm solar flux (Fs) for the period from 1979 to 2010. Shaded gray regions represent values that do not satisfy a 95 percent level of confidence.

Although the inverse correlation is well established (Yu, 2002; Haigh, 2003; Voliculescu et al., 2006; Lockwood and Frohlich, 2007; Gray et al., 2010), there exists differentiation concerning heliospheric cosmic ray transport during different epochs of the 22-year solar magnetic polarity Hale cycle. Additionally, the NARR time domain (1979-2010) only accommodates three complete (~11 year) solar activity cycles (solar cycles 21, 22, and 23) and does not cover two complete (~22 year) magnetic Hale cycles. Nor does it address identified prolonged solar minima epochs within the climate record.

However, given these potential caveats, the results of this study indicate that regionally significant positive and negative correlations exist between solar flux and low, mid-level and high cloud cover. These respective correlations are highly regionally specific such as the marine layer, the arctic, moist continental landmasses, etc. Fundamentally, determination of cloud-cover modulated radiative flux and quantification of the atmospheric radiation budget are essential for accurate climatological modeling. Identifying specific geographic locations that exhibit strong correlation between cloud cover and solar activity, improves the assessment of the regional solar/climatic impact.

4.6 ACKNOLEDGEMENTS

Solar flux and NARR Reanalysis data provided by the NOAA/OAR/ESRL PSD, Boulder, Colorado, USA, (http://www.esrl.noaa.gov/psd/)

CHAPTER 5

CONCLUSIONS

5.1 SUMMARY OF RESULTS

In this chapter, I summarize the results of the initial posited research questions, around which my dissertation is constructed. In addition, I provide a discussion of future research and the overall significance of each investigation with the overall importance of this entire work. First, my three fundamental research questions are:

(A) What are the biweekly declination effects of lunar gravitation upon the middle and upper tropospheric geopotential heights? The justification for this question is that several lunar declination periodicities exits in the climate record. These correlations have been found to vary with several large-scale oscillatory modes of the coupled atmosphere and ocean. The Moon obtains its maximum distance from the equator approximately every two weeks. Due to the current limitations facing numerical forecasting, validates the exploration of short term biweekly lunar declination connections upon tropospheric circulation.

(B) How do United States severe weather reports, specifically tornadoes, hail and damaging wind reports, correlate with heliospheric current sheet crossings at Earth's orbit? The justification for this query is due to the established connection between solar wind magnetic sector crossings and atmospheric vorticity. Since tornado formation necessitates spin in the atmosphere, U.S. severe weather reports acts as an adequate measure for assessing the impact of the Wilcox effect upon tropospheric weather patterns.

(C) How does cloud cover reconstructions spatially and temporally vary with respect to galactic cosmic rays? The justification for this question is that the correlation between cloud cover and galactic cosmic rays was the first hypothesis to substantiate the connection between terrestrial climate change with solar activity.

Several reviews and synopses of the literature readily admit a lack of discrimination between cloud types at various altitudes and their respective geographic spatial variance. It is this void in the literature which motivated this inquiry.

I will first summarize the framework and the results of each of these inquiries individually.

5.1.1 Lunar Declination and Circulation

To address this question, we conducted a study comparing global geopotential tropospheric height values provided by the NCEP/NCAR Reanalysis, versus instances of maximum lunar declination. The NCEP/NCAR reanalysis provides data from 1948 to present. Lunar orbital parameters were obtained using ephemeris modules and cross-checked using NASA's JPL online Horizons Ephemeris. Our analysis focused on circulation anomalies which exist during the transition from positive maximum lunar declination (North of the Equator) to negative maximum lunar declination (South of the Equator) and vice versa.

Fundamentally, our results confirm the hypothesis in which atmospheric pressure variations correspond with the position of the Moon above or below the equator. Our finding acts to contradict the hypotheses in which atmospheric tides are solely influenced by diurnal heating. Through a lunar synodic revolution lasting 27.3 days, a maximum effect is experience by both hemispheres every 13.66 days. The effect is largely, but not entirely, hemispherically symmetrical.

Currently, meteorological forecasting is limited to two weeks. Our findings show a coherent spatial consistency concerning lunar declination extremes upon Rossby longwave characteristics. Due to the influence of Rossby longwaves on synoptic scale mid-latitude storm tracks and on surface/thermal pressure patterns, our findings suggest that the incorporation of lunar declination parameters into forecasting algorithms could theoretically extend/improve meteorological forecasting.

5.1.2 The Solar Wind and Severe Weather

To address this question, analyzed solar wind data and U.S. severe weather reports. OMNIweb solar wind data was provided by the National Space Science Data Center. Instances of solar wind magnetic sector crossings (hemispheric current sheet crossings) were obtained by smoothing the solar wind time series and locating where the radial component of the magnetic field reverses. Additionally, data for the dynamic solar wind plasma was used to test the authenticity of these dates, specifically: the magnetic field vectors, bulk flow velocity, density, proton count, etc. were subjected to superposed epoch analysis using the calculated HCS crossing dates. All of the plasma wind parameters exhibited stepwise changes through the SPE analysis. United States severe weather reports (tornadoes, hail, and damaging wind), provided by NOAA's Storm Prediction Center, where then analyzed with respect to their nearest respective HCS crossing date.

Our results indicate a preference for violent tornadoes to occur prior to a heliospheric current sheet crossing, specifically a transition from a negative to a positive radial magnetic field. Violent tornadoes (EF3+) are almost 10% more probable to occur near a N2P crossing, and 4% less probable to occur immediately following the HCS crossing. There exists a similar anomaly for positive to negative crossing events, however the signal is muted.

The distribution of other severe weather reports, used as a control, generally does not mirror the tornado reports distribution. Hail reports exhibits the closest signal during a negative to positive sector crossing, however it is noticeably suppressed. Damaging wind report distribution is completely irregular from the distribution of tornado reports about HCS crossings. Our results do not attempt to prove either hypothesis regarding the Wilcox effect (HCS crossing correlation with atmospheric vorticity), however, our results do indicate that the polarity of the HCS crossing is critical in quantifying the atmospheric response.

5.1.3 Solar Flux, Cosmic Rays and Cloud Cover Reanalysis

To address this research question, I conducted a study comparing solar flux versus a reanalysis of cloud cover over North America. Solar flux is well established as a surrogate for inversely estimating galactic cosmic ray flux. North American cloud cover values were provided by the North American Regional Reanalysis project. Cloud cover monthly mean values were obtained for low-level, mid-level, and high-level altitudes for the time range of the NARR (1979-present). Solar variability was provided by terrestrial solar radio flux monitors (at 10.7cm wavelength or 2800 MHz). Each grid-point in the high resolution NARR dataset was subjected to several correlation analyses with respect to monthly smoothed values of solar flux.

My results confirm previous negative correlation between solar flux and low-level marine-layer cloud cover, specifically over the central, northeast Pacific, and the central Atlantic oceans. Additionally, negative correlation is observed in high cloud cover over the majority of Canada.

However, the fine-resolution NARR dataset also indicates a positive correlation exists between solar activity and low-level cloud cover over the Arctic and tropical continental Central America. Additionally, positive correlations between solar flux and mid-level cloud cover are observed throughout the ITCZ, the subtropics, the southern, gulf coast, Atlantic seaboard states and the Arctic. These results indicate substantial regional variability between cloud cover altitude and solar flux, and inversely galactic cosmic rays.

5.2 FUTURE RESEARCH

The aforementioned research investigations are either currently under peer review for publication or have been published in the scientific literature. Prospects for future research per the respective investigations are as follows.

5.2.1 Lunar Declination Biweekly Tropospheric Anomalies

Our research indicates a biweekly lunar declination influence upon Rossby longwaves and correspondingly, synoptic storm tracks. An interesting test would be to analyze forecast

model output statistics and their correlation with lunar declination. Our primary investigation was concerned with identifying the correlation between Rossby longwaves, via geopotential height values from the NCEP/NCAR reanalysis. A logical supplement would be to extend the correlation of lunar declination to other diagnostic variables provided in the analysis.

Additionally, the analysis could be expanded to include a full period of declination transition. Instead of focusing on maximum declination extremes, expand the analysis to visualize the transition from absolute negative declination to maximum positive. This type of analysis may reveal the synoptic longwave deformation and jet stream reorganization.

5.2.2 Solar Wind Magnetic Sectors and U.S. Severe Weather Occurrence

To probe the connection between HCS crossings and mid-latitude cyclones, we require extensive conglomerate case studies which explore the genesis and maturity of baroclinic disturbances in relation to heliospheric events. Multiple case studies for mid-latitude cyclones which occur in proximity to HCS crossings, versus those that do not. This comparison would help elucidate the causes of the Wilcox effect.

An interesting hypothesis is that severe weather reports (tornadoes) in the Southern hemisphere would have a preference for positive to negative HCS crossings as opposed to a negative to positive one. Noting a polar asymmetry in the Wilcox effect has wide reaching implications from seasonal forecasting to large scale oscillatory phenomenon.

5.2.3 Solar Flux, Cosmic Rays and Cloud Cover Reanalysis

The global electric circuit represents a new frontier in analyzing the spatial physical processes of our planet, and idealistically, requires the construction and maintenance of a global network of sensors solely designed for observing atmospheric electromagnetic phenomenon.

My analysis was performed upon the North American Regional Reanalysis, used due to its incorporation of satellite remotely sensed data. The logical next step would be to expand this to a global reanalysis data set. Additionally, other variables complementary to cloud cover

provided in the analysis (radiative flux coefficients, opacity, vertical column moisture, etc.) could be analyzed in an identical fashion.

The establishment of a census of energetic particles, categorized by energy level, would be useful for future case studies, measuring the amount of change in cloud properties per energetic particle flux events. Additionally, it would be interesting to compare terrestrial cloud cover response, to the other rocky planets with atmospheres: Mars and Venus. Observing similar or dissimilar impacts on other worlds would serve to test our fundamental understanding of energetic particle and specific cloud processes.

5.3 SIGNIFICANCE TO FIELD

This dissertation establishes the significance of short term meteorological and climatological impacts of exogenic forcing. Thorough analysis of exogenic forcing acts to tether the newly defined field of heliophysics with the well-established fields of meteorology and climatology. Ultimately, this dissertation serves to extend short term meteorological forecasting, enhance climatological modeling and through analysis of severe violent weather and heliospheric events, protect property and save lives.

Fundamentally, I discern a significant impact on our planet's circulation due to the inclination of lunar orbit. Not only is this periodicity approximately the same length as our current limitation of numerical forecasting, but is also relatively uncomplicated to obtain. If these forcings can be correctly incorporating into forecast models, it is my belief that these results could significantly improve and extend numerical forecasts.

I find a unique correlation between the magnetic structure of the solar wind with U.S. violent tornadoes. Heliosphereic current sheet crossings, through the Wilcox effect, appear to have the capacity to inject sufficient vorticity into the atmosphere to affect tornado occurrence. The results indicate that the polarity of the solar wind magnetic sector is not trivial. Tornado fatalities are primarily due to violent (EF3+) tornadoes. Essentially, this type of research could be used to establish additional severe weather indices, with the ultimate goal of saving lives.

Several authors (Gray et al., 2010, Haigh 2011), admit a deficiency in the correlation with cloud cover and solar flux (inversely with GCRs), primarily with respect to cloud cover height and specific regionality. My study provides fine resolution of the spatial correlation between solar flux and cloud cover, while simultaneously employing multiple cloud cover altitudes using the NARR reanalysis dataset. Understanding the atmospheric altitude and spatially depended response to exogenic forcing on clouds are essential for climate modeling which incorporate radiative flux computations.

To conclude, the findings of this dissertation compel us to accept that our current understanding of Earth's dynamic systems, though extremely advanced, is woefully incomplete. If this dissertation accomplishes anything, it is the authors hope that a greater reverence is gleaned concerning the remarkably unique conditions in which our civilization has prospered, and that there is much more to be done.

REFERENCES

Adderley, E., and E. G. Bowen, 1962: Lunar component in precipitation data. Science, 137(3532), 749-750.

American Meteorological Society, 2008: Space Weather: A policy statement of the American Meteorological Society. Bullitin of the American Meteorological Society, 16-18.

Balling Jr., R. C., and R. S. Cerveny, 1995: Influence of lunar phase on daily global temperatures. *Science*, *267*(5203), 1481–3.

Barnston, A. G., and R. E. Livezey, 1987: Classification, Seasonality and Persistence of Low-Frequency Atmospheric Circulation Patterns. Monthly Weather Review, 115,1083-1126.

Balling Jr., R. C., and R. S. Cerveny, 2003: Cosmic ray flux impact on clouds? An analysis of radiosonde, cloud cover, and surface temperature records from the United States. Theoretical and Applied Climatology, 75(3-4), 225-231.

Beer, J., 2010: Astrophysical influences on planetary climates. In Heliophysics: Evolving Solar Activity and the Climates of Space and Earth. C. J. Schrijver and G. L. Sisko (eds.), Vol 3, Cambridge University Press, 300pp.

Beer, J., M. Vonmoos, and R. Muscheler, 2006: Solar Variability Over the Past Several Millennia, *Space Science Reviews*, *125*(1-4), 67–79.

Berger, A., 1992: Astronomical solutions for paleoclimate studies over the last 3 million years. *Earth and Planetary Science Letters*, *111*, 369–382.

Berger, A., and M. Loutre, 1989: Pre-quaternary Milankovitch frequencies. Nature, 342, 133.

Berner, K. S., N. Koç, F. Godtliebsen, and D. Divine, 2011: Holocene climate variability of the Norwegian Atlantic Current during high and low solar insolation forcing. *Paleoceanography*, *26*(2), 1–15.

Bhatnagar, V. P., and T. Jakobsson, 1978: Lack of effects of solar magnetic-sector crossings on the troposphere. Geophysical Research Letters 5(3), 180-182.

Bisi, M. M. et al., 2010: From the Sun to the Earth: The 13 May 2005 Coronal Mass Ejection. *Solar Physics*, *265*(1-2), 49–127.

Bjerknes, J., 1969: Atmospheric Teleconnections from the Equatorial Pacific. Monthly Weather Review, 97(3), 163-173.

Bond, G., B. Kromer, J. Beer, R. Muscheler, M. N. Evans, W. Showers, S. Hoffmann, R. Lotti-Bond, I. Hajdas, and G. Bonani, 2001: Persistent solar influence on North Atlantic climate during the Holocene. *Science*, *294*(5549), 2130–6.

Bradley, D., and M. Woodbury, 1962: Lunar synodical period and widespread precipitation. *Science*, *6*(3), 3–5.

Brier, G., and D. Bradley, 1964: The lunar synodical period and precipitation in the United States. *Journal of the Atmospheric Sciences*, *21*, 386-395.

Burns, G. B., B. A. Tinsley, A. V. Frank-Kamenetsky, and E. A. Bering, 2007: Interplanetary magnetic field and atmospheric electric circuit influences on ground-level pressure at Vostok. *Journal of Geophysical Research*, 30, 112(D4), 2-11.

Burroughs, W. J., 2003: Weather Cycles: Real or Imaginary? Cambridge University Press, Cambridge, U.K., 371pp.

Cerveny, R., and R. C. Balling, 1999: Lunar influence on diurnal temperature range. *Geophysical research letters*, *26*(11), 1605–1607.

Cerveny, R. S., and J. A. Shaffer, 2001: The Moon and El Nino. Geophysical Research Letters, 28(1), 25-28.

Cerveny, R. S., B. M. Svoma, and R. S. Vose, 2010: Lunar tidal influence on inland river streamflow across the conterminous United States. *Geophysical Research Letters*, *37*(22), 1–5.

Chapman, S., and R. S. Lindzen, 1970: Atmospheric Tides: Thermal and Gravitational. D. Reidel, Dordrecht, Netherlands, 200pp.

Charvatova, I., 1997: Solar-terrestrial and climatic phenomena in relation to solar inertial motion. *Surveys in geophysics*, 18, 131–146.

Cordero, E. C., and T. R. Nathan, 2005: A new pathway for communicating the 11-year solar cycle signal to the QBO. *Geophysical Research Letters*, *32*(18), 1–5.

Cressie, N., 1991: Statistics for Spatial Data. John Wiley, Chichester, U.K.

Currie, R. G., 1996: Variance contribution of luni-solar (M(n)) and solar cycle (S-c) signals to climate data. International Journal of Climatology, 16(12), 1343-1364.

Delaygue, G., and E. Bard, 2010: An Antarctic view of Beryllium-10 and solar activity for the past millennium. *Climate Dynamics*, *36*(11-12), 2201–2218.

Dengel, S., D. Aeby, and J. Grace, 2009: A relationship between galactic cosmic radiation and tree rings. *The New phytologist*, *184*(3), 545–51.

Doswell, C. A., H. E. Brooks, and N. Dotzek, 2009: On the implementation of the enhanced Fujita scale in the USA. Atmospheric Research 93(1-3), 554-563.

Dyre, J. C., C. V. Voorhies, R. C. Balling, and R. S. Cerveny, 1995: Lunar phase influence on global temperatures. *Science*, *269*(5228), 1285.

Eddy, J., 1976: The maunder minimum. *Science*, 192(4245), 1189-1202.

Eddy, J., P. Gilman, and D. Trotter, 1977: Anomalous solar rotation in the early 17th century. *Science*, *198*(4319), 824–829.

Eddy, J., F. Stephenson, and K. K. C. Yau, 1989: On pre-telescopic sunspot records. *Quarterly Journal of the Royal Astronomical Society*, 30, 65–73.

Elkibbi, M., and J. A. Rial, 2001: An outsider's review of the astronomical theory of the climate: is the eccentricity-driven insolation the main driver of the ice ages? *Earth-Science Reviews*, *56*, 161–177.

Emile-Geay, J., M. Cane, R. Seager, A. Kaplan, and P. Almasi, 2007: El Niño as a mediator of the solar influence on climate. *Paleoceanography*, *22*(3), 1–16.

Fazel, Z., J. P. Rozelot, S. Lefebvre, a. Ajabshirizadeh, and S. Pireaux, 2008: Solar gravitational energy and luminosity variations. *New Astronomy*, *13*(2), 65–72.

Forbes, J. M., M. E. Hagan, S. Miyahara, Y. Miyoshi, and X. Zhang, 2003: Diurnal nonmigrating tides in the tropical lower atmosphere. Earth Planets Space, 55(7), 419-426.

Foukal, P., and J. Lean, 1988: Magnetic modulation of solar luminosity by photospheric activity. *The Astrophysical Journal*, 328, 347-357.

Frohlich, C., and J. Lean, 1998: The Sun's total irradiance: Cycles, trends and related climate change uncertainties since 1976. *Geophysical Research Letters*, *25*(23), 4377–4380.

Fujita, T.T., 1981: Tornadoes and Downbursts in the context of generalized planetary scales. Journal of the Atmospheric Sciences 38(8), 1511-1534.

Fujita, T.T., D. L. Bradbury, and C.F. Vanthull, 1970: Palm Sunday Tornadoes of April 11, 1965. Monthly Weather Review 98(1), 29.

Gavin, D. G., A. C. G. Henderson, K. S. Westover, S. C. Fritz, I. R. Walker, M. J. Leng, and F. S. Hu, 2011: Abrupt Holocene climate change and potential response to solar forcing in western Canada. *Quaternary Science Reviews*, *30*(9-10), 1243–1255.

Gray, L. J., J. Beer, M. Geller, J. D. Haigh, M. Lockwood, K. Matthes, U. Cubasch, D. Fleitmann, G. Harrison, L. Hood, J. Luterbacher, G. A. Meehl, D. Shindell, B. van Geel, and W. White, 2010: Solar influences on climate. Reviews of Geophysics, 48, RG4001.

Guo, X.L., and M. Y. Huang, 2002: Hail formation and growth in a 3D cloud model with hail-bin microphysics. Atmospheric Research 63(1-2), 59-99.

Hagan, M. E., and J. M. Forbes, 2003: Migrating and nonmigrating semi-diurnal tides in the upper atmosphere excited by tropospheric latent heat release. Journal of Geophysical Research, 108(A2), 1062.

Hagan, M. E., J. M. Forbes, and A. Richmond, 2003: Atmospheric tides, in Encyclopedia of Atmospheric Sciences, Academic, San Diego, California, 1, 159-165.

Haigh, J., 1996: The Impact of Solar Variability on Climate. *Science, 272*(5264), 981–984.

Haigh, J., 2003: The effects of solar variability on the Earth's climate. Philosophical Transactions of the Royal Society A: Mathematical, Physical and Engineering Sciences, 361(1802), 95-111.

Haigh, J., 2011: Solar influences on Climate Executive summary. *Weather*, (5).

Haigh, J., M. Blackburn, and R. Day, 2005: The response of tropospheric circulation to perturbations in lower-stratospheric temperature. *Journal of Climate*, *18*, 3672–3685.

Hanson, K., G. A. Maul, and W. McLeish, 1987: Precipitation and the lunar synodic cycle- Phase progression across the United States, *Journal of climate and Applied Meteorology, 26, 1358-1362*.

Hansteen, V. H., 2010: Stellar winds and magnetic fields. In Heliophysics: Plasma Physics of the Local Cosmos. C. J. Schrijver and G. L. Sisko (eds.), Vol 1, Cambridge University Press, 225pp.

Hoyt, D., and J. Eddy, 1983: Solar irradiance modulation by active regions from 1969 through 1981. *Geophysical research letters*, *10*(7), 509–512.

Imbrie, J., A. Berger, E. Boyle, and S. Clemens, 1993: On the structure and origin of major glaciation cycles 2. The 100,000-year cycle. *Paleoceanography*, *8*(6), 699–735.

Isaaks, E. H., R. M. Srivastava, 1989: An Introduction to Applied Geostatistics, Oxford University Press, Oxford, U.K.

Javaraiah, J., 2005: Sun's retrograde motion and violation of even-odd cycle rule in sunspot activity. *Monthly Notices of the Royal Astronomical Society*, *362*(4), 1311–1318.

Jokipii, J. R., 2010: The heliosphere and cosmic rays. In Heliophysics: Evolving Solar Activity and the climates of space and earth. C. J. Schrijver and G. L. Sisko (eds.), Vol 3, Cambridge University Press, 243pp.

Jose, P., 1965: Sun's motion and sunspots. *The Astronomical Journal*, *70*(3), 193-200.

Kalnay, E., and Coauthors, 1996: The NCEP/NCAR 40-year reanalysis project. Bulletin of the American Meteorological Society, 77, 437-471.

Keeling, C. D., and T. P. Whorf, 1997: Possible forcing of global temperature by the oceanic tides. *Proceedings of the National Academy of Sciences of the United States of America*, *94*(16), 8321–8328.

Keeling, C. D., and T. P. Whorf, 2000: The 1,800-year oceanic tidal cycle: a possible cause of rapid climate change. *Proceedings of the National Academy of Sciences of the United States of America*, *97*(8), 3814–3819.

Kniveton, D.R., B. A. Tinsley, G. B. Burns, E. A. Bering, and O. A. Troshichev, 2008: Variations in global cloud cover and the fair-weather vertical electric field. Journal of Atmospheric and Solar-Terrestrial Physics 70(13), 1663-1642.

Kristjansson, J., J. Kristiansen, and E. Kaas, 2004: Solar activity, cosmic rays, clouds and climate – an update. Advances in Space Research, 34(2), 407-415.

Krahenbuhl, D. S., M. B. Pace, R. S. Cerveny, and R. C. Balling, 2011: Monthly lunar declination extremes' influence on tropospheric circulation patterns. *Journal of Geophysical Research*, *116*(D23), 1–5.

Labitzke, K., and H. van Loon, 1992: On the association between the QBO and the extratropical stratosphere. *Journal of atmospheric and terrestrial physics*, *54*(11), 1453–1463.

Landscheidt, T., 1999: Extrema in sunspot cycle linked to sun's motion. *Solar Physics*, 415–426.

Laut, P., 2003: Solar activity and terrestrial climate: an analysis of some purported correlations. Journal of Atmospheric and Solar-Terrestrial Physics, 65(7), 801-812.

Lean, J., J. Beer, and R. Bradley, 1995: Reconstruction of solar irradiance since 1610: Implications for climate change. *Geophysical Research Letters*, *22*(23), 3195–3198.

Lean, J., and D. Rind, 1998: Climate forcing by changing solar radiation. *Journal of Climate*, 11, 3069–3094.

Lethbridge, M., 1970: Relationship between thunderstorm frequency and lunar phase and declination. *Journal of Geophysical Research*, *75*(27), 5149–5154.

Li, G., 2005: 27.3-day and 13.6-day atmospheric tide and lunar forcing on atmospheric circulation. Advances in Atmospheric Science, 22(3), 359-374.

Li, G., and H. Zong, 2007: 27.3-day and 13.6-day atmospheric tide. Science in China Series D: Earth Sciences, 50.9, 1380-1395.

Li, G., H. Zong., and Q. Zhang, 2011: 27.3-day and average 13.6-day periodic oscillations in the Earth's rotation rate and atmospheric pressure fields due to celestial gravitation forcing. Advances in Atmospheric Science, 28(1), 45-58.

Li, K. J., X. J. Shi, H. F. Liang, L. S. Zhan, J. L. Xie, and W. Feng, 2011: Variations of Solar Rotation and Sunspot Activity. *The Astrophysical Journal*, *730*(1), 49.

Lindzen, R. S., 2005: Dynamics in Atmospheric Physics. Cambridge University Press, Cambridge, U.K., 310 pp.

Lockwood, M., 2006: What do Cosmogenic Isotopes tell us about past solar forcing of Climate? Space Science Reviews, 125(1-4), 95-109.

Lockwood, M., and C. Fröhlich, 2007: Recent oppositely directed trends in solar climate forcings and the global mean surface air temperature. *Proceedings of the Royal Society A: Mathematical, Physical and Engineering Sciences*, *463*(2086), 2447–2460.

Lockwood, M., R. G. Harrison, T. Woollings, and S. K. Solanki, 2010: Are cold winters in Europe associated with low solar activity? *Environmental Research Letters*, *5*(2), 024001.

Loon, H. V., and D. J. Shea, 2000: The global 11-year solar signal in July-August. *Geophysical Research Letters*, *27*(18), 2965–2968.

Ludecke, H., 2011: Long-term instrumental and reconstructed temperature records contradict anthropogenic global warming, *Energy & Environment*, 22(6).

Marsh, N., and H. Svensmark, 2000: Cosmic rays, clouds, and climate. Space Science Reviews, 94, 215-230.

Meeus, J., 1991: Astronomical Algorithms. Willmann-Bell, Richmond, Va., 429 pp.

Merkel, A. W., J. W. Harder, D. R. Marsh, A. K. Smith, J. M. Fontenla, and T. N. Woods, 2011: The impact of solar spectral irradiance variability on middle atmospheric ozone. *Geophysical Research Letters*, *38*(13), 1–6.

Mesinger, M., G. Dimego, E. Kalnay, K. Mitchell, P. C. Shafran, W. Ebisuzaki, D. Jovic et al., 2006: North American Regional Reanalysis: A long-term, consistent, high-resolution climate dataset for the North American Domain. Bulletin of the American Meteorological Society. 87(3), 342-360.

Mironova, I., B. Tinsley, and L. M. Zhou, 2012: The links between atmospheric vorticity, radiation belt electrons, and the solar wind. Advances in Space Research 50(6), 783-790.

Mufti, S., and G. N. Shah, 2011: Solar-geomagnetic activity influence on Earth's climate. *Journal of Atmospheric and Solar-Terrestrial Physics*, *73*(13), 1607–1615.

Muller, R. A., and G. J. MacDonald, 1997: Glacial Cycles and Astronomical Forcing. *Science*, *277*(5323), 215–218.

Nathan, T. R., and E. C. Cordero, 2007: An ozone-modified refractive index for vertically propagating planetary waves. *Journal of Geophysical Research*, *112*(D2), 1–12.

O'Brien, D. P., and R. G. Currie, 1992: Observations of the 18.6-year cycle in air pressure and a theoretical model to explain certain aspects of this signal. Climate Dynamics, 8, 287-298.

Odenwald, S., 2010: The heliosphere and cosmic rays. In Heliophysics: Space Storms and Radiation. C. J. Schrijver and G. L. Sisko (eds.), Vol 2, Cambridge University Press, 15pp.

Palle, E., 2005: Possible satellite perspective effects on the reported correlation between solar activity and clouds. Geophysical Research Letters, 32(3), L03802.

Paluš, M., J. Kurths, U. Schwarz, N. Seehafer, D. Novotná, and I. Charvátová, 2007: The solar activity cycle is weakly synchronized with the solar inertial motion, *Physics Letters A*, *365*(5-6), 421–428.

Park, C.G., 1976: Solar magnetic-sector effects of vertical atmospheric electric-field at Vostok, Antarctica. Geophysical Research Letters 3(8), 475-478.

Perryman, M. A. C., and T. Schulze-Hartung, 2010: The barycentric motion of exoplanet host stars Tests of solar spin – orbit coupling. *Astronomy & Astrophysics*, (1).

Pertsev, N., and P. Dalin, 2010: Lunar semimonthly signal in cloudiness: Lunar-phase or lunar-declination effect? Journal of Atmospheric and Solar-Terrestrial Physics, 72, 713-717.

Polvani, L. M., and P. J. Kushner, 2002: Tropospheric response to stratospheric perturbations in a relatively simple general circulation model. *Science, 29*(7), 40–43.

Prikryl, P., V. Rusin, and M. Rybansky, 2009a: The influence of solar wind on extratropical cyclones – Part 1: Wilcox effect revisited. Annales Geophysicae 27(1), 1-30.

Prikryl, P., D. B. Muldrew, and G. J. Sofko, 2009b: The influence of solar wind on extratropical cyclones – Part 2: A link mediated by auroral atmospheric gravity waves? Annales Geophysicae 27(1), 31-57.

Pudovkin, M. and S. Babushkina, 1992: Influence of solar flares and disturbances of the interplanetary medium on the atmospheric circulation. *Journal of Atmospheric and Terrestrial Physics*, *54*(7-8), 841–846.

Pustilnik, L., and G. Y. Din, 2004: Space Climate Manifestation in Earth Prices – From Medievel England up to modern U.S.A.. *Solar Physics*, (2004), 473–481.

Roldugin, V.C., and B. A. Tinsley, 2004: Atmospheric transparency changes associated with solar wind-induced atmospheric electricity variations. Journal of Atmospheric and Solar-Terrestrial Physics 66(13-14), 1143-1149.

Roy, I., and J. D. Haigh, 2010: Solar cycle signals in sea level pressure and sea surface temperature. *Atmospheric Chemestry and Physics, 10,* 3147–3153.

Roy, I., and J. D. Haigh, 2011: The influence of solar variability and the quasi-biennial oscillation on lower atmospheric temperatures and sea level pressure. *Atmospheric Chemistry and Physics*, *11*(22), 11679–11687.

Rusov, V. D., A. V. Glushkov, V. N. Vaschenko, O. T. Myhalus, Y. a. Bondartchuk, V. P. Smolyar, E. P. Linnik, S. C. Mavrodiev, and B. I. Vachev, 2010: Galactic cosmic rays-clouds effect and bifurcation model of the Earth global climate. Part 1. Theory, *Journal of Atmospheric and Solar-Terrestrial Physics*, *72*(5-6), 398–408.

Ruzmaikin, A., 2004: The pattern of northern hemisphere surface air temperature during prolonged periods of low solar output. *Geophysical Research Letters*, *31*(12), 2–5.

Ruzmaikin, A., 2007: Effect of solar variability on the Earth's climate patterns. *Advances in Space Research*, *40*(7), 1146–1151.

Ruzmaikin, A., J. Feynman, and Y. L. Yung, 2006: Is solar variability reflected in the Nile River? *Journal of Geophysical Research*, *111*(D21), 1–8.

Rycroft, M. ., S. Israelsson, and C. Price, 2000: The global atmospheric electric circuit, solar activity and climate change. *Journal of Atmospheric and Solar-Terrestrial Physics*, *62*(17-18), 1563–1576.

Salby, M. L., and P. F. Callaghan, 2006: Evidence of the solar cycle in the tropical troposphere. *Journal of Geophysical Research*, *111*(D21), 1–8.

Scafetta, N., 2012: Multi-scale harmonic model for solar and climate cyclical variation throughout the Holocene based on Jupiter–Saturn tidal frequencies plus the 11-year solar dynamo cycle. *Journal of Atmospheric and Solar-Terrestrial Physics*, *80*, 296–311.

Scafetta, N., P. Grigolini, T. Imholt, J. Roberts, and B. West, 2004: Solar turbulence in earth's global and regional temperature anomalies. *Physical Review E*, *69*(2), 1–13.

Scafetta, N., and B. J. West, 2006: Phenomenological solar signature in 400 years of reconstructed Northern Hemisphere temperature record. *Geophysical Research Letters*, *33*(17), 1–5.

Scafetta N., and B. J. West, 2006: Phenomenological solar contribution to the 1900-2000 global surface warming. Geophysical Research Letters, 33(5), 2-5.

Schaefer, B. E., J. R. King, and C. P. Deliyannis, 2000: Superflares on ordinary solar-type stars. The Astrophysical Journal, 529, 1026-1030.

Shaffer, J., and R. S. Cerveny, 1998: Long-term equilibrium tides, *Journal of geophysical research*, *103(C9)*, 18801- 18807.

Shaffer, J., R. Cerveny, and R. C. Balling, 1997: Polar temperature sensitivity to lunar forcing? *Geophysical research letters*, *24*(1), 29–32.

Shapiro, R., 1976: Solar magnetic-sector structure and terrestrial atmospheric vorticity. Journal of the Atmospheric Sciences 33(5), 865-870.

Siingh, D., R. P. Singh, A. K. Singh, M. N. Kulkarni, a. S. Gautam, and A. K. Singh, 2011: Solar Activity, Lightning and Climate. *Surveys in Geophysics*, *32*(6), 659–703.

Simpson, I. R., M. Blackburn, and J. D. Haigh, 2009: The Role of Eddies in Driving the Tropospheric Response to Stratospheric Heating Perturbations. *Journal of the Atmospheric Sciences*, *66*(5), 1347–1365.

Solanki, S. K., and N. Krivova, 2003a: Can solar variability explain global warming since 1970? *Journal of Geophysical Research*, *108*(A5), 1200.

Solanki, S. K., and N. A. Krivova, 2005: Solar irradiance variations: from current measurements to long-term estimates. *Solar Physics*, (2004), 197–208.

Solanki, S. K., I. G. Usoskin, B. Kromer, M. Schüssler, and J. Beer, 2004: Unusual activity of the Sun during recent decades compared to the previous 11,000 years. *Nature*, *431*(7012), 1084–1087.

Stager, J. C., A. Ruzmaikin, D. Conway, P. Verburg, and P. J. Mason, 2007: Sunspots, El Niño, and the levels of Lake Victoria, East Africa. *Journal of Geophysical Research*, *112*(D15), 1–13.

Stuiver, M., and T. F. Braziunas, 1993: Sun, ocean, climate and atmospheric 14CO2 : an evaluation of causal and spectral relationships. *The Holocene*, *3*(4), 289–305.

Svensmark, H., 2000: Cosmic rays and earth's climate. Space Science Reviews, 93, 155-166.

Svensmark, H., and E. Friis-Christensen, 1997: Variation of cosmic ray flux and global cloud coverage—a missing link in solar-climate relationships. Journal of Atmospheric and Solar-Terrestrial Physics, 59(11), 1225-1232.

Thejll, P., B. Christiansen, and H. Gleisner, 2003: On correlations between the North Atlantic Oscillation, geopotential heights, and geomagnetic activity. *Geophysical Research Letters*, *30*(6), 1–4.

Tinsley, B.A., 1996: Correlations of atmospheric dynamics with solar wind-induced changes of air-earth current density into cloud tops. Journal of Geophysical Research-Atmospheres 101(D23), 29701-29714.

Tinsley, B.A., 2000: Influence of solar wind on the global electric circuit, and inferred effects on cloud microphysics, temperature, and the dynamics in the troposphere. Space Science Reviews 94(1-2), 231-258.

Tinsley, B. A., 2012: A working hypothesis for connections between electrically-induced changes in cloud microphysics and storm vorticity, with possible effects on circulation, *Advances in Space Research*, 50(6), 791-805.

Tinsley, B. A., G. B. Burns, and L. Zhou, 2007: The role of the global electric circuit in solar and internal forcing of clouds and climate. *Advances in Space Research*, *40*(7), 1126–1139.

Tinsley, B., J. Hoeksema, and D. Baker, 1994: Stratospheric volcanic aerosols and changes in air-earth current density at solar wind magnetic sector boundaries as conditions for the Wilcox tropospheric vorticity. *Journal of geophysical research*, *99*, 805–813.

Usoskin, I. G., and G. A. Kovaltsov, 2008: Cosmic rays and climate of the Earth: Possible connection. Comptes Rendus Geoscience, 340(7), 441-450.

van Loon, H., G. A. Meehl, and D. J. Shea: 2007: Coupled air-sea response to solar forcing in the Pacific region during northern winter. *Journal of Geophysical Research*, *112*(D2), 1–8.

Veretenenko, S., and P. Thejll, 2004: Effects of energetic solar proton events on the cyclone development in the North Atlantic. Journal of Atmospheric and Solar-Terrestrial Physics 66(5), 393-405.

Voiculescu, M., I. G. Usoskin, and K. Mursula, 2006: Different response of clouds to solar input. Geophysical Research Letters, 33(21), L21802.

Voiculescu, M., and I. Usoskin, 2012: Persistent solar signatures in cloud cover: spatial and temporal analysis. Environmental Research Letters, 7(4), 044004.

Wilcox, J.M., P. H. Scherrer, L. Svalgaar, W. O. Roberts, R. H. Olson, and R. L. Jenne, 1974: Influence of solar magnetic-sector structure on terrestrial atmospheric vorticity. Journal of the Atmospheric Sciences 31(2), 581-588.

Yu, F., 2002: Altitude variations of cosmic ray induced productions of aerosols: Implications for global cloudiness and climate. Journal of Geophysical Research, 107(A7), 1118.

APPENDIX A

GLOSSARY

AO	Arctic Oscillation

Ap	Ap Geomagnetic Index
CCN	Cloud Condensation Nuclei
CME	Coronal Mass Ejection
EF	Enhanced Fujita
ENSO	El Nino Southern Oscillation
EUV	Extreme Ultra-Violet
GCR	Galactic Cosmic Ray
GEC	Global Electric Circuit
HCS	Heliospheric Current Sheet
hPa	hecto-Pascals
IMF	Interplanetary Magnetic Field
ISCCP	International Satellite Cloud Climatology Project
ITCZ	Inter-Tropical Convergence Zone
LIA	Little Ice Age
MLD	Maximum Lunar Declination
N2P	Negative to Positive
NAM	Northern Annular Mode
NAO	North Atlantic Oscillation
NARR	North American Regional Reanalysis
NASA JPL	National Aeronautics and Space Administration Jet Propulsion Laboratory
NCAR	National Center for Atmospheric Research
NCEP	National Centers for Environmental Prediction
NSSDC	National Space Science Data Center
NWS	National Weather Service
OMRI	Ozone-Modified Refractive Index
P2N	Positive to Negative
PDO	Pacific Decadal Oscillation

QBO	Quasi-Biennial Oscillation
REF	Relativistic Electron Flux
Rz	Sunspot Number
SPC	Storm Prediction Center
SPE	Superposed Epoch Analysis
SSN	Sunspot Number
TSI	Total Solar Irradiance
UV	Ultra-Violet
VAI	Vorticity Area Index
VEI	Volcanic Explosively Index

APPENDIX B

HCS CROSSING DATES

Positive to Negative Magnetic Sector Crossing Dates

1963/11/29 15:00:00
1963/12/12 22:00:00
1963/12/27 15:00:00
1964/1/8 10:00:00
1964/1/26 16:00:00
1964/2/4 21:00:00
1965/6/7 13:59:59
1965/6/20 01:00:00
1965/7/11 22:59:59
1965/7/26 22:59:59
1965/8/28 01:59:59
1965/9/22 13:00:00
1965/10/27 06:00:00
1965/11/24 13:00:00
1965/12/5 01:59:59
1965/12/23 06:00:00
1966/1/3 19:00:00
1966/1/21 07:00:00
1966/7/7 21:00:00
1966/8/18 13:59:59
1966/9/7 07:59:59
1966/9/13 00:00:00
1966/10/12 12:00:00
1966/10/20 21:00:00
1966/11/9 03:00:00
1966/12/4 22:59:59
1967/1/1 21:00:00
1967/1/12 19:00:00
1967/2/8 07:00:00
1967/3/9 16:59:59
1967/3/15 13:59:59
1967/4/1 21:00:00
1967/5/10 18:00:00
1967/6/26 13:59:59
1967/7/10 16:00:00
1967/8/9 15:00:00
1967/9/6 10:59:59
1967/10/3 15:00:00
1967/10/29 16:59:59
1967/11/7 03:00:00
1967/12/5 15:00:00
1967/12/31 22:59:59
1968/1/29 22:59:59
1968/2/27 07:00:00
1968/3/24 00:00:00
1968/4/22 04:59:59
1968/5/18 00:00:00
1968/6/1 19:00:00
1968/6/12 04:59:59
1968/6/28 13:59:59
1968/7/10 15:00:00
1968/7/26 04:00:00
1968/8/6 15:00:00
1968/8/21 19:59:59
1968/9/4 21:00:00
1968/9/19 18:00:00
1968/9/29 19:59:59
1968/10/16 00:00:00
1968/11/13 16:59:59
1968/12/10 16:59:59
1969/1/7 13:00:00
1969/2/3 12:00:00
1969/3/5 18:00:00
1969/4/1 06:00:00
1969/4/14 10:00:00
1969/5/13 15:00:00
1969/5/27 16:59:59
1969/6/23 13:00:00
1969/7/21 15:00:00
1969/8/19 10:00:00
1969/9/14 03:00:00
1969/10/16 10:00:00
1969/11/11 13:00:00
1969/12/10 04:00:00
1970/1/6 13:00:00
1970/2/3 16:00:00
1970/3/1 01:59:59
1970/4/16 13:00:00
1970/5/12 01:59:59
1970/5/22 07:59:59
1970/6/8 15:00:00
1970/7/6 03:00:00
1970/8/2 07:00:00
1970/9/2 06:00:00
1970/9/28 19:59:59
1970/10/27 18:00:00
1970/11/15 22:59:59
1970/11/25 16:00:00
1970/12/14 18:00:00
1970/12/23 10:59:59
1971/1/19 22:59:59
1971/2/2 19:59:59
1971/3/15 01:59:59
1971/3/30 10:00:00
1971/4/8 00:00:00
1971/5/7 07:00:00
1971/5/22 22:59:59
1971/6/2 09:00:00
1971/6/29 06:00:00
1971/7/18 16:59:59

1971/8/16 16:59:59
1971/8/24 16:00:00
1971/9/19 16:59:59
1971/10/7 01:00:00
1971/11/6 19:00:00
1971/12/2 16:00:00
1971/12/29 04:59:59
1972/1/22 09:00:00
1972/2/17 00:00:00
1972/3/16 01:00:00
1972/3/31 12:00:00
1972/4/11 01:00:00
1972/4/27 19:00:00
1972/5/9 16:59:59
1972/5/23 09:00:00
1972/6/4 22:00:00
1972/6/16 22:59:59
1972/6/21 12:00:00
1972/7/3 22:00:00
1972/7/16 01:00:00
1972/8/4 22:00:00
1972/9/4 12:00:00
1972/10/1 04:00:00
1972/11/4 00:00:00
1972/11/12 09:00:00
1972/11/22 07:00:00
1972/12/2 10:00:00
1972/12/21 07:59:59
1973/1/2 07:59:59
1973/1/20 07:59:59
1973/2/17 12:00:00
1973/3/18 15:00:00
1973/4/16 16:59:59
1973/5/13 16:59:59
1973/6/11 21:00:00
1973/7/8 19:59:59
1973/7/23 10:59:59
1973/8/11 15:00:00
1973/9/10 16:00:00
1973/9/13 21:00:00
1973/10/9 04:59:59
1973/10/24 04:59:59
1973/11/5 09:00:00
1973/11/21 13:00:00
1973/12/4 16:00:00
1973/12/17 22:59:59
1973/12/28 01:00:00
1974/1/24 10:59:59
1974/2/21 04:00:00
1974/3/21 01:59:59
1974/4/17 01:59:59
1974/5/13 18:00:00
1974/6/9 07:59:59
1974/7/8 00:00:00
1974/8/3 01:59:59
1974/8/30 01:00:00
1974/9/26 22:59:59
1974/10/20 18:00:00
1974/11/20 10:00:00
1974/12/3 07:00:00
1974/12/17 13:00:00
1974/12/31 01:59:59
1975/1/13 06:00:00
1975/2/10 18:00:00
1975/3/7 13:59:59
1975/4/2 07:59:59
1975/4/30 09:00:00
1975/5/29 00:00:00
1975/6/27 16:00:00
1975/7/26 00:00:00
1975/8/21 15:00:00
1975/9/17 07:59:59
1975/10/16 04:00:00
1975/11/17 16:00:00
1975/12/11 07:59:59
1976/1/31 07:59:59
1976/2/26 10:59:59
1976/3/25 06:00:00
1976/4/20 19:00:00
1976/5/16 15:00:00
1976/5/26 00:00:00
1976/6/27 19:00:00
1976/8/17 18:00:00
1976/11/18 19:00:00
1976/12/2 22:00:00
1976/12/15 00:00:00
1976/12/26 12:00:00
1977/1/14 16:00:00
1977/3/21 18:00:00
1977/4/3 12:00:00
1977/4/30 16:00:00
1977/5/14 19:59:59
1977/6/2 22:59:59
1977/6/9 19:00:00
1977/6/28 19:00:00
1977/7/11 04:00:00
1977/8/4 13:00:00
1977/8/31 13:00:00
1977/9/27 06:00:00
1977/10/26 01:59:59
1977/11/19 19:59:59
1977/12/25 07:59:59
1978/1/30 16:00:00
1978/3/19 00:00:00
1978/4/26 22:59:59
1978/5/11 18:00:00
1978/6/20 07:00:00
1978/7/21 22:00:00

1978/8/15 22:59:59
1978/9/10 01:59:59
1978/9/13 01:59:59
1978/9/26 09:00:00
1978/10/8 00:00:00
1978/11/7 04:59:59
1978/12/3 18:00:00
1978/12/29 04:00:00
1979/1/2 12:00:00
1979/1/24 22:00:00
1979/2/24 15:00:00
1979/3/24 00:00:00
1979/4/21 10:00:00
1979/5/18 13:00:00
1979/6/1 19:00:00
1979/6/16 07:59:59
1979/7/12 10:59:59
1979/8/11 00:00:00
1979/9/14 06:00:00
1979/10/5 03:00:00
1979/10/14 03:00:00
1979/12/7 01:59:59
1980/1/3 01:59:59
1980/1/23 22:00:00
1980/1/28 07:00:00
1980/2/24 19:59:59
1980/3/14 21:00:00
1980/3/26 04:00:00
1980/4/11 13:59:59
1980/5/6 04:00:00
1980/6/1 01:59:59
1980/6/8 01:59:59
1980/6/25 19:59:59
1980/7/21 06:00:00
1980/8/3 10:00:00
1980/8/18 12:00:00
1980/8/29 16:00:00
1980/9/14 07:59:59
1980/9/28 01:59:59
1980/10/8 00:00:00
1980/10/24 15:00:00
1980/11/5 22:00:00
1980/11/21 18:00:00
1980/12/4 00:00:00
1981/1/1 12:00:00
1981/1/18 18:00:00
1981/1/27 10:00:00
1981/2/23 22:00:00
1981/3/25 22:00:00
1981/4/20 01:59:59
1981/5/15 16:00:00
1981/6/15 18:00:00
1981/7/11 21:00:00
1981/7/27 19:59:59
1981/8/7 16:59:59
1981/8/24 15:00:00
1981/9/3 13:00:00
1981/9/18 19:00:00
1981/9/29 21:00:00
1981/10/13 15:00:00
1981/10/27 00:00:00
1981/11/10 04:59:59
1981/11/25 13:59:59
1981/12/12 09:00:00
1981/12/23 16:59:59
1982/1/6 19:00:00
1982/2/3 12:00:00
1982/2/22 03:00:00
1982/3/7 01:59:59
1982/3/30 10:59:59
1982/4/28 07:00:00
1982/5/27 01:59:59
1982/6/24 03:00:00
1982/7/14 12:00:00
1982/7/20 01:59:59
1982/8/15 21:00:00
1982/9/3 06:00:00
1982/10/9 04:00:00
1982/11/7 06:00:00
1982/12/3 13:00:00
1982/12/30 16:00:00
1983/1/25 18:00:00
1983/3/19 03:00:00
1983/4/15 22:59:59
1983/5/12 06:00:00
1983/6/17 16:59:59
1983/7/9 04:59:59
1983/7/21 16:59:59
1983/8/3 03:00:00
1983/8/30 13:59:59
1983/10/5 15:00:00
1983/11/2 10:59:59
1983/11/15 13:59:59
1983/12/12 04:59:59
1984/1/6 22:59:59
1984/2/2 16:00:00
1984/2/26 22:59:59
1984/3/28 16:59:59
1984/5/18 07:00:00
1984/6/16 06:00:00
1984/7/13 06:00:00
1984/8/8 07:00:00
1984/8/31 04:59:59
1984/9/26 16:00:00
1984/10/29 10:59:59
1985/2/18 10:00:00
1985/3/20 15:00:00
1985/4/12 09:00:00

1985/5/3 22:59:59
1985/5/31 22:00:00
1985/6/25 15:00:00
1985/7/23 09:00:00
1985/8/18 07:59:59
1985/9/16 00:00:00
1985/10/11 16:59:59
1985/11/10 07:59:59
1986/1/6 01:00:00
1986/2/7 03:00:00
1986/3/5 10:00:00
1986/4/5 00:00:00
1986/4/30 13:59:59
1986/5/30 19:00:00
1986/6/27 16:59:59
1986/7/25 21:00:00
1986/11/2 21:00:00
1986/12/6 07:00:00
1987/4/2 09:00:00
1987/4/30 22:00:00
1987/5/22 18:00:00
1987/6/16 22:00:00
1987/7/14 00:00:00
1987/8/14 03:00:00
1987/9/8 04:59:59
1987/10/7 09:00:00
1987/11/3 19:00:00
1987/12/6 06:00:00
1987/12/31 13:00:00
1988/1/13 19:59:59
1988/1/26 22:59:59
1988/2/23 22:00:00
1988/3/23 01:59:59
1988/4/16 16:00:00
1988/5/18 15:00:00
1988/6/14 04:00:00
1988/6/30 01:59:59
1988/8/20 18:00:00
1988/9/15 18:00:00
1988/10/11 01:59:59
1988/11/11 09:00:00
1988/12/11 16:00:00
1988/12/31 13:59:59
1989/1/2 15:00:00
1989/1/31 21:00:00
1989/2/24 19:59:59
1989/3/28 18:00:00
1989/4/26 10:00:00
1989/5/24 16:59:59
1989/6/19 19:59:59
1989/7/9 22:59:59
1989/7/23 22:00:00
1989/8/19 10:59:59
1989/9/3 19:00:00
1989/10/3 12:00:00
1989/10/30 00:00:00
1989/11/23 01:59:59
1989/12/19 04:00:00
1990/1/16 00:59:59
1990/2/12 18:00:00
1990/3/17 02:00:00
1990/5/10 15:59:59
1990/6/6 20:00:00
1990/6/30 03:00:00
1990/7/26 03:00:00
1990/8/27 06:00:00
1990/9/26 00:00:00
1990/10/23 08:00:00
1990/11/15 06:59:59
1990/12/12 17:00:00
1991/1/13 00:59:59
1991/2/8 06:59:59
1991/3/3 14:00:00
1991/4/24 03:00:00
1991/5/22 21:59:59
1991/6/18 11:00:00
1991/7/20 06:59:59
1991/8/8 00:59:59
1991/9/9 09:59:59
1991/10/5 21:00:00
1991/11/28 21:59:59
1991/12/30 09:00:00
1992/1/25 09:00:00
1992/2/20 05:00:00
1992/3/21 12:59:59
1992/4/23 02:00:00
1992/5/18 14:00:00
1992/6/16 12:00:00
1992/7/9 00:59:59
1992/7/31 08:00:00
1992/8/16 15:00:00
1992/9/12 20:00:00
1992/10/6 03:59:59
1992/11/11 15:59:59
1992/12/9 21:59:59
1993/1/31 05:00:00
1993/3/3 21:59:59
1993/3/27 14:00:00
1993/5/7 06:00:00
1993/7/25 12:00:00
1993/8/18 15:00:00
1993/9/22 06:00:00
1993/11/21 00:59:59
1993/12/16 11:00:00
1994/1/11 18:00:00
1994/2/8 12:00:00
1994/3/6 12:59:59
1994/4/3 00:00:00

1994/5/2 21:59:59
1994/5/28 12:00:00
1994/6/25 14:00:00
1994/7/24 06:59:59
1994/8/17 21:59:59
1994/9/17 06:59:59
1994/10/14 08:00:00
1994/11/12 15:00:00
1994/12/7 05:00:00
1994/12/21 06:59:59
1995/1/3 00:59:59
1995/1/17 09:59:59
1995/1/29 08:00:00
1995/2/11 21:00:00
1995/2/26 17:00:00
1995/3/10 12:59:59
1995/3/25 21:59:59
1995/4/7 05:00:00
1995/4/20 18:00:00
1995/5/3 03:59:59
1995/5/17 20:00:00
1995/5/31 08:00:00
1995/6/14 23:00:00
1995/6/26 00:00:00
1995/7/11 15:59:59
1995/7/24 20:00:00
1995/8/7 02:00:00
1995/8/20 06:59:59
1995/9/17 21:59:59
1995/9/29 11:00:00
1995/10/18 12:00:00
1995/10/27 00:00:00
1995/11/14 15:00:00
1995/11/22 21:00:00
1995/12/6 09:59:59
1995/12/12 06:59:59
1995/12/20 20:00:00
1995/12/31 21:59:59
1996/1/25 14:00:00
1996/2/18 08:00:00
1996/3/10 02:00:00
1996/4/10 15:00:00
1996/5/1 23:00:00
1996/5/14 06:59:59
1996/5/31 12:59:59
1996/6/15 03:00:00
1996/6/28 08:00:00
1996/7/12 06:59:59
1996/8/7 11:00:00
1996/9/4 20:00:00
1996/9/29 20:00:00
1996/10/28 00:00:00
1996/11/24 18:59:59
1996/12/5 00:59:59
1996/12/21 20:00:00
1996/12/26 14:00:00
1997/1/19 15:59:59
1997/2/13 21:00:00
1997/3/12 11:00:00
1997/3/22 18:59:59
1997/4/3 09:59:59
1997/4/17 15:00:00
1997/4/29 20:00:00
1997/5/18 06:00:00
1997/5/27 15:59:59
1997/6/19 11:00:00
1997/6/27 00:59:59
1997/7/8 03:59:59
1997/7/25 03:59:59
1997/8/4 15:00:00
1997/8/26 03:00:00
1997/9/4 20:00:00
1997/9/19 03:59:59
1997/10/3 18:59:59
1997/10/23 18:59:59
1997/11/1 20:00:00
1997/11/8 06:00:00
1997/11/17 14:00:00
1997/11/24 20:00:00
1997/12/8 03:00:00
1998/1/11 09:00:00
1998/1/30 23:00:00
1998/2/27 09:00:00
1998/3/10 21:59:59
1998/3/26 09:59:59
1998/4/8 00:59:59
1998/4/24 17:00:00
1998/5/5 09:00:00
1998/5/21 08:00:00
1998/6/4 02:00:00
1998/6/19 03:59:59
1998/7/2 00:00:00
1998/7/16 15:59:59
1998/7/29 21:00:00
1998/8/20 20:00:00
1998/9/4 21:00:00
1998/9/28 23:00:00
1998/10/15 03:00:00
1998/10/27 21:00:00
1998/11/11 17:00:00
1998/11/24 08:00:00
1998/12/12 03:00:00
1998/12/30 12:59:59
1999/1/6 02:00:00
1999/2/3 06:00:00
1999/3/1 00:00:00
1999/3/29 23:00:00
1999/4/26 15:59:59

1999/5/13 17:00:00
1999/5/24 18:59:59
1999/6/9 03:00:00
1999/6/24 11:00:00
1999/7/3 17:00:00
1999/7/31 11:00:00
1999/8/11 00:59:59
1999/8/25 14:00:00
1999/9/7 09:00:00
1999/9/22 14:00:00
1999/10/3 18:59:59
1999/10/20 21:00:00
1999/10/31 03:59:59
1999/11/18 21:00:00
1999/11/26 08:00:00
1999/12/15 06:00:00
1999/12/28 15:00:00
2000/1/10 05:00:00
2000/1/23 20:00:00
2000/2/6 00:59:59
2000/3/6 08:00:00
2000/3/31 21:59:59
2000/4/28 11:00:00
2000/5/25 20:00:00
2000/6/22 17:00:00
2000/7/18 15:00:00
2000/8/16 00:59:59
2000/8/18 03:59:59
2000/9/11 03:00:00
2000/9/16 15:59:59
2000/10/7 06:00:00
2000/10/15 20:00:00
2000/11/1 09:00:00
2000/11/9 15:00:00
2000/11/25 00:59:59
2000/12/7 17:00:00
2000/12/25 11:00:00
2001/1/4 21:00:00
2001/1/21 11:00:00
2001/2/14 12:59:59
2001/3/13 00:00:00
2001/3/24 03:00:00
2001/4/7 05:00:00
2001/5/7 08:00:00
2001/6/3 03:00:00
2001/6/28 12:00:00
2001/7/25 14:00:00
2001/8/11 03:59:59
2001/8/20 09:59:59
2001/9/15 09:00:00
2001/10/6 00:00:00
2001/10/14 00:00:00
2001/10/24 21:59:59
2001/11/4 20:00:00
2001/11/25 05:00:00
2001/12/25 06:00:00
2002/1/19 21:59:59
2002/2/16 18:00:00
2002/3/22 15:59:59
2002/4/16 08:00:00
2002/5/7 06:59:59
2002/6/2 11:00:00
2002/6/29 14:00:00
2002/7/25 02:00:00
2002/8/20 18:00:00
2002/9/17 06:00:00
2002/10/15 00:59:59
2002/11/10 02:00:00
2002/12/7 09:00:00
2003/1/3 21:59:59
2003/1/29 11:00:00
2003/2/27 03:59:59
2003/3/26 23:00:00
2003/4/21 00:00:00
2003/5/19 00:59:59
2003/6/14 05:00:00
2003/7/12 17:00:00
2003/8/4 15:00:00
2003/9/1 12:59:59
2003/10/1 17:00:00
2003/10/24 06:00:00
2003/11/22 18:00:00
2003/12/19 15:00:00
2004/1/13 06:00:00
2004/2/11 06:59:59
2004/3/10 21:59:59
2004/4/4 09:00:00
2004/5/1 14:00:00
2004/5/29 18:00:00
2004/6/26 11:00:00
2004/7/20 06:59:59
2004/7/30 06:00:00
2004/8/14 15:59:59
2004/8/25 20:00:00
2004/8/31 12:59:59
2004/9/11 17:00:00
2004/9/20 03:00:00
2004/10/9 02:00:00
2004/10/18 12:59:59
2004/11/3 12:59:59
2004/11/13 08:00:00
2004/11/29 15:00:00
2004/12/15 06:59:59
2004/12/25 12:59:59
2005/1/9 11:00:00
2005/1/22 12:00:00
2005/2/6 06:00:00
2005/3/5 03:59:59

2005/3/16 21:00:00
2005/4/2 09:00:00
2005/4/29 15:00:00
2005/5/9 02:00:00
2005/5/21 15:59:59
2005/5/28 03:59:59
2005/6/5 00:00:00
2005/6/22 03:00:00
2005/7/2 09:59:59
2005/7/19 17:00:00
2005/7/29 00:59:59
2005/8/14 09:59:59
2005/8/25 06:00:00
2005/9/10 21:00:00
2005/9/25 05:00:00
2005/10/7 11:00:00
2005/10/22 02:00:00
2005/11/2 15:59:59
2005/11/19 06:00:00
2005/11/29 00:00:00
2005/12/24 00:59:59
2006/1/26 08:00:00
2006/2/8 11:00:00
2006/2/18 21:59:59
2006/3/6 15:00:00
2006/3/18 15:00:00
2006/4/13 06:00:00
2006/5/11 08:00:00
2006/5/26 12:59:59
2006/6/6 15:59:59
2006/6/22 15:59:59
2006/7/4 23:00:00
2006/7/31 06:00:00
2006/8/17 09:00:00
2006/8/27 06:00:00
2006/9/10 14:00:00
2006/9/24 17:00:00
2006/10/7 14:00:00
2006/10/19 18:59:59
2006/11/4 15:00:00
2006/11/16 15:59:59
2006/12/2 03:59:59
2006/12/10 09:00:00
2006/12/29 12:59:59
2007/1/8 14:00:00
2007/1/26 18:59:59
2007/2/4 20:00:00
2007/2/22 21:00:00
2007/3/5 00:00:00
2007/3/22 00:59:59
2007/4/1 15:00:00
2007/4/16 08:00:00
2007/4/27 03:00:00
2007/5/15 09:00:00
2007/5/24 15:00:00
2007/6/8 03:00:00
2007/6/22 00:00:00
2007/7/3 17:00:00
2007/7/19 12:00:00
2007/7/29 03:59:59
2007/8/15 14:00:00
2007/9/14 09:59:59
2007/10/11 18:00:00
2007/11/8 03:00:00
2007/12/3 23:00:00
2007/12/25 14:00:00
2008/1/4 08:00:00
2008/1/31 11:00:00
2008/2/27 09:59:59
2008/3/26 06:59:59
2008/4/15 09:59:59
2008/4/22 18:59:59
2008/5/20 02:00:00
2008/6/7 18:00:00
2008/7/4 23:00:00
2008/7/31 06:59:59
2008/8/25 21:00:00
2008/9/20 20:00:00
2008/10/19 06:00:00
2008/11/15 12:00:00
2008/12/11 15:00:00
2008/12/22 12:00:00
2009/1/9 09:59:59
2009/2/4 00:00:00
2009/3/11 00:00:00
2009/4/8 15:00:00
2009/5/6 08:00:00
2009/5/19 00:59:59
2009/5/27 02:00:00
2009/6/3 18:59:59
2009/6/21 17:00:00
2009/7/10 02:00:00
2009/7/22 00:59:59
2009/8/6 03:00:00
2009/8/18 03:59:59
2009/9/14 17:00:00
2009/9/30 06:00:00
2009/10/11 17:00:00
2009/10/29 18:59:59
2009/12/5 05:00:00
2009/12/14 20:00:00
2010/1/7 02:00:00
2010/1/31 17:00:00
2010/3/2 08:00:00
2010/3/30 18:59:59
2010/4/20 03:59:59
2010/4/30 14:00:00
2010/5/17 00:59:59

2010/5/26 14:00:00
2010/6/14 00:00:00
2010/6/25 14:00:00
2010/7/13 14:00:00
2010/7/19 12:00:00
2010/8/14 06:59:59
2010/8/21 09:00:00
2010/9/9 18:59:59
2010/10/19 11:00:00
2010/11/6 18:59:59
2010/11/13 18:59:59
2010/12/8 06:59:59
2011/1/6 09:59:59
2011/1/26 11:00:00
2011/2/2 03:59:59
2011/2/19 18:00:00
2011/2/28 17:00:00
2011/3/20 21:00:00
2011/4/3 09:59:59
2011/4/29 05:00:00
2011/5/27 09:00:00
2011/6/22 03:00:00
2011/7/18 12:59:59
2011/8/13 21:00:00
2011/9/10 06:00:00
2011/9/19 05:00:00
2011/9/30 12:00:00
2011/10/10 09:59:59
2011/11/7 15:00:00
2011/12/8 00:59:59
2011/12/20 08:00:00
2011/12/30 06:59:59
2012/1/7 00:59:59
2012/1/15 11:00:00
2012/2/3 06:59:59
2012/2/14 14:00:00
2012/3/2 03:59:59
2012/3/13 12:59:59
2012/3/27 06:00:00
2012/4/11 12:59:59
2012/5/9 17:00:00
2012/5/21 15:59:59
2012/6/4 12:00:00

Negative to Positive Magnetic Sector Crossing Dates

1963/12/4 12:00:00
1963/12/20 22:00:00
1964/1/4 13:59:59
1964/1/18 10:00:00
1964/1/27 15:00:00
1964/2/12 07:59:59
1965/6/12 18:00:00
1965/7/6 22:59:59
1965/7/22 09:00:00
1965/8/20 18:00:00
1965/9/16 06:00:00
1965/10/25 12:00:00
1965/11/18 16:59:59
1965/12/1 13:59:59
1965/12/17 01:59:59
1965/12/25 03:00:00
1966/1/16 19:59:59
1966/7/6 10:59:59
1966/8/14 18:00:00
1966/9/4 16:59:59
1966/9/8 10:59:59
1966/10/5 01:59:59
1966/10/16 22:59:59
1966/10/30 16:59:59
1966/11/28 16:59:59
1966/12/24 16:00:00
1967/1/20 09:00:00
1967/2/24 09:00:00
1967/3/12 15:00:00
1967/3/24 04:00:00
1967/4/24 13:00:00
1967/6/23 10:00:00
1967/7/8 10:59:59
1967/8/4 13:00:00
1967/8/31 04:00:00
1967/9/28 03:00:00
1967/10/25 19:00:00
1967/11/5 09:00:00
1967/11/22 15:00:00
1967/12/20 19:00:00
1968/1/19 04:59:59
1968/2/13 03:00:00
1968/3/13 15:00:00
1968/4/6 21:00:00
1968/5/3 03:00:00
1968/5/30 22:59:59
1968/6/7 04:59:59
1968/6/22 09:00:00
1968/7/3 18:00:00
1968/7/18 10:59:59
1968/8/1 15:00:00
1968/8/14 07:59:59
1968/8/31 19:00:00
1968/9/10 07:00:00
1968/9/28 16:00:00
1968/10/7 04:59:59
1968/11/2 10:00:00
1968/11/30 07:59:59
1968/12/25 22:59:59
1969/1/23 16:00:00
1969/2/19 01:00:00
1969/3/25 22:00:00
1969/4/12 10:00:00
1969/4/21 04:00:00
1969/5/19 04:59:59
1969/6/15 03:00:00
1969/7/13 00:00:00
1969/8/7 21:00:00
1969/9/5 16:00:00
1969/10/2 01:59:59
1969/10/31 04:00:00
1969/11/27 15:00:00
1969/12/24 07:59:59
1970/1/18 19:59:59
1970/2/9 22:00:00
1970/3/9 07:00:00
1970/4/30 03:00:00
1970/5/16 21:00:00
1970/5/27 04:00:00
1970/6/23 10:00:00
1970/7/25 03:00:00
1970/8/18 16:00:00
1970/9/13 10:00:00
1970/10/11 10:00:00
1970/11/9 12:00:00
1970/11/21 06:00:00
1970/12/4 01:00:00
1970/12/17 10:59:59
1970/12/31 04:00:00
1971/1/28 00:00:00
1971/2/25 22:00:00
1971/3/23 16:00:00
1971/4/4 07:00:00
1971/4/20 01:00:00
1971/5/18 07:00:00
1971/5/29 21:00:00
1971/6/16 18:00:00
1971/7/13 12:00:00
1971/8/9 06:00:00
1971/8/20 13:00:00

1971/9/5 10:59:59
1971/9/30 18:00:00
1971/10/28 09:00:00
1971/11/23 01:59:59
1971/12/16 04:59:59
1972/1/16 22:59:59
1972/2/11 07:00:00
1972/3/7 12:00:00
1972/3/27 19:59:59
1972/4/4 03:00:00
1972/4/24 10:00:00
1972/5/2 06:00:00
1972/5/17 00:00:00
1972/5/28 18:00:00
1972/6/11 01:00:00
1972/6/19 10:00:00
1972/6/25 07:59:59
1972/7/12 01:00:00
1972/7/23 10:59:59
1972/8/18 00:00:00
1972/9/9 09:00:00
1972/10/10 18:00:00
1972/11/8 09:00:00
1972/11/14 16:59:59
1972/11/28 15:00:00
1972/12/13 10:59:59
1973/1/7 22:59:59
1973/2/5 13:00:00
1973/3/6 06:00:00
1973/4/3 03:00:00
1973/4/24 22:59:59
1973/5/27 22:00:00
1973/6/24 01:00:00
1973/7/18 13:59:59
1973/7/24 04:59:59
1973/8/22 19:00:00
1973/9/12 22:00:00
1973/9/20 03:00:00
1973/10/15 10:59:59
1973/10/28 07:00:00
1973/11/14 03:00:00
1973/11/24 13:59:59
1973/12/14 09:00:00
1973/12/19 10:59:59
1974/1/14 16:59:59
1974/2/10 22:59:59
1974/3/12 06:00:00
1974/4/4 07:59:59
1974/5/2 07:00:00
1974/5/30 16:00:00
1974/6/26 10:00:00
1974/7/23 18:00:00
1974/8/20 21:00:00
1974/9/13 22:00:00
1974/10/13 04:59:59
1974/11/9 13:00:00
1974/12/1 19:00:00
1974/12/7 18:00:00
1974/12/28 04:59:59
1975/1/4 01:59:59
1975/1/24 04:59:59
1975/2/20 10:59:59
1975/3/22 00:00:00
1975/4/15 03:00:00
1975/5/16 15:00:00
1975/6/11 01:00:00
1975/7/8 10:00:00
1975/8/2 06:00:00
1975/8/28 21:00:00
1975/9/25 18:00:00
1975/10/28 01:59:59
1975/11/22 15:00:00
1975/12/25 13:00:00
1976/1/21 07:00:00
1976/2/16 19:59:59
1976/3/14 04:59:59
1976/4/13 22:00:00
1976/5/9 01:00:00
1976/5/23 13:59:59
1976/6/5 07:59:59
1976/6/30 21:00:00
1976/8/20 15:00:00
1976/11/25 13:00:00
1976/12/8 13:59:59
1976/12/22 04:00:00
1977/1/6 01:59:59
1977/3/12 19:59:59
1977/3/30 16:00:00
1977/4/15 04:00:00
1977/5/9 13:59:59
1977/5/15 10:59:59
1977/6/4 16:00:00
1977/6/17 04:00:00
1977/7/2 10:59:59
1977/7/14 16:00:00
1977/8/16 04:00:00
1977/9/9 18:00:00
1977/10/10 22:59:59
1977/11/3 04:00:00
1977/12/11 13:00:00
1978/1/8 18:00:00
1978/2/9 07:00:00
1978/4/17 21:00:00
1978/5/1 16:00:00
1978/6/15 19:59:59
1978/6/28 00:00:00
1978/8/4 01:00:00
1978/8/26 03:00:00

1978/9/12 06:00:00
1978/9/21 22:00:00
1978/9/27 13:00:00
1978/10/18 01:00:00
1978/11/16 06:00:00
1978/12/17 13:59:59
1979/1/1 01:59:59
1979/1/14 06:00:00
1979/2/12 01:00:00
1979/3/12 07:00:00
1979/4/6 21:00:00
1979/5/6 01:59:59
1979/5/29 13:00:00
1979/6/5 03:00:00
1979/7/3 13:00:00
1979/7/29 01:00:00
1979/8/24 22:00:00
1979/9/20 13:00:00
1979/10/7 19:00:00
1979/10/20 18:00:00
1979/12/14 04:59:59
1980/1/7 19:00:00
1980/1/25 19:00:00
1980/2/4 12:00:00
1980/3/3 22:00:00
1980/3/16 06:00:00
1980/3/29 19:59:59
1980/4/26 03:00:00
1980/5/20 16:00:00
1980/6/4 07:00:00
1980/6/15 16:59:59
1980/7/12 19:00:00
1980/7/29 00:00:00
1980/8/9 16:00:00
1980/8/28 13:59:59
1980/9/7 01:00:00
1980/9/23 07:59:59
1980/10/3 16:00:00
1980/10/17 21:00:00
1980/10/31 01:59:59
1980/11/16 04:00:00
1980/11/27 13:59:59
1980/12/14 00:00:00
1981/1/10 19:00:00
1981/1/22 13:00:00
1981/2/8 22:59:59
1981/3/7 04:59:59
1981/4/5 01:59:59
1981/5/1 04:59:59
1981/5/29 04:00:00
1981/6/23 07:59:59
1981/7/22 03:00:00
1981/7/31 21:00:00
1981/8/17 13:00:00
1981/8/26 22:00:00
1981/9/12 10:59:59
1981/9/24 12:00:00
1981/10/7 19:59:59
1981/10/20 18:00:00
1981/11/4 21:00:00
1981/11/15 15:00:00
1981/12/2 19:00:00
1981/12/18 04:00:00
1981/12/27 07:00:00
1982/1/15 10:00:00
1982/2/16 01:59:59
1982/2/24 21:00:00
1982/3/18 04:00:00
1982/4/12 12:00:00
1982/5/9 16:00:00
1982/6/6 01:59:59
1982/7/5 06:00:00
1982/7/17 22:59:59
1982/8/2 21:00:00
1982/8/28 21:00:00
1982/9/22 10:59:59
1982/10/23 09:00:00
1982/11/20 13:00:00
1982/12/15 19:59:59
1983/1/4 06:00:00
1983/3/7 10:59:59
1983/4/5 13:59:59
1983/4/29 22:59:59
1983/5/23 13:59:59
1983/6/26 12:00:00
1983/7/12 01:59:59
1983/7/24 22:00:00
1983/8/21 09:00:00
1983/10/4 04:00:00
1983/10/10 16:00:00
1983/11/5 10:59:59
1983/11/24 13:00:00
1983/12/23 01:00:00
1984/1/27 12:00:00
1984/2/23 00:00:00
1984/3/9 10:59:59
1984/5/1 19:00:00
1984/5/25 04:59:59
1984/6/29 22:00:00
1984/8/2 07:00:00
1984/8/20 06:00:00
1984/9/21 09:00:00
1984/10/17 07:59:59
1984/11/17 01:00:00
1985/1/31 21:00:00
1985/3/3 19:59:59
1985/3/28 15:00:00
1985/4/13 04:00:00

1985/5/22 09:00:00
1985/6/18 00:00:00
1985/7/13 01:59:59
1985/8/10 13:00:00
1985/9/2 19:00:00
1985/9/29 06:00:00
1985/10/30 10:00:00
1985/12/23 01:00:00
1986/1/13 10:59:59
1986/2/13 16:00:00
1986/3/8 13:00:00
1986/4/16 01:59:59
1986/5/8 22:00:00
1986/6/18 16:59:59
1986/7/21 09:00:00
1986/10/29 19:00:00
1986/11/26 06:00:00
1986/12/22 13:59:59
1987/4/2 19:00:00
1987/5/10 10:00:00
1987/5/31 18:00:00
1987/7/3 01:59:59
1987/8/3 03:00:00
1987/8/30 16:00:00
1987/9/22 09:00:00
1987/10/23 19:00:00
1987/11/17 01:00:00
1987/12/18 10:00:00
1988/1/3 22:00:00
1988/1/17 21:00:00
1988/2/10 07:00:00
1988/3/5 07:00:00
1988/4/10 03:00:00
1988/4/29 15:00:00
1988/5/23 16:00:00
1988/6/25 13:00:00
1988/8/13 06:00:00
1988/9/11 01:00:00
1988/10/8 13:00:00
1988/11/2 21:00:00
1988/11/28 19:00:00
1988/12/22 07:59:59
1989/1/25 01:59:59
1989/2/12 15:00:00
1989/3/10 01:59:59
1989/4/11 06:00:00
1989/5/12 03:00:00
1989/6/5 22:00:00
1989/6/30 10:00:00
1989/7/20 13:59:59
1989/8/8 03:00:00
1989/8/31 07:00:00
1989/9/23 16:59:59
1989/10/17 00:00:00
1989/11/14 07:59:59
1989/12/11 21:00:00
1990/1/1 07:59:59
1990/1/12 03:00:00
1990/2/7 00:00:00
1990/3/4 12:59:59
1990/5/6 08:00:00
1990/5/23 21:00:00
1990/6/18 21:59:59
1990/7/21 08:00:00
1990/8/8 12:59:59
1990/9/12 03:59:59
1990/10/10 05:00:00
1990/11/4 21:00:00
1990/11/28 18:00:00
1990/12/30 12:00:00
1991/1/26 02:00:00
1991/2/19 21:00:00
1991/4/10 15:00:00
1991/5/7 21:00:00
1991/6/4 09:00:00
1991/7/1 09:59:59
1991/7/26 03:59:59
1991/8/27 15:00:00
1991/9/25 03:59:59
1991/10/22 00:59:59
1991/12/12 00:59:59
1992/2/5 08:00:00
1992/3/1 12:00:00
1992/4/2 18:59:59
1992/4/28 21:59:59
1992/5/29 20:00:00
1992/6/17 00:59:59
1992/7/20 09:59:59
1992/8/5 08:00:00
1992/8/20 03:59:59
1992/9/26 21:59:59
1992/10/22 06:00:00
1992/11/23 00:59:59
1992/12/18 15:59:59
1993/1/23 12:00:00
1993/2/13 03:00:00
1993/3/20 00:00:00
1993/4/14 12:00:00
1993/5/18 08:00:00
1993/8/6 23:00:00
1993/9/7 15:59:59
1993/10/5 18:00:00
1993/11/27 21:59:59
1993/12/29 03:00:00
1994/1/26 23:00:00
1994/2/23 17:00:00
1994/3/21 08:00:00
1994/4/15 03:59:59

1994/5/10 11:00:00
1994/6/10 12:00:00
1994/7/6 18:00:00
1994/8/4 21:00:00
1994/9/5 00:00:00
1994/10/1 02:00:00
1994/10/25 06:00:00
1994/11/19 21:59:59
1994/12/15 09:59:59
1994/12/24 18:59:59
1995/1/11 00:00:00
1995/1/22 20:00:00
1995/2/6 12:00:00
1995/2/17 12:00:00
1995/3/5 05:00:00
1995/3/18 02:00:00
1995/3/31 06:59:59
1995/4/15 18:59:59
1995/4/26 15:00:00
1995/5/13 21:59:59
1995/5/24 00:00:00
1995/6/8 14:00:00
1995/6/20 08:00:00
1995/7/6 09:00:00
1995/7/12 15:59:59
1995/8/2 09:59:59
1995/8/8 21:00:00
1995/8/26 17:00:00
1995/9/24 00:00:00
1995/10/3 06:00:00
1995/10/21 20:00:00
1995/10/31 02:00:00
1995/11/19 00:59:59
1995/11/27 21:00:00
1995/12/9 12:00:00
1995/12/15 20:00:00
1995/12/21 18:59:59
1996/1/20 21:00:00
1996/2/17 06:00:00
1996/3/7 18:00:00
1996/4/6 21:00:00
1996/4/26 14:00:00
1996/5/10 03:00:00
1996/5/23 18:59:59
1996/6/5 06:00:00
1996/6/20 03:59:59
1996/6/30 20:00:00
1996/7/18 14:00:00
1996/8/14 06:59:59
1996/9/11 06:59:59
1996/10/9 12:00:00
1996/11/5 06:00:00
1996/12/3 12:59:59
1996/12/9 11:00:00
1996/12/24 05:00:00
1997/1/8 06:59:59
1997/2/4 12:59:59
1997/3/6 06:00:00
1997/3/20 11:00:00
1997/4/1 09:59:59
1997/4/12 15:59:59
1997/4/29 00:00:00
1997/5/12 02:00:00
1997/5/20 06:59:59
1997/6/13 00:00:00
1997/6/22 18:59:59
1997/7/4 18:00:00
1997/7/10 11:00:00
1997/7/29 15:59:59
1997/8/10 06:59:59
1997/8/28 23:00:00
1997/9/9 05:00:00
1997/9/19 06:59:59
1997/10/8 12:00:00
1997/10/25 11:00:00
1997/11/4 05:00:00
1997/11/9 18:59:59
1997/11/22 00:59:59
1997/12/3 18:00:00
1997/12/30 02:00:00
1998/1/19 03:59:59
1998/2/24 12:00:00
1998/3/5 00:59:59
1998/3/22 12:00:00
1998/4/3 15:59:59
1998/4/15 12:59:59
1998/5/1 09:00:00
1998/5/16 09:00:00
1998/5/29 02:00:00
1998/6/12 02:00:00
1998/6/25 00:00:00
1998/7/10 08:00:00
1998/7/21 20:00:00
1998/8/3 11:00:00
1998/8/23 03:59:59
1998/9/12 14:00:00
1998/10/7 12:00:00
1998/10/18 14:00:00
1998/11/3 09:59:59
1998/11/19 03:00:00
1998/12/2 03:59:59
1998/12/19 09:00:00
1998/12/31 12:59:59
1999/1/13 18:00:00
1999/2/11 18:00:00
1999/3/11 14:00:00
1999/4/10 03:59:59
1999/5/5 03:59:59

1999/5/17 03:59:59
1999/6/2 00:59:59
1999/6/16 06:59:59
1999/6/24 15:00:00
1999/7/13 21:59:59
1999/8/6 06:59:59
1999/8/16 18:59:59
1999/8/30 12:59:59
1999/9/13 08:00:00
1999/9/28 06:00:00
1999/10/10 05:00:00
1999/10/23 21:00:00
1999/11/7 12:59:59
1999/11/22 21:00:00
1999/12/4 12:59:59
1999/12/23 17:00:00
2000/1/1 02:00:00
2000/1/20 17:00:00
2000/1/28 09:00:00
2000/2/16 14:00:00
2000/3/16 12:59:59
2000/4/14 15:00:00
2000/5/12 23:00:00
2000/6/7 08:00:00
2000/7/5 18:00:00
2000/7/28 15:00:00
2000/8/17 00:59:59
2000/8/28 14:00:00
2000/9/11 21:00:00
2000/9/24 21:59:59
2000/10/9 06:59:59
2000/10/22 20:00:00
2000/11/4 05:00:00
2000/11/19 00:59:59
2000/12/1 06:00:00
2000/12/16 18:59:59
2000/12/29 21:59:59
2001/1/11 11:00:00
2001/1/29 00:00:00
2001/2/27 12:00:00
2001/3/21 09:59:59
2001/3/26 02:00:00
2001/4/23 18:00:00
2001/5/18 02:00:00
2001/6/16 02:00:00
2001/7/11 18:59:59
2001/8/6 14:00:00
2001/8/13 18:59:59
2001/9/2 00:00:00
2001/9/29 12:00:00
2001/10/8 14:00:00
2001/10/16 02:00:00
2001/10/26 21:59:59
2001/11/15 06:00:00
2001/12/10 21:59:59
2002/1/7 20:00:00
2002/2/5 08:00:00
2002/3/3 12:59:59
2002/3/27 15:00:00
2002/4/21 21:00:00
2002/5/19 09:59:59
2002/6/16 15:00:00
2002/7/12 20:00:00
2002/8/8 23:00:00
2002/9/3 15:00:00
2002/9/30 00:59:59
2002/10/24 06:00:00
2002/11/22 05:00:00
2002/12/19 08:00:00
2003/1/17 20:00:00
2003/2/13 05:00:00
2003/3/12 09:00:00
2003/4/8 02:00:00
2003/5/4 15:59:59
2003/5/30 15:00:00
2003/6/27 09:00:00
2003/7/26 23:00:00
2003/8/21 14:00:00
2003/9/15 20:00:00
2003/10/13 09:00:00
2003/11/9 00:00:00
2003/12/5 23:00:00
2003/12/31 18:59:59
2004/1/28 15:00:00
2004/2/27 00:59:59
2004/3/24 20:00:00
2004/4/21 08:00:00
2004/5/19 08:00:00
2004/6/13 08:00:00
2004/7/9 12:59:59
2004/7/22 20:00:00
2004/8/6 14:00:00
2004/8/20 06:00:00
2004/8/30 15:00:00
2004/9/5 00:59:59
2004/9/16 00:00:00
2004/10/2 11:00:00
2004/10/12 03:00:00
2004/10/30 06:00:00
2004/11/7 14:00:00
2004/11/24 00:59:59
2004/12/7 03:59:59
2004/12/22 08:00:00
2004/12/31 02:00:00
2005/1/17 00:00:00
2005/1/28 02:00:00
2005/2/24 09:59:59
2005/3/14 18:00:00

2005/3/24 00:59:59
2005/4/19 21:59:59
2005/5/6 08:00:00
2005/5/12 09:00:00
2005/5/23 02:00:00
2005/6/2 00:00:00
2005/6/12 18:59:59
2005/6/28 06:59:59
2005/7/9 14:00:00
2005/7/26 12:59:59
2005/8/4 18:59:59
2005/8/22 03:59:59
2005/9/1 02:00:00
2005/9/15 03:59:59
2005/9/27 03:59:59
2005/10/15 08:00:00
2005/10/25 21:00:00
2005/11/11 02:00:00
2005/11/22 00:59:59
2005/12/9 06:00:00
2006/1/3 14:00:00
2006/2/1 00:00:00
2006/2/10 06:00:00
2006/2/28 03:59:59
2006/3/9 06:00:00
2006/3/27 09:59:59
2006/4/20 06:59:59
2006/5/17 06:59:59
2006/5/31 18:00:00
2006/6/14 14:00:00
2006/6/27 05:00:00
2006/7/11 02:00:00
2006/8/7 00:59:59
2006/8/19 08:00:00
2006/9/3 00:00:00
2006/9/16 18:00:00
2006/10/1 09:59:59
2006/10/12 00:59:59
2006/10/27 12:59:59
2006/11/9 12:00:00
2006/11/23 06:59:59
2006/12/6 08:00:00
2006/12/15 21:00:00
2007/1/2 17:00:00
2007/1/16 23:00:00
2007/1/30 03:00:00
2007/2/13 14:00:00
2007/2/27 05:00:00
2007/3/13 05:00:00
2007/3/26 08:00:00
2007/4/9 02:00:00
2007/4/22 17:00:00
2007/5/8 08:00:00
2007/5/19 05:00:00
2007/6/2 06:59:59
2007/6/14 03:59:59
2007/6/29 09:59:59
2007/7/11 21:00:00
2007/7/26 08:00:00
2007/8/6 00:59:59
2007/9/1 03:59:59
2007/9/27 21:59:59
2007/10/25 15:59:59
2007/11/22 06:00:00
2007/12/17 18:00:00
2007/12/28 09:00:00
2008/1/12 02:00:00
2008/2/8 15:59:59
2008/3/8 12:00:00
2008/4/3 09:59:59
2008/4/17 18:00:00
2008/5/1 09:00:00
2008/5/28 23:00:00
2008/6/25 09:59:59
2008/7/22 02:00:00
2008/8/17 15:59:59
2008/9/14 09:00:00
2008/10/11 00:00:00
2008/11/7 15:59:59
2008/12/4 00:59:59
2008/12/19 03:59:59
2008/12/30 03:00:00
2009/1/24 00:00:00
2009/2/20 06:59:59
2009/3/15 08:00:00
2009/4/17 14:00:00
2009/5/15 03:59:59
2009/5/21 11:00:00
2009/6/1 02:00:00
2009/6/10 17:00:00
2009/7/7 20:00:00
2009/7/13 21:00:00
2009/8/3 18:59:59
2009/8/11 11:00:00
2009/9/11 03:00:00
2009/9/27 12:00:00
2009/10/9 09:00:00
2009/10/23 15:59:59
2009/11/25 03:59:59
2009/12/13 09:59:59
2009/12/22 21:59:59
2010/1/18 00:00:00
2010/2/18 00:59:59
2010/3/16 00:00:00
2010/4/14 12:59:59
2010/4/22 06:00:00
2010/5/11 08:00:00
2010/5/20 00:59:59

2010/6/7 20:00:00
2010/6/15 14:00:00
2010/7/8 21:00:00
2010/7/14 03:00:00
2010/8/9 11:00:00
2010/8/16 11:00:00
2010/9/6 23:00:00
2010/10/5 00:00:00
2010/11/2 18:59:59
2010/11/7 15:00:00
2010/11/28 03:00:00
2010/12/24 09:00:00
2011/1/17 18:59:59
2011/1/30 15:59:59
2011/2/14 18:59:59
2011/2/26 00:59:59
2011/3/13 12:00:00
2011/3/23 05:00:00
2011/4/11 17:00:00
2011/5/13 09:59:59
2011/6/12 23:00:00
2011/7/9 21:59:59
2011/8/8 08:00:00
2011/9/2 06:59:59
2011/9/18 17:00:00
2011/9/28 02:00:00
2011/10/1 17:00:00
2011/10/30 23:00:00
2011/12/1 08:00:00
2011/12/18 11:00:00
2011/12/28 09:59:59
2011/12/31 23:00:00
2012/1/13 20:00:00
2012/1/26 23:00:00
2012/2/9 15:59:59
2012/2/23 06:59:59
2012/3/9 06:59:59
2012/3/23 06:00:00
2012/4/6 09:59:59
2012/5/3 23:00:00
2012/5/19 06:00:00
2012/5/29 03:00:00
2012/6/12 20:00:00

BIOGRAPHICAL SKETCH

Daniel Krahenbuhl is a Ph.D. candidate in the school of Geographical Sciences and Urban Planning at Arizona State University. An adaptation of his Master's thesis was published in the Journal of Geophysical Research-Atmospheres. He participated in NASA/UCAR's visiting science program for Heliophysics during summer 2011. He has contributed to several diverse research investigation ranging from remote sensing of arid geomorphological landforms, cloud/cosmic ray correlations, the expansion/contraction of global pressure systems, heliophysical modeling and solar cycle forecasting. He has acted as software developer for several Python open source code projects, specifically involving 3D meteorological visualization, climatological modeling, gridded database maintenance and manipulation, and geospatial analysis. He has served as laboratory instructor and supervisor for over 4 years for several courses including: Physical Geography, Geomorphology, Meteorology and Climatology.